nature portfolio

Peer Review File

Transformability of Dynamics on Higher-order Networks

Corresponding Author: Professor Shibo He

This file contains all reviewer reports in order by version, followed by all author rebuttals in order by version.

Attachments originally included by the reviewers as part of their assessment can be found at the end of this file.

Version 0:

Reviewer comments:

Reviewer #1

(Remarks to the Author)
The authors deal with dynamic processes on networks and study the possibility of transforming higher-order dynamic processes on hypergraphs into lower-order processes, identifying the specific conditions that enable such transformation. They focus specifically on contagion and opinion diffusion. Furthermore, they identify the structural and dynamic contributions that drive this transformability.

The work is original and scientifically sound: I appreciate the concepts proposed and the general idea, that make the topic potentially suitable for Communications Physics. However, I have several major and minor concerns that make the paper unsuitable for publication in its current form. Above all, there are issues related to the relevance of the results and to the notation, which require an extensive reformulation.

**Major issues:
1. The transformability of higher-order dynamical process on hypergraphs into dynamics on simplices or graphs is presented as a main result. By focusing on contagion processes, the authors estimate the conditions on the contagion probabilities that allow obtaining the same dynamics on the hypergraph and on its corresponding simplicial complex or graph. These results are quite trivial, since they simply show that higher-order nonlinear processes are a generalization of pairwise processes, containing the latter as a special case. The authors have only found the conditions that make higher-order processes not higher-order anymore reducing them to their pairwise counterpart. For example, it is obvious that if β_δ=0 for δ>1 then the process is equal to a pairwise process, or that if the non-linear probability coefficients are rescaled with X^v then all nonlinearities disappear, since in both cases the higher-order terms and mechanisms are removed.

The authors emphasize these results, but in my opinion they appear rather trivial. On the contrary, the second part of the paper, on the structural and dynamical contribution to the difference between higher-order and pairwise processes, seems much more interesting and should be further expanded.

2. The limitations of the proposed approach are not highed enough. One of the main limitations is that a Q^* must exist, and this may not be the case for all higher-order processes. The authors should discuss further under what conditions Q^* exists or not. Moreover, there could be several possible Q^* potentially giving different results, and this possibility is not discussed in the text. In higher-order contagion on hypergraphs the coefficient λ is usually constant [A], while here the authors consider λ to depend on m and X, to make the model easier to be reduced to the simplicial or pairwise case. What is the meaning of this dependence? Is this necessary to obtain Q^*? For example, the nonlinearities can be removed also considering v=1.

3. There are several problems of notation and errors: I will list here the main ones, but there are much more. In Eq. (1): what are h and A? Shouldn't the second term depend on i? The product Π on X considers all possible number of infected in the hyperedge, instead of considering the true number of infected nodes in the group at time t, and this is incorrect; similarly, the product Π on m is incorrect; the product Π should be unique and on all hyperedges in which the node i is involved. Furthermore, the mapping ratio k is introduced without explaining what it is. Similarly, i is used as a node index, but then in Eq. (2,3) it is used as an index of the summation. Eq. (8) in the Methods is different from the corresponding one in the main text (Eq. (1)) and still is incorrect. In Eqs. (9,10), the variable I(t) is indicated with and without subscripts. In the SI: in Eq. (1) there is a summation over i but then i does not appear, and the meaning of Δ is not indicated. In Eq.(2) the notation of the summation is incorrect. Furthermore, Eqs. (4,5) are not consistent with Eqs. (1,2) when obtaining Eq.(5) from Eq. (4). In Eq.

(11) <Θ> is not defined. In Eq. (18) the subscripts of λ are missing, the product on h disappears but the index remains and again a product on X is introduced, even if X is fixed.

4. It is important to describe also in the main text the higher-order generalization of the opinion dynamics introduced, given that numerous possible versions exist (moreover, the higher-order version of the Voter model is not presented anywhere). Also the conditions for Q^* in the two opinion dynamics processes should be provided (analogously to the contagion processes) and more details on how the system instability is evaluated. Moreover, no references have been cited for the higher-order DW generalization considered, whose mechanisms seem not being fully higher-order since they correspond to considering a tolerance based on the link weights. Truly higher-order DW generalizations are proposed in [B,C]: the authors should consider these cases.

5. The text lacks crucial information on how the numerical simulations of the processes are performed. For example, Fig. 3 caption states that the simulations use numerical integration methods. The numerical integration is used to solve the mean-field equations, right? While how are conducted the numerical simulations?

6. The caption of Fig. 3 states that ΔΦ^* is compared to the sum of the absolute values of $\Delta\Phi_1$ and $\Delta\Phi_2$. However, this is incorrect if compared to the definition provided: the definition adopted should be uniform.

7. The synthetic networks considered are generated with N=|E|, hence producing an average hyperdegree <D>=2. The network is very sparse, and the overlap of hyperedges is lost, eventually impeding opinion convergence due to the nodes' isolation. Larger values of |E| should be considered.

8. Some considerations in Supp. Note 4 are incorrect. If a group of size m has X infected and is projected onto simplices with ratio k, with m>k: the maximum number of infected in a generated simplex is not k, since X could be lower than k; the minimum is not k+1-(m-X). For example, in a triangle with 1 infected (m=3, X=1 and k=2): the minimum and maximum according to the authors would be 1 and 2 respectively, but instead there is a simplex of size 2 with 0 infected and the maximum is 1.

9. In Supp. Note 6, the authors consider the specific case of contagion on simplicial complexes: similar results should be shown for hypergraphs and the other processes. Moreover, in Supp. Note 7, the authors discuss heterogeneous mean-field equations but do not present them: they should be reported.

**Minor issues:
1. In the text often the authors use the terms "network dynamics" and "dynamical networks": these terms are misleading because they are generally used to describe temporal networks in which interactions evolve over time. It would be preferable use "dynamics on networks" to avoid misunderstandings. Moreover, the authors discuss the "interplay" of the processes at different orders or the presence of "mutual dependence": I think these terms are misleading since they suggest a coupling of different processes.

2. In Section 2.3, an α parameter is introduced without specifying its meaning. Moreover, in Fig. 4, which synthetic graph is considered, and for what model parameter values are the simulations conducted? In SI Fig. 3, there are inconsistencies between the caption and the plot, in the colours and descriptions of the panels. Furthermore, what do the colours under the black curves indicate?

3. In schools datasets, contacts are collected as pairwise interactions. How are the groups defined?

4. Which configuration model is used? Is the model proposed in [D]?

5. In the SI: Table 2 is unclear because it shows a list of properties but not which network they correspond to: different N and |E|? Fig. 2 is unclear and more comments should be added to describe it: why the infection rate reach values of 10^14? It would be better to indicate the values of m and X on the heatmaps.

[A] St-Onge, G., Iacopini, I., Latora, V. et al. Influential groups for seeding and sustaining nonlinear contagion in heterogeneous hypergraphs. Commun Phys 5, 25 (2022).
[B] Schawe, H., Hernández, L. Higher order interactions destroy phase transitions in Deffuant opinion dynamics model. Commun Phys 5, 32 (2022).
[C] Hickok, A., et al. A bounded-confidence model of opinion dynamics on hypergraphs. SIAM Journal on Applied Dynamical Systems 21.1 (2022): 1-32.
[D] Iacopini, I., Petri, G., Barrat, A. et al. Simplicial models of social contagion. Nat Commun10, 2485 (2019).

Reviewer #2

(Remarks to the Author)
See attached.

Version 1:

Reviewer comments:

Reviewer #1

(Remarks to the Author)
During this revision phase, the authors have made a wide set of modifications to the original version of the paper. I appreciate the attention they paid to the reviewers' suggestions.

I consider the paper significantly improved in terms of clarity and structure. However, I’m not fully satisfied by the modifications and I still have some major and minor concerns that the authors should address before considering the paper for publication in Communication Physics. I detail my concerns below.

**Major issues:
1. Fig. 4 is obtained for a specific value of m and of X: what if they are changed? For example, if the size of interactions is larger? Or with a larger number of infected? Moreover, these results are obtained for a specific structure? If yes, which one (it’s not specified in the caption)?
The existence of Q^* should be investigated in more details and overall for different m and X: what if Q^* exists for m=3 but not for m=4? It’s easier to satisfy the condition for smaller m? And for smaller X? And what is the role of the structure underlying the process? For example, Fig. 3 of SI already partially goes in this direction: for that Fig. what would be Q^*?

2. Fig. 4 and Eq. (4) show that Q is different for different m and X. If in the hypergraphs there are different hyperedges of different sizes and with different number of infected, how this is impacting Q^*? The entropy is calculated for Q^* fixing the parameters differently for each m and X? For example, in caption of Fig. 3 the authors say “… where \lambda satisfies Eq. 3”, so this means a different \lambda for different m and X?

3. I still find quite unclear how the authors treat the \lambda parameter: if it “represents a constant infection rate” how it can “assume different values under different settings of m and X”? In particular, the conditions for mapping the process to the simplicial contagion case are different for different m and X, but a general hypergraph is made by different hyperedges of different sizes (m) and with a different number of infected nodes over time within them (X): so the conditions for a specific m and X are usually not valid for others and cannot be fulfilled all simultaneously, since \lambda is constant? This is partially linked to the previous point.

4. The discussion on the limitations of the work are improved, however I think that the discussion on the existence of Q^* should also be more stressed in the main text (not only in the Discussion): especially regarding the GDW opinion dynamics, which shows that intrinsically higher-order processes do not fall (easily) in the group of transformable processes (and this is very relevant). Moreover, I was expecting them to be transformable at least from the structural point of view, if the underlying hypergraph has only pairwise interactions.

**Minor issues:
1. There are still many notation problems and inaccuracies (some even if I already highed them in the previous review round): for example, the definition of X is introduced in page 13, but should appear before, in page 5 already (since it’s used there). In Eq.s (12,13) on the right-hand side there should be a subscript as at the first member. What is the "bound c" in Fig. 5 caption? Maybe it should be \epsilon? A statement in Supp. Note 4 is still incorrect: the minimum number of infected in the simplex could be 0 potentially. There is still usage of “network dynamics” in the text. Fig. 4 of SI: still panels a and b are inverted with respect to the caption and a colorbar should be added to indicate the meaning of the colours under the curves. In SI, at the end of page 11: \Delta I_1 and I_2 are not defined for hypergraphs. The last paragraph of the Introduction “To the best of our… dynamical systems” is repeated twice. In Fig. 2 caption, \beta is said to vary from 0.005 to 0.1, but it varies from 0.01 (see legend). Sometimes panels are indicated in bold and sometimes with “( )”. What is U in Eq. (9)? At the end of Sec. 4.3, there is a typo (repeated twice) with a dot after “\mathcal(D)” that should not be there. Caption of Fig. 3 is unclear: what are the “dotted line”, “dark-colored” and “-colored” bars cited in the caption referring to panels a and b?

2. In caption of Fig. 4 should be stated what is \alpha (since here it appears before than the Sec. in which it is introduced)

3. The information on numerical simulations is not enough: how are the different realizations created? Different initial conditions or different networks? When are the simulations stopped, and which initial conditions are used? This should be added in the text, for example with a dedicated small paragraph in the methods or in the captions. Moreover, the authors should check all the captions to see if everywhere is indicated: (i) how simulations are run; (ii) on which structure.

4. Why when increasing the density of the hypergraphs, the dynamical factor is more relevant? A short justification should be added in the main text.

Reviewer #2

(Remarks to the Author)
The revised article, “Transformability of Higher-order Network Dynamics” greatly improves upon its original draft. Some lingering issues/comments:
* I realized that Ref. 25 is not about contagion so shouldn’t be cited when talking about contagion. I think that Ref. 28 or https://doi.org/10.1063/5.0020034 might be more appropriate in the second paragraph of the introduction.
* Not to be pedantic, but the manuscript states, “Secondly, the contagion dynamics are governed by the evolution of

individual node states (e.g., infection probabilities), which gives rise to disorder at the system level, hereafter referred to as system disorder." I don't think that "governed" is the appropriate word here. I would say that temporal node states describe the system and infection probabilities govern these transitions.
* The last paragraph of the introduction is much improved.
I recommend that it be published after these minor corrections are made.

Version 2:

Reviewer comments:

Reviewer #1

(Remarks to the Author)
During this second revision phase, the authors addressed my concerns and amended the text accordingly. Some of the modifications and responses are in the right direction, however some parts seem not convincing to me. I detail the reasons for these considerations below: these points should be addressed by the authors before accepting the paper for publication in Communication Physics.

**Issues:
1. Many of the figures' captions still lack crucial information or present contrasting information, despite having requested to clarify this part in both my first and second report. For example, the caption of Fig. 3 says that the simulations are run on the primary and high-school dataset, but only one curve is shown, and then also an SSC random networks is cited; Fig. 4 does not indicate the value of \nu; Fig. 5a,d do not indicate the underlying network;...

2. The framework is now much clearer: to transform the higher-order process into the pairwise one, the higher-order contagion probabilities must have specific values for each size of the group (m) and for each number of infected individuals in it (X). This has clarified the framework, showing that the constraints for transformability are very strong (and potentially unrealistic).

However the authors' considerations on the existence of Q^* are unclear: I am mainly referring to the paragraphs "As shown in Fig. 4a-c, … hypergraphs with larger hyperedges." at the end of pag. 8 and beginning of pag. 9. The authors claim that when the group size is small (m=2) and there are few infected individuals (X=1) the range of parameters for which the higher-order/pairwise mapping can occur is broader than the case with large sizes and many infected individuals (m=4, X=3). However, Fig. 4 shows that for each value of \beta there exists a single \lambda_m,X that allows transformability for each m,X considered in the same way. It seems that the authors are changing point of view, assuming that \lambda_m,X is fixed and \beta is searched for the mapping: therefore if (m,X) are large and \lambda_m,X is large then the corresponding allowed \beta does not exist. This approach is a bit confusing, since for the full transformability to exist \beta must exist and be the same for every m,X and the point of view is different from the rest of the paper. The authors should clarify this point better and make it less confusing.

3. \Lambda_m,X is still a good measure: if it becomes 0, it means that regardless of \beta, the only way to transform one process into the other is if there is zero probability of infection for those m,X. In Fig. 4d, it is not clear whether some (m,X) give \Lambda_m,X=0 or simply very small. Perhaps it is better to use a logarithmic scale of the colorbar and indicate if the values are zero? If they are zeros, the authors should also comment on this in the text.

4. For which value of \nu are the results in Fig. 4 obtained? \nu determines the non-linearity of the higher-order process, so I imagine it plays a key role in the existence of Q^*.

Version 3:

Reviewer comments:

Reviewer #1

(Remarks to the Author)
In this final round of review, the authors carefully addressed all my concerns and revised the manuscript accordingly.
I am satisfied with the changes implemented and with their response.
I consider the actual version of the paper ready, hence I suggest publication of the paper in Communications Physics.

Finally, I would like to express my appreciation to the authors for their work of revision, which was very attentive and effective, improving the paper significantly.

Article title:
- Original title: Transformability of Higher-order Network Dynamics
- Updated title: Transformability of Dynamics on Higher-order Networks
Manuscript Number: COMMSPHYS-25-1130A

Response to the comments of Reviewer #1

Reviewer #1 (Remarks to the Author):

The authors deal with dynamic processes on networks and study the possibility of transforming higher-order dynamic processes on hypergraphs into lower-order processes, identifying the specific conditions that enable such transformation. They focus specifically on contagion and opinion diffusion. Furthermore, they identify the structural and dynamic contributions that drive this transformability.

The work is original and scientifically sound: I appreciate the concepts proposed and the general idea, that make the topic potentially suitable for Communications Physics. However, I have several major and minor concerns that make the paper unsuitable for publication in its current form. Above all, there are issues related to the relevance of the results and to the notation, which require an extensive reformulation.

Reply: We thank the reviewer for their insightful comments. Below are our responses addressing each of them.

Major issues.

1 The transformability of higher-order dynamical process on hypergraphs into dynamics on simplices or graphs is presented as a main result. By focusing on contagion processes, the authors estimate the conditions on the contagion probabilities that allow obtaining the same dynamics on the hypergraph and on its corresponding simplicial complex or graph. These results are quite trivial, since they simply show that higher-order nonlinear processes are a generalization of pairwise processes, containing the latter as a special case. The authors have only found the conditions that make higher-order processes not higher-order anymore reducing them to their pairwise counterpart. For example, it is obvious that if $\beta\delta=0$ for $\delta>1$ then the process is equal to a pairwise process, or that if the non-linear probability coefficients are rescaled with Xv then all nonlinearities disappear, since in both cases the higher-order terms and mechanisms are removed.

The authors emphasize these results, but in my opinion they appear rather trivial.

On the contrary, the second part of the paper, on the structural and dynamical contribution to the difference between higher-order and pairwise processes, seems much more interesting and should be further expanded.

Reply: We sincerely thank the reviewer for this comment. We realize that the presentation of our manuscript may not sufficiently emphasize the intended scope, which has given the impression that Part 1 constitutes the main result. We have now revised the text to make our aims clearer in the Introduction. The central theme of our study is the *transformability* of higher-order dynamical processes. In this context, Part 1 is primarily introduced as a methodological tool that sets up the formal framework. The main emphasis of our work lies in Part 2 and Part 3, where we (i) disentangle the structural and dynamical origins underlying the (non-)transformability of higher-order processes, and (ii) explore the extensibility of our proposed scheme to different classes of dynamics. Both aspects are essential for advancing the understanding of transformability in higher-order dynamics, and they constitute the key contributions of our manuscript.

In response to the concern, we have first updated the Introduction to more explicitly highlight the objectives of our study. Additionally, we have readjusted and streamlined the discussion regarding the case $\beta_\delta = 0$ for $\delta > 1$ in the main text.

Furthermore, we have significantly explored the second part of the manuscript, which focuses on the structural and dynamical contributions to the differences between higher-order and pairwise processes. Specifically:

In Section 2.2, we examined and discussed the variation of the Q value and the existence of Q^* during dynamic transformations (see Fig. R1). Our analysis reveals that, for a hypergraph contagion process to be mapped onto its multi-edge graph counterpart, the parameter λ cannot take excessively large values.

In Section 2.3, we included additional validation of our proposed framework across networks with different densities (Fig. R2-1 and Fig. R2-2).

These additions emphasized on the novel contributions of our work regarding the interplay between structure and dynamics in higher-order processes. The specific revisions implemented in both the main manuscript and the Supplementary Information are detailed below.

Page 8, Section 2.2:

Q^* as a criterion for dynamic transformation. *The feasibility of decomposition into structural and dynamical components critically depends on the value of Q^*. As shown in Fig. 4a–b, sufficiently small values of λ (e.g., $\lambda \ll \beta$ when $\beta_\Delta = 0$) enable contagion dynamics on hypergraphs to be mapped onto equivalent dynamics on* *projected multi-edge dyadic graphs, thereby allowing decomposition. In contrast, when $\lambda > 0.2$, no valid mapping β exists, and the decomposition becomes infeasible. A similar condition arises in simplicial complexes, where $\beta_\Delta = 0$ determines whether decomposition is attainable. These results highlight a fundamental finding, i.e., the existence of Q^* is not guaranteed universally but is restricted to specific parameter regimes. Consequently, the applicability of our framework depends on whether the underlying dynamics fall within these regimes. This observation underscores the importance of Q^* not only as a technical requirement, but also as a critical criterion delineating when higher-order contagion processes can, or cannot, be faithfully reduced to lower-order representations.*

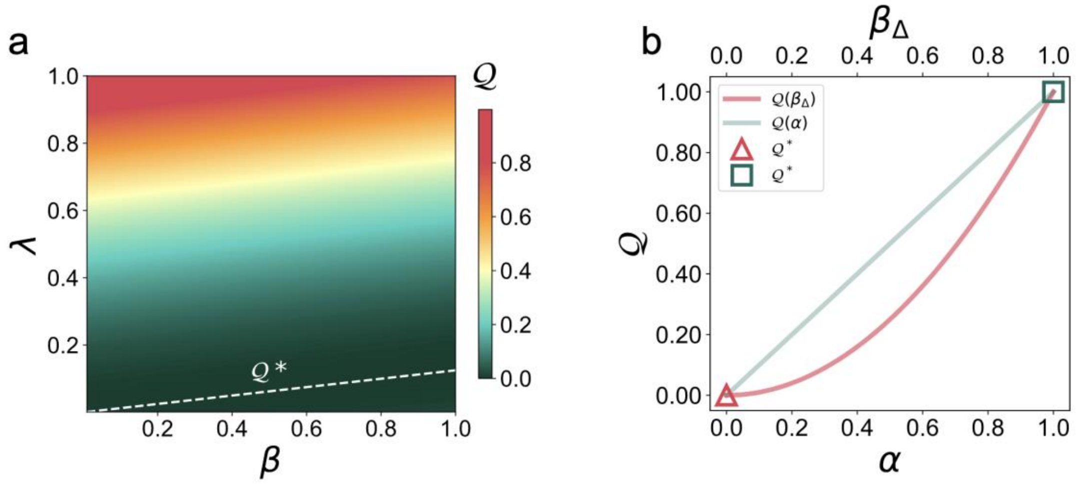

Fig.R1. (Fig. 4 in the revised manuscript) *Q^* in dynamics on hypergraphs and simplicial complexes.* ***a*** *Variation of Q with respect to λ and β in contagion dynamics on hypergraphs ($I_{\Upsilon=\mathcal{H}}$) with $m = 3$ and $\chi = 2$. The dashed line indicates the condition $Q = Q^*$.* ***b*** *Variation of Q with respect to β_Δ in contagion dynamics on simplicial complexes (red line), where the red triangle denotes $Q = Q^*$. The green line shows Q for two opinion dynamics on hypergraphs, with the green square indicating Q^*.*

Page 10, Section 2.3:

We further examine the effect of network density on performance (see Supplementary Information). The proposed method remains consistently effective across synthetic hypergraphs of varying densities. Notably, in denser hypergraphs the relative contribution of the dynamical factor becomes more pronounced than that of the structural factor.

Page 19, Supplementary Note 9:

To assess the effectiveness of the proposed scheme in hypergraphs with varying densities, we next evaluate its performance under different network density conditions. To this end, we generate synthetic hypergraphs with $N = 100$ nodes and different numbers of hyperedges, $|E| = \{200,300,500,1000\}$. As shown in Fig. 11 and Fig. 12, *the proposed method remains effective across all densities considered. Moreover, we find that in denser hypergraphs the relative contribution of the dynamical factor becomes more pronounced compared to that of the structural factor.*

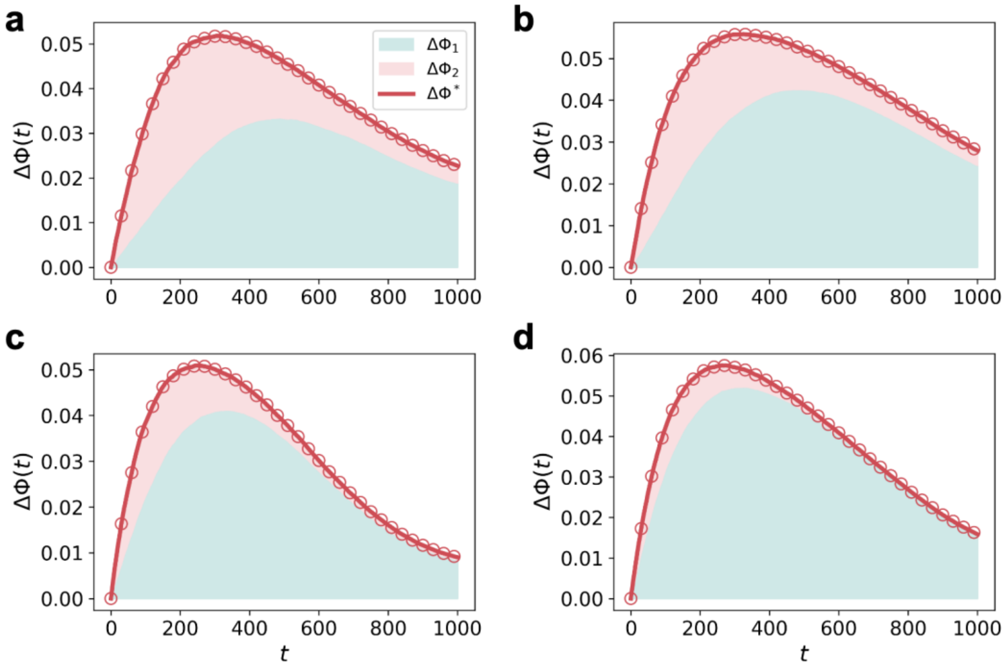

Fig. R2-1. (Fig. 11 in the revised Supplementary Note 9) ***a-d*** *The relationships between the dynamical contribution* $\Delta\Phi_1 = \mathcal{D}^{\alpha}_{\mathcal{H}}(t) - \mathcal{D}^{\alpha_1}_{\mathcal{H}}(t)$*, the structural contribution* $\Delta\Phi_2 = \mathcal{D}_{\widehat{\mathcal{H}}}(t) - \mathcal{D}_{\widehat{\mathcal{H}}}(t)$*, and the total information loss* $\Delta\Phi^*$ *under DW process are examined in synthetic hypergraphs of **(a)*** $\mathcal{H}(V = 100, |E| = 200)$*, **(b)*** $\mathcal{H}(V = 100, |E| = 300)$*, **(c)*** $\mathcal{H}(V = 100, |E| = 500)$*, **(d)*** $\mathcal{H}(V = 100, |E| = 1000)$*. All results are averaged over 10 numerical simulations with the time steps* $t = 10^3$.

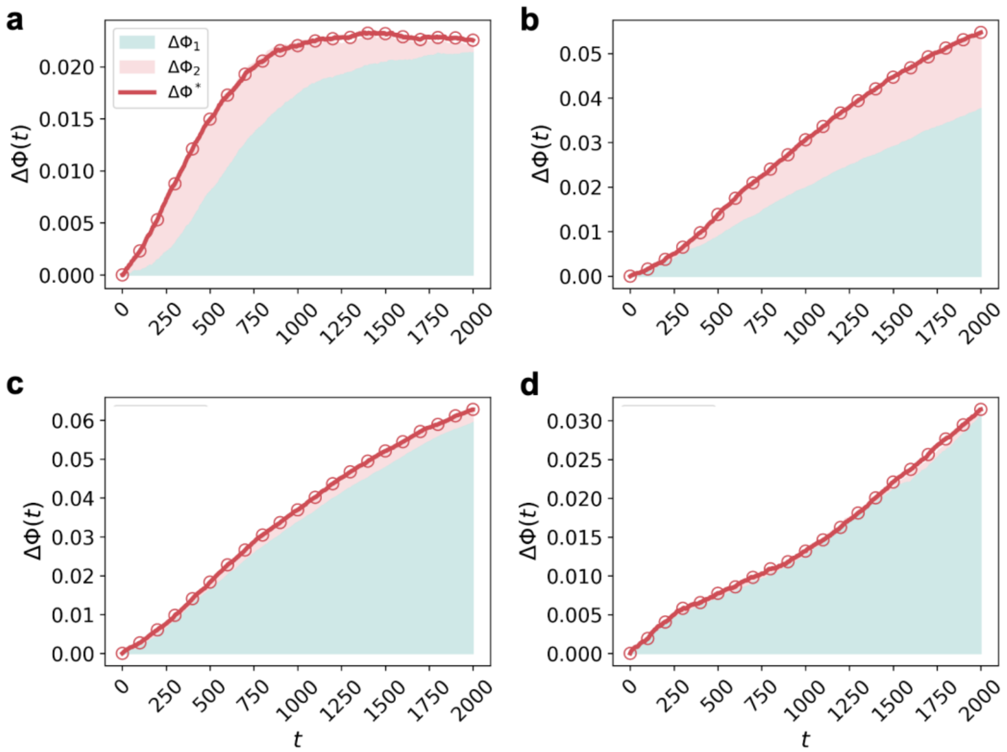

Fig. R2-2. (Fig. 12 in the revised Supplementary Note 9) ***a-d*** *The relationships between the dynamical contribution* $\Delta\Phi_1 = \mathcal{D}_{\mathcal{H}}^{\alpha}(t) - \mathcal{D}_{\mathcal{H}}^{\alpha_1}(t)$, *the structural contribution* $\Delta\Phi_2 = \mathcal{D}_{\widehat{\mathcal{H}}}(t) - \mathcal{D}_{\widehat{\mathcal{H}}}(t)$, *and the total information loss* $\Delta\Phi^*$ *under Voter process are examined in synthetic hypergraphs of (**a**)* $\mathcal{H}(V = 100, |E| = 200)$, *(**b**)* $\mathcal{H}(V = 100, |E| = 300)$, *(**c**)* $\mathcal{H}(V = 100, |E| = 500)$, *(**d**)* $\mathcal{H}(V = 100, |E| = 1000)$. *All results are averaged over 10 numerical simulations with the time steps* $t = 2 \times 10^3$.

2.1 The limitations of the proposed approach are not highlighted enough. One of the main limitations is that a Q^* must exist, and this may not be the case for all higher-order processes.

Reply: We sincerely thank the reviewer for this insightful and constructive comment. We agree with the reviewer that the limitations were not sufficiently highlighted in the original version. To address this concern, we have revised the Discussion section to explicitly discuss the dependence of our framework on the existence of Q^*. We now emphasize that Q^* may not exist for all higher-order processes, which constitutes a central limitation of our approach. While we have already analyzed the possible existence of Q^* in terms of decomposition into structural and dynamical components, additional forms of decomposition beyond these two could also be explored in future work. This new discussion has been added in the revised manuscript (Discussion, page 12):

Page 12, Section 3:

Moreover, our proposed scheme relies on the existence of Q^*, which may not be guaranteed for all higher-order processes, such as the group-updated DW (GDW) model [40, 46]. This is due to fundamental differences in the update mechanisms: the expected increment for each node pair often deviates from that in the corresponding multigraph, and the tolerance condition is evaluated across all nodes in a hyperedge (e.g., maximal opinion difference), making it inherently a higher-order criterion that cannot be reduced to a simple pairwise threshold in the multigraph. Nevertheless, the statistical behavior of hypergraph-based dynamics can be brought close to that of multigraph dynamics under a set of macro-level conditions. These include decomposing hyperedge updates into pairwise linear increments scaled by edge weights, updating randomly selected node pairs rather than all nodes simultaneously, adjusting tolerance thresholds according to hyperedge size or structure, and weighting hyperedge selection probabilities to match their expected contribution to the global variance. While these conditions do not guarantee the strict existence of Q^*, they allow for practical equivalence in ensemble-averaged dynamics. Although we have discussed its potential existence under structural and dynamical decompositions, alternative decomposition schemes could also be explored in future studies to further generalize the applicability of the proposed framework.

2.2 The authors should discuss further under what conditions Q^* exists or not. Moreover, there could be several possible Q^* potentially giving different results, and this possibility is not discussed in the text.

Reply: Thanks for your suggestion. We have expanded our analysis of Q^* in the main text and added new results (Fig. 4a and Fig. 4b). Our findings show that the feasibility of decomposing transformations between higher-order networks and their projected graphs depends on the value of Q^*. Specifically, for contagion dynamics on hypergraphs, sufficiently small value of λ (much smaller than β when $\beta_\Delta = 0$) enables such decomposition. In contrast, when $\lambda > 0.2$, there is no corresponding β that can map the two contagion dynamics, which makes the decomposition infeasible. A similar observation holds for simplicial complexes, where the condition $\beta_\Delta = 0$ characterizes when decomposition is possible. The following text and Fig. R1 (now Fig. 4 in the revised manuscript) have been added to Section 2.2:

Page 8, Section 2.2:

Q^* as a criterion for dynamic transformation. *The feasibility of decomposition into structural and dynamical components critically depends on the value of Q^*. As shown in Fig. 4a–b, sufficiently small values of λ (e.g., $\lambda \ll \beta$ when $\beta_\Delta = 0$) enable* *contagion dynamics on hypergraphs to be mapped onto equivalent dynamics on projected multi-edge dyadic graphs, thereby allowing decomposition. In contrast, when* $\lambda > 0.2$*, no valid mapping* β *exists, and the decomposition becomes infeasible. A similar condition arises in simplicial complexes, where* $\beta_\Delta = 0$ *determines whether decomposition is attainable. These results highlight a fundamental finding, i.e., the existence of* Q^* *is not guaranteed universally but is restricted to specific parameter regimes. Consequently, the applicability of our framework depends on whether the underlying dynamics fall within these regimes. This observation underscores the importance of* Q^* *not only as a technical requirement, but also as a critical criterion delineating when higher-order contagion processes can, or cannot, be faithfully reduced to lower-order representations.*

2.3 In higher-order contagion on hypergraphs the coefficient λ is usually constant [A], while here the authors consider λ to depend on m and X, to make the model easier to be reduced to the simplicial or pairwise case. What is the meaning of this dependence? Is this necessary to obtain Q^*? For example, the nonlinearities can be removed also considering v=1.

[A] St-Onge, G., Iacopini, I., Latora, V. et al. Influential groups for seeding and sustaining nonlinear contagion in heterogeneous hypergraphs. Commun Phys 5, 25 (2022).

Reply: We thank the reviewer for raising this important point. We would like to clarify that λ does not functionally depend on m or χ. Rather, it represents a constant infection rate, which may be assigned with different values under different settings of m and χ to enable meaningful comparisons across distinct dynamical processes. In other words, within each specific scenario defined by m and χ, λ is fixed, serving as a reference to indicate whether a higher-order contagion process can be consistently mapped onto another dynamical process. This clarification has been explicitly added in Section 2.1. Detailed descriptions are as follows:

Page 5, Section 2.1:

Here, λ *does not functionally depend on* m *or* χ*; rather, it represents a constant infection rate that may assume different values under different settings of* m *and* χ *to facilitate meaningful comparisons across distinct dynamical processes.*

Furthermore, as correctly noted, the nonlinearities in our model can be removed by setting $\nu = 1$. Our formulation naturally encompasses this linear case as a special instance, highlighting that the introduced dependence of λ on scenario parameters does not preclude simpler dynamics. The revised description is as follows:

Page 5, Section 2.1:

We note that the proposed formulation is flexible, the case $\nu = 1$ corresponds merely to the linear limit, serving as a special instance within this general framework.

3.1 There are several problems of notation and errors: I will list here the main ones, but there are much more. In Eq. (1): what are h and A? Shouldn't the second term depend on i? The product Π on X considers all possible number of infected in the hyperedge, instead of considering the true number of infected nodes in the group at time t, and this is incorrect; similarly, the product Π on m is incorrect; the product Π should be unique and on all hyperedges in which the node i is involved.

Reply: We sincerely thank the reviewer for these comments. We have carefully addressed each point in this revision.

Firstly, we have clarified the definitions of h and A_h^m in both Eq. 1 and Eq. 10 in the Methods section. Specifically, h denotes each hyperedge adjacent to the *S*-state node i, while A_h^m represents the m-th order adjacency tensor, which encodes the presence of m-node hyperedges. In the revised manuscript, we have explicitly provided these definitions as:

Pages 13-14, Section 4.2.1:

The infection probability across each neighboring hyperedge is contingent upon the quantity of I-state nodes present, which can be articulated through the propagation rate $\lambda \cdot \chi^{\nu}$ [54], where λ and ν are adjustable parameters, and $\chi = \chi_h(t)$ denotes the number of I-state nodes in each hyperedge h $(h \in \mathcal{E}_i)$ adjacent to the S-state node i at time step t, where $\mathcal{E}_i$ is the set of hyperedges incident to node i. This quantity can be written as $\chi_h(t) = \sum_{j\in h,\, j\neq i} I_{\{j\in I(t)\}}$, where $I_{\{\cdot\}}$ is the indicator function.

In a hypergraph, the m-th order adjacency tensor A_h^m encodes the presence of m-node hyperedges. Specifically, for a given node i, we denote the set of nodes involved as $J = \{i, j_1, j_2, \dots, j_{m-1}\}$. The tensor entry is defined as:

$$A_h^m = \begin{cases} 1, & if\, J \in E \text{ and } |J| = m \\ 0, & otherwise \end{cases}, \tag{11}$$

where E denotes the set of hyperedges. The maximum order of A_h^m corresponds to the largest hyperedge size in the hypergraph, formally given by $M = \max_{h\in E}|h|$.

Page 5, Section 2.1:

Here, h denotes a hyperedge incident to the S-state node i, A_h^m is the m-th order adjacency tensor, encoding the presence of hyperedges of size m, and M denotes the maximum hyperedge size, see Methods section for details.

Secondly, we have clarified the definition of χ, and accordingly reformulated the product. We define the χ as $\chi = \chi_h(t)$, which denotes the number of *I*-state nodes in each hyperedge $h\,(h \in \mathcal{E}_i)$ adjacent to the *S*-state node i at time step t, where $\mathcal{E}_i$ is the set of hyperedges incident to node i. Such quantity is expressed as $\chi_h(t) = \sum_{j\in h,\, j\neq i} I_{\{j\in I(t)\}}$, where $I_{\{\cdot\}}$ is the indicator function. The details are revised in the Methods section as follows:

Page 13, Section 4.2.1:

The infection probability across each neighboring hyperedge is contingent upon the quantity of I-state nodes present, which can be articulated through the propagation rate $\lambda \cdot \chi^{\nu}$ [54], where λ and ν are adjustable parameters, and $\chi = \chi_h(t)$ denotes the number of I-state nodes in each hyperedge $h\,(h \in \mathcal{E}_i)$ adjacent to the S-state node i at time step t, where $\mathcal{E}_i$ is the set of hyperedges incident to node i. This quantity can be written as $\chi_h(t) = \sum_{j\in h,\, j\neq i} I_{\{j\in I(t)\}}$, where $I_{\{\cdot\}}$ is the indicator function.

Page 13, Section 4.2.2:

$$P_{\mathcal{H}}^{i}(t) = 1 - \prod_{m=2}^{M} \prod_{h\in\mathcal{E}_i, |h|=m} \left(1 - \lambda \cdot \left(\chi_h(t)\right)^{\nu} \cdot A_h^m\right) \tag{10}$$

Pages 13-14, Section 4.2.2:

In a hypergraph, the m-th order adjacency tensor A_h^m encodes the presence of m-node hyperedges. Specifically, for a given node i, we denote the set of nodes involved as $J = \{i, j_1, j_2, \dots, j_{m-1}\}$. The tensor entry is defined as:

$$A_h^m = \begin{cases} 1, & \text{if } J \in E \text{ and } |J| = m \\ 0, & \text{otherwise} \end{cases}, \tag{11}$$

where E denotes the set of hyperedges. The maximum order of A_h^m corresponds to the largest hyperedge size in the hypergraph, formally given by $M = \max_{h\in E} |h|$.

Additionally, we have revised Eq. 1 in Section 2.1 and supplemented it with clarifying descriptions. The updated equation now reads as follows:

Page 5, Section 2.1:

For the contagion dynamics on hypergraphs, we isolate the effects of higher-order interactions by defining $\lambda \cdot \chi^{\nu}$ as the infection rate within an m-sized hyperedge containing χ nodes in the infected (I) state [41], see Methods. Here, λ does not functionally depend on m or χ; rather, it represents a constant infection rate that may assume different values under different settings of m and χ to facilitate meaningful comparisons across distinct dynamical processes. Accordingly, the infection probability of a susceptible node i under SI model in $\mathcal{H}$, denoted as $P_{\mathcal{H}}^{i}(t)$, can be refined as follows:

$$P_{\mathcal{H}}^{i}(t) = 1 - \prod_{m=2}^{M} \prod_{h \in \mathcal{E}_i, |h|=m} \left(1 - \lambda_{m,\chi} \cdot \chi^{\nu} \cdot A_h^m\right). \tag{1}$$

Here, h denotes a hyperedge incident to the S-state node i, A_h^m is the m-th order adjacency tensor, encoding the presence of hyperedges of size m, and M denotes the maximum hyperedge size, see Methods section for details.

Finally, since Eq. 1 and Eq. 10 have been modified in the main text, we have updated the Eq. 18 (now Eq. 17 in Supplementary Note 4), as detailed in following description.

Page 6, Supplementary Note 4:

$$P_{\mathcal{H}}^{i}(t) = 1 - \prod_{m=2}^{M} \prod_{h \in \mathcal{E}_i, |h|=m} \left(1 - \lambda_{m,\chi}^{\kappa} \cdot \chi^{\nu} \cdot A_h^m\right). \tag{17}$$

3.2 Furthermore, the mapping ratio k is introduced without explaining what it is.

Reply: We sincerely thank the reviewer for this comment. To clarify the definition of mapping ratio κ, we have added detailed descriptions in the main text, which now reads:

Page 5, Section 2.1:

We then determine the transformable conditions and show that the SI process on any hypergraph, with hyperedges of arbitrary size m and an arbitrary mapping ratio κ, where restricts hyperedges larger than $\kappa+1$ to subsets of size at most $\kappa+1$, and yields a κ-simplicial complex with $max\{\delta\} = \kappa$ (see Methods for details), can be consistent with contagion process on the simplicial complex representation.

3.3 Similarly, i is used as a node index, but then in Eq. (2,3) it is used as an index of the summation.

Reply: We sincerely thank the reviewer for this comment. To resolve the ambiguity arising from the double use of the notation i, we have replaced the i used as the index in the original summation with the notation a throughout both the main text and the Supplementary Information. Additionally, we have identified a similar ambiguity with the notation j, which has been replaced by the notation b. The details of the modifications are as follows.

Page 5, Section 2.1:

$$\lambda_{m,\chi}^{\kappa} = \frac{1}{\chi^{\nu}} \sum_{a=\tau}^{\tau^*} \binom{\chi}{a} \binom{m-\chi-1}{\kappa-a} \sum_{b=1}^{a} \binom{a}{b} \beta_b. \tag{2}$$

Page 5, Section 2.1:

$$\lambda_{m,\chi}^{\kappa} = \frac{1}{\chi^{\nu}} \sum_{a=\tau}^{\tau^*} a \cdot \binom{\chi}{a} \binom{m-\chi-1}{\kappa-a} \beta. \tag{3}$$

Page 14, Section 4.2.3:

$$\lambda_{m,\chi}^{\kappa} \cdot \chi^{\nu} = \sum_{a=max(1,\kappa+1-(m-\chi))}^{min(\kappa,\chi)} \binom{\chi}{a} \binom{m-\chi-1}{\kappa-a} \sum_{b=1}^{a} \binom{a}{b} \beta_b. \tag{14}$$

$$\lambda_{m,\chi}^{\kappa} \cdot \chi^{\nu} = \sum_{a=1}^{\chi} \binom{\chi}{a} \beta_a. \tag{15}$$

$$\lambda_{m,\chi}^{\kappa} = \frac{1}{\chi^{\nu}} \sum_{a=\tau}^{\tau^*} \binom{\chi}{a} \binom{m-\chi-1}{\kappa-a} \sum_{b=1}^{a} \binom{a}{b} \beta_b. \tag{16}$$

$$\lambda_{m,\chi}^{\kappa} = \frac{1}{\chi^{\nu}} \sum_{a=\tau}^{\tau^*} a \cdot \binom{\chi}{a} \binom{m-\chi-1}{\kappa-a} \beta. \tag{17}$$

Pages 6-7, Supplementary Note 4:

$$\sum_{b=1}^{a} \binom{a}{b} \beta_b. \tag{18}$$

$$\lambda_{m,\chi}^{\kappa} \cdot \chi^{\nu} = \sum_{a=max(1,\kappa+1-(m-\chi))}^{min(\kappa,\chi)} \binom{\chi}{a} \binom{m-\chi-1}{\kappa-a} \sum_{b=1}^{a} \binom{a}{b} \beta_b. \tag{19}$$

$$\lambda_{m,\chi}^{\kappa} \cdot \chi^{\nu} = \sum_{a=1}^{\chi} \binom{\chi}{a} \beta_a. \tag{20}$$

$$\lambda_{m,\chi}^{\kappa} = \frac{1}{\chi^{\nu}} \left[\begin{array}{c} \mathbb{I}_{\kappa<m} \cdot \sum_{a=max(1,\kappa+1-(m-\chi))}^{min(\kappa,\chi)} \binom{\chi}{a} \binom{m-\chi-1}{\kappa-a} \sum_{b=1}^{a} \binom{a}{b} \beta_b \\ + \mathbb{I}_{\kappa>=m} \cdot \sum_{a=1}^{\chi} \binom{\chi}{a} \beta_a] \end{array} \right] \tag{21}$$

$$\lambda_{m,\chi}^{\kappa} = \frac{1}{\chi^{\nu}} \sum_{a=\tau}^{\tau^*} \binom{\chi}{a} \binom{m-\chi-1}{\kappa-a} \sum_{b=1}^{a} \binom{a}{b} \beta_b. \tag{22}$$

$$\lambda_{m,\chi}^{\kappa} = \frac{1}{\chi^{\nu}} \sum_{a=\tau}^{\tau^*} a \cdot \binom{\chi}{a} \binom{m-\chi-1}{\kappa-a} \beta. \tag{23}$$

3.4 Eq. (8) in the Methods is different from the corresponding one in the main text (Eq. (1)) and still is incorrect.

Reply: We are grateful to the reviewer for pointing this out. As described above, we have revised the original Eq. 8 (now Eq. 10 in the updated manuscript) and have added additional clarifying descriptions to improve readability.

3.5 In Eqs. (9,10), the variable I(t) is indicated with and without subscripts.

Reply: We thank the reviewer for this comment. Regarding the confusing subscripts in Eqs. 9 and 10 (now Eqs. 12-13 in the revised manuscript), we have carefully modified and clarified the notation. In particular, the previously ambiguous subscripts in Eq. 13 have been corrected to properly indicate the power (exponent) values. The updated expression now reads as follows:

Page 14, Section 4.2.2:

$$\frac{dI_{\mathcal{C}}(t)}{dt} = \sum_{\delta=1}^{max|u|,u\in U} (1 - I(t)) \cdot \langle k_\delta^* \rangle \cdot \beta_\delta \cdot (I(t))^\delta. \tag{13}$$

3.6 In the SI: in Eq. (1) there is a summation over i but then i does not appear, and the meaning of Δ is not indicated. In Eq. (2) the notation of the summation is incorrect. Furthermore, Eqs. (4,5) are not consistent with Eqs. (1,2) when obtaining Eq.(5) from Eq. (4).

Reply: We sincerely thank the reviewer for this comment. In the Supplementary Information, we have revised Eqs. 1-2 and their corresponding descriptions, and now the Eqs. 4-5 are consistent with Eqs. 1-2 in deriving Eq. 5 from Eq. 4. The updated versions are presented as follows:

Page 4, Supplementary Note 2:

$$\Gamma_i^{tri}(t) = \beta I_{j_1}(t) + \beta I_{j_2}(t) + \beta_\Delta I_{j_1}(t) \cdot I_{j_2}(t), \tag{1}$$

$$\Gamma_i^{\mathrm{bi}}(t) = \beta I_{j_3}(t). \tag{2}$$

Here, nodes j_1 and j_2 denote the other two nodes forming the 2-simplex (triangle) with node i, while j_3 is a neighboring node connected to i by a binary link. The terms $I_{j_1}(t)$, $I_{j_2}(t)$ and $I_{j_3}(t)$ represent the infection probabilities of these neighbors at time t. The parameter β is the transmission rate for pairwise interactions, while β_Δ captures the enhanced transmission due to simultaneous exposure within a 2-simplex, reflecting higher-order group effects.

3.7 In Eq.(11) <Θ> is not defined.

Reply: We sincerely thank the reviewer for this comment. Additionally, we have added a description to clarify the meaning of $\langle\Theta\rangle$, which has been updated to:

Page 4, Supplementary Note 2:

Here, $\langle\Theta\rangle$ quantifies the average reduction in effective edges when collapsing the multi-edge graph $\tilde{\Upsilon}$ into the ordinary graph $\hat{\Upsilon}$ by merging redundant edges. This correction term accounts for the diminished transmission capacity due to edge de-duplication, reflecting that some transmission pathways are no longer independent in the ordinary graph.

3.8. In Eq. (18) the subscripts of λ are missing, the product on h disappears but the index remains and again a product on X is introduced, even if X is fixed.

Reply: We sincerely thank the reviewer for this comment. As we have updated the Eq.1 and Eq. 10 in the main text, we have also revised both the corresponding descriptions of λ in Supplementary Information and the equation (previously Eq. 18, now Eq. 17 in the Supplementary Note 4). The details of these revisions are as follows.

Page 6, Supplementary Note 4:

We isolate the effects of hyperedge sizes m, the number of infected nodes χ, and the mapping ratio κ. Accordingly, the formula of $P_{\mathcal{H}}^{i}(t)$ in the main text can be updated as follows:

$$P_{\mathcal{H}}^{i}(t) = 1 - \prod_{m=2}^{M} \prod_{h\in\mathcal{E}_i, |h|=m} \left(1 - \lambda_{m,\chi}^{\kappa} \cdot \chi^{\nu} \cdot A_h^m\right), \tag{17}$$

where M represents the maximum observed value of m.

4.1 It is important to describe also in the main text the higher-order generalization of the opinion dynamics introduced, given that numerous possible versions exist (moreover, the higher-order version of the Voter model is not presented anywhere).

Reply: Thank you for your suggestion. Firstly, we have added detailed descriptions of the higher-order generalizations of both the DW model and the Voter model in the main text. Specifically, these descriptions are now included in Section 2.3 as well as in the Methods section, as detailed below:

Page 9, Section 2.3:

We then extend both the two dynamic models in hypergraphs, as detailed in the Methods section. Specifically, in the proposed DW model, the tolerance parameter is linked to the influence of commonly shared groups; accordingly, the update rule is *formulated as* $\frac{1}{\sum_s |h_s|^{\alpha}}\left(o_i - o_j\right)^2 \le \epsilon, (i,j) \in h_s$. *Here, where* $|h_s|$ *denotes the size of hyperedge* h_s, *i.e., the number of nodes it contains.*

Physically, α *is an adjustable parameter controlling the nonlinear scaling of influence from neighboring hyperedges on opinion updates. It modulates how the size of these hyperedges affects their contribution, with its value capturing diminishing or amplifying effects of group size on opinion dynamics. Additionally, we design a multivariate Voter model sharing the consistent bound criterion as the extended DW model to test the persistence of observed phenomena under a distinct update mechanism: while the DW process features continuous mutual convergence, the Voter process involves discrete state adoption without averaging (see Method for details).*

Page 15, Section 4.2.5:

For the Voter model, we further design a multivariate variant with the consistent bound criterion as in our extended DW model [44, 45]. The purpose is to examine whether the phenomena observed in the DW dynamics persist under a fundamentally different update mechanism. Although the confidence bound is identical, the two models differ markedly in their microdynamics: in the DW process, interacting nodes adjust their opinions by mutual convergence in a continuous space, whereas in the Voter process, a node directly adopts the discrete opinion state of a neighbor without any averaging. Such differences can substantially alter convergence speed, consensus probability, and the structure of the final opinion distribution, meaning that consistency of results across both models is not a priori guaranteed. Unlike the DW model, the opinion values of individuals in the Voter model are multivariate and discontinuous. Specifically, in this model, each agent i *holds a discrete multivariate opinion value.*

$$o_i(t) = \{1,2,\cdots,\mathcal{Y}\}, \tag{19}$$

where $\mathcal{Y}$ *denotes the opinion multivariate types. Here, in our experiments, we set* $\mathcal{Y} = 10$.

The update rule of the proposed Voter model is as follows: (i) At each time step t, *a node* i *is chosen uniformly at random. (ii) A neighbor* j *is selected from* i*'s adjacency set. (iii) If the confidence condition of Eq. 18 is satisfied (where* ϵ *is the confidence bound), then:*

$$o_i(t+1) = o_j(t). \tag{20}$$

Otherwise, the state remains unchanged, i.e., $o_i(t+1) = o_i(t)$. *This rule differs fundamentally from the proposed DW model, in which opinions are continuous and updated via averaging within a confidence bound. Our discrete, multivariate formulation captures higher-order opinion interactions more faithfully while preserving the stochastic nature of the Voter process.*

4.2 Also, the conditions for Q^* in the two opinion dynamics processes should be provided (analogously to the contagion processes) and more details on how the system instability is evaluated.

Reply: Thanks for your suggestion. We have added detailed descriptions of the conditions for Q^* in the two opinion dynamics processes, as well as an explanation of how system disorder (previously referred to as system instability) is evaluated. These additions now read as follows:

Page 10, Section 2.3:

In the two opinion dynamics, the value of Q equals α in general, with the special case that when $\alpha = 1$ (α_1) it coincides with the reference value Q^*, all taking the value unity. This relationship can be compactly expressed using an indicator function $I_{\{\cdot\}}$ that returns 1 if the condition in the subscript is satisfied and 0 otherwise:

$$Q = \alpha + (1-\alpha)\mathbb{I}_{\alpha=1}, \tag{7}$$

where $Q^* = 1$ in this context.

Page 10, Section 2.3:

Then, the system disorder is quantified by the variance of opinion values across all nodes at time t. Specifically,

$$\Phi(t) = \frac{1}{N}\sum_{i=1}^{N}\left(o_i(t) - \bar{o}(t)\right)^2, \tag{6}$$

where N is the total number of nodes, $o_i(t)$ denotes the opinion of node i at time t, and $\bar{o}(t) = \frac{1}{N}\sum_{i=1}^{N} o_i(t)$ is the mean opinion at time t. A larger value of $\Phi(t)$ indicates greater dispersion of opinions, which corresponds to higher system disorder.

4.3 Moreover, no references have been cited for the higher-order DW generalization considered, whose mechanisms seem not being fully higher-order since they correspond to considering a tolerance based on the link weights. Truly higher-order DW generalizations are proposed in [B,C]: the authors should consider these cases.

[B] Schawe, H., Hernández, L. Higher order interactions destroy phase transitions in Deffuant opinion dynamics model. Commun Phys 5, 32 (2022).

[C] Hickok, A., et al. A bounded-confidence model of opinion dynamics on hypergraphs. SIAM Journal on Applied Dynamical Systems 21.1 (2022): 1-32.

Reply: Thanks for your suggestion. We have first cited prior work that serves as the basis for our higher-order DW generalization.

Page 15, Section 4.2.5:

In the Deffuant-Weisbuch (DW) model [42, 43] on graphs involving multiple edges, *the influence of these edges is incorporated such that a greater number of repeated edges η between two nodes leads to a reduced opinion gap, expressed as* $\frac{1}{\eta} \cdot \left(o_i - o_j\right)^2 \leq \epsilon$.

We then sincerely thank the reviewer for providing the references [B, C] on fully higher-order generalizations of the DW model. Following your suggestion, we have carefully analyzed the two opinion dynamics presented in [B, C]. In these models, at each iteration a hyperedge is randomly selected, and if the opinion differences among its nodes are below a tolerance threshold, all nodes adopt the hyperedge's average state. Hereafter, we refer to these models as the group-updated DW (GDW) model.

Given the central role of Q^* in our proposed scheme, we further examined its existence in these GDW opinion dynamics by investigating how hypergraph-based dynamics can be projected onto multigraphs, where each edge update follows a linear increment inversely proportional to its edge weight. Our analysis reveals several fundamental challenges in directly mapping the GDW model to the multigraph DW: (i) the expected increment for each node pair does not align with that of the multigraph DW, particularly when nodes participate in multiple hyperedges; and (ii) the tolerance condition in GDW is evaluated over the entire hyperedge (e.g., maximal opinion difference), making it inherently higher-order and incompatible with the pairwise threshold used in the multigraph.

To discuss these points, we have included a discussion of the limitations of our work in the Discussion, citing the suggested references [B,C] ([40] and [46] in the revised manuscript). We explicitly discuss the existence of Q^* and provide the key principles that a hypergraph opinion dynamics model should satisfy to ensure the effectiveness of our scheme. In addition, we discuss future directions for applying the scheme to diverse hypergraph-based opinion dynamics and highlight promising avenues for further research. The added descriptions are presented as follows:

Page 12, Section 3:

Moreover, our proposed scheme relies on the existence of Q^*, which may not be guaranteed for all higher-order processes, such as the group-updated DW (GDW) model [40, 46]. This is due to fundamental differences in the update mechanisms: the expected increment for each node pair often deviates from that in the corresponding multigraph, and the tolerance condition is evaluated across all nodes in a hyperedge (e.g., maximal opinion difference), making it inherently a higher-order criterion that cannot be reduced to a simple pairwise threshold in the multigraph. Nevertheless, the statistical behavior of hypergraph-based dynamics can be brought close to that of multigraph dynamics under a set of macro-level conditions. These include decomposing *hyperedge updates into pairwise linear increments scaled by edge weights, updating randomly selected node pairs rather than all nodes simultaneously, adjusting tolerance thresholds according to hyperedge size or structure, and weighting hyperedge selection probabilities to match their expected contribution to the global variance. While these conditions do not guarantee the strict existence of Q^*, they allow for practical equivalence in ensemble-averaged dynamics. Although we have discussed its potential existence under structural and dynamical decompositions, alternative decomposition schemes could also be explored in future studies to further generalize the applicability of the proposed framework.*

5 The text lacks crucial information on how the numerical simulations of the processes are performed. For example, Fig. 3 caption states that the simulations use numerical integration methods. The numerical integration is used to solve the mean-field equations, right? While how are conducted the numerical simulations?

Reply: We thank the reviewer for pointing out the need for clarification. In the revised manuscript, we have added a more detailed explanation of both the simulation procedure and the mean-field analysis. Specifically, the contagion dynamics are simulated through extensive Monte Carlo realizations, while the mean-field equations are solved by numerically integrating the corresponding system of differential equations using the LSODA algorithm implemented in the function *scipy.integrate.solve_ivp*. For clarity, we have also revised the caption of Fig. 3 (previously Fig. R3 in the original version) accordingly.

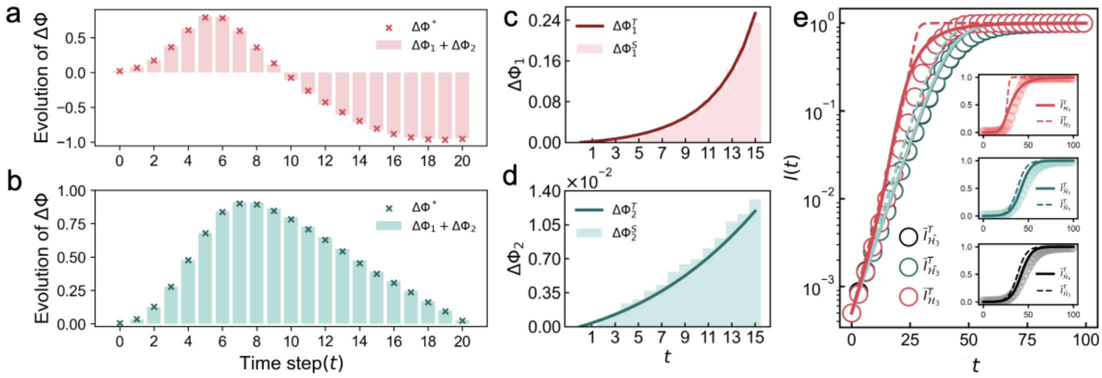

***Fig.R3 (Fig. 3 in the revised main text). Identification and quantification of contributing factors in contagion dynamics. a-b** Temporal evaluation of $\Delta\Phi_1(t) + \Delta\Phi_2(t)$ in SI contagion processes simulated on real-world datasets of primary school and high school interactions. In **a**, $\Delta\Phi_1(t)$ is calculated as $\Delta\Phi_1(t) = \Phi^{Q}(t) - \Phi^{Q^*}(t)$, with $Q(\lambda = 0.005, \nu = 4)$ and $Q^*(\nu = 1)$, where λ satisfies Eq.3 for Q^*. $\Delta\Phi_2(t)$ is derived as $\Phi_{\widetilde{\mathcal{H}}}(t) - \Phi_{\widehat{\mathcal{H}}}(t)$. In **b**, for the simplicial complex $\mathcal{C}$, $\Delta\Phi_1(t)$ is evaluated by setting $Q(\beta_\Delta = 0.9)$ and*

*$Q^*(\beta_\Delta = 0)$, while $\Delta\Phi_2(t)$ is calculated similarly to **a**. The total entropy difference, $\Delta\Phi^*$ (dotted line), closely matches the sum of $\Delta\Phi_1(t)$ (dark-colored bars) and $\Delta\Phi_2(t)$ (light-colored bars) over time. Note that, for clarity, $\Delta\Phi^*$ (scatter points marked with "×") is compared with the sum of $\Delta\Phi_1$ and $\Delta\Phi_2$ (shown as bars). Results are averaged over 500 independent simulations. **c-d** Comparison of theoretical predictions ($\Delta\Phi^T$, solid lines) from the SI model with simulation results ($\Delta\Phi^S$, bars) for $\Delta\Phi_1(t)$ and $\Delta\Phi_2(t)$. Strong agreement is observed between theory and simulation. **e** Comparison of quantitative evaluation of the mean infection density $\bar{I}(t)$ between the original and the refined models. Theoretical predictions $\bar{I}^T(t)$ (solid lines) align closely with simulation results $\bar{I}^S(t)$ (dots), as shown for simplicial complexes $\bar{I}_{\mathcal{H}_3}(t)$, projected multi-edge graphs $\bar{I}_{\widetilde{\mathcal{H}}_3}(t)$, and simple graphs $\bar{I}_{\widehat{\mathcal{H}}_3}(t)$. The inset presents the non-logarithmic results of $\bar{I}(t)$ with error bars. Note that the simplicial complexes utilized here are shown in SSC networks in Supplementary in detail. Simulation of contagion dynamics are over 500 independent Monte Carlo realizations. The mean-field solutions for $\bar{I}_{\mathcal{H}_3}(t)$ are obtained by numerically integrating the corresponding differential equations using the LSODA algorithm.*

6 The caption of Fig. 3 states that ΔΦ^* is compared to the sum of the absolute values of ΔΦ1 and ΔΦ2. However, this is incorrect if compared to the definition provided: the definition adopted should be uniform.

Reply: Thanks for the suggestion. We have corrected this inconsistency in the revised manuscript. Specifically, Figs. 3a and 3b (corresponding to Figs. R3a and R3b in this response) have been updated to ensure that $\Delta\Phi^*$ is consistently compared with the sum of the absolute values of $\Delta\Phi_1$ and $\Delta\Phi_2$, in full accordance with the adopted definition. In addition, the caption of Fig. 3 has been revised to explicitly reflect this correction. The updated description now reads:

Page 6, Section 2.2:

Note that, for clarity, $\Delta\Phi^*$ (scatter points marked with "×") is compared with the sum of $\Delta\Phi_1$ and $\Delta\Phi_2$ (shown as bars).

7 The synthetic networks considered are generated with N=|E|, hence producing an average hyperdegree <D>=2. The network is very sparse, and the overlap of hyperedges is lost, eventually impeding opinion convergence due to the nodes' isolation. Larger values of |E| should be considered.

Reply: Thanks for your suggestion. Following the suggestion, we performed additional experiments to examine the robustness of our proposed scheme under different network densities. Specifically, we generated synthetic hypergraphs with $N = 100$ nodes and varying numbers of hyperedges, $|E| = \{200,300,500,1000\}$, and conducted the corresponding analyses under both DW and Voter process. The results are provided in Fig. 11 and Fig. 12 of Supplementary Note 9 (with Fig. R2-1 and Fig. R2-2 provided above in this response). Our findings confirm that the proposed method remains consistently effective across all tested densities. Moreover, we observe that in denser hypergraphs the relative influence of the dynamical factor becomes more pronounced compared to the structural factor. These results not only address the reviewer's concern regarding the sparsity of the original setting but also provide new insights into the interplay between structural and dynamical contributions. The details of the descriptions are as follows:

Page 19, Supplementary Note 9:

To assess the effectiveness of the proposed scheme in hypergraphs with varying densities, we next evaluate its performance under different network density conditions. To this end, we generate synthetic hypergraphs with $N = 100$ *nodes and different numbers of hyperedges,* $|E| = \{200,300,500,1000\}$*. As shown in Fig. 11 and Fig. 12, the proposed method remains effective across all densities considered. Moreover, we find that in denser hypergraphs the relative contribution of the dynamical factor becomes more pronounced compared to that of the structural factor.*

To improve clarity, we have updated the Supplementary Information by including a detailed description of the new experimental setup (see Supplementary Note 1), which now reads as follows:

Page 2, Supplementary Note 1:

In addition, we construct four synthetic hypergraphs with $N = 100$ *nodes and* $|E| = \{200,300,500,1000\}$ *hyperedges to further assess the performance of the proposed scheme under different network densities.*

Furthermore, in the main text we have incorporated a summary of these findings as follows:

Page 10, Section 2.3:

We further examine the effect of network density on performance (see Supplementary Information). The proposed method remains consistently effective across synthetic hypergraphs of varying densities. Notably, in denser hypergraphs the relative contribution of the dynamical factor becomes more pronounced than that of the structural factor.

8 Some considerations in Supp. Note 4 are incorrect. If a group of size m has X infected and is projected onto simplices with ratio k, with m>k: the maximum number of infected in a generated simplex is not k, since X could be lower than k; the minimum is not k+1-(m-X). For example, in a triangle with 1 infected (m=3, X=1 and k=2): the minimum and maximum according to the authors would be 1 and 2 respectively, but instead there is a simplex of size 2 with 0 infected and the maximum is 1.

Reply: We sincerely thank the reviewer for pointing out this inaccuracy. We have carefully revised Supplementary Note 4 to provide a more precise and consistent description. In particular, we have corrected the expressions for the minimum and maximum numbers of infected nodes in the case of $m > \kappa$. The revised text in the Supplementary Note now reads:

Page 6, Supplementary Note 4:

In the case where $\kappa < m$, the m-sized hyperedge should first be mapped to κ-simplices. Let χ represent the number of infected nodes within the hyperedge. The minimum number of infected nodes in the mapped κ-simplices is given by $max\big(1, \kappa + 1 - (m - \chi)\big)$, and the maximum number is $min(\kappa, \chi)$. For a susceptible (S-state) node i in the hyperedge, we must select an additional κ nodes to complete the κ-simplex. Given that a infected nodes have already been chosen from the hyperedge, the remaining task is to select $\kappa - a$ susceptible nodes from the remaining $m - 1 - \chi$ susceptible nodes in the hyperedge.

For clarity, we have also explicitly included the corresponding expressions in Eq. 20 of the Supplementary Note 4. The revised form is given as:

Page 6, Supplementary Note 4:

$$\lambda_{m,\chi}^{\kappa} \cdot \chi^{\nu} = \sum_{a=max\left(1,\kappa+1-(m-\chi)\right)}^{min(\kappa,\chi)} \binom{\chi}{a}\binom{m-\chi-1}{\kappa-a}\sum_{b=1}^{a}\binom{a}{b}\beta_b. \tag{19}$$

As a concrete example, in the case of a triangle with one infected node ($m = 3$, $\chi = 1$ and $\kappa = 2$), the corrected formulation yields a maximum of 1, which is fully consistent with the reviewer's observation.

9 In Supp. Note 6, the authors consider the specific case of contagion on simplicial complexes: similar results should be shown for hypergraphs and the other processes. Moreover, in Supp. Note 7, the authors discuss heterogeneous mean-field equations but do not present them: they should be reported.

Reply: Thanks for the suggestion. We have updated previous Supplementary Note 6 (now Supplementary Note 7) to include the demonstration of the two underlying factors governing the transformation of dynamics for hypergraphs. Specifically, we provide the rate equations describing the evolution of the infected population in both hypergraph contagion dynamics and in the corresponding projected multi-edge graphs. We show that, when $Q = Q^*$, these two descriptions are equivalent, allowing the transformation to be decomposed into two distinct contributions: structural and dynamical impacts. The revisions made on pages 10–11 of Supplementary Note 7 are summarized below.

Pages 10-11, Supplementary Note 7:

We then focus on the hypergraphs, a canonical representation of higher-order network structures. In close analogy to the formulation on simplicial complexes, the problem can be reformulated as follows:

$$\frac{dI_{\mathcal{H}}^{Q}(t)}{dt} - \frac{dI_{\mathcal{H}}^{Q^*}(t)}{dt} + \frac{dI_{\widetilde{\mathcal{H}}}(t)}{dt} - \frac{dI_{\widehat{\mathcal{H}}}(t)}{dt} = \frac{dI_{\mathcal{H}}^{Q}(t)}{dt} - \frac{dI_{\widehat{\mathcal{H}}}(t)}{dt}. \tag{39}$$

We consider a node i that, on average, is incident to $\langle k_{e_3}\rangle$ three-body hyperedges and $\langle k_{e_2}\rangle$ pairwise hyperedges under the condition $\kappa = 2$. Within this setting, the rate equation governing the evolution of the infected population in the hypergraph contagion dynamics can be written as:

$$\frac{dI_{\mathcal{H}}^{Q}(t)}{dt} = \big(1 - I(t)\big) \cdot \begin{bmatrix} \langle k_{e_3}\rangle \cdot \left(\lambda_{3,1}^{2} \cdot 1^{\nu} \cdot 2I(t) \cdot \big(1 - I(t)\big) + \lambda_{3,2}^{2} \cdot 2^{\nu} \cdot (I(t))^2\right) \\ +\langle k_{e_2}\rangle \cdot \lambda_{2,1}^{2} \cdot 1^{\nu} I(t) \end{bmatrix}. \tag{40}$$

Here, for a three-body hyperedge containing a single infected node, the transmission probability is given by $2I(t) \cdot \big(1 - I(t)\big)$, and the corresponding contribution takes the form $\lambda_{3,1}^{2} \cdot 1^{\nu} \cdot 2I(t) \cdot ((1 - I(t))$. Conversely, when the hyperedge contains two infected nodes, the transmission probability becomes $(I(t))^2$, yielding a contribution of $\lambda_{3,2}^{2} \cdot 2^{\nu} \cdot (I(t))^2$.

Building on this formulation, we next examine the relationship between $\frac{dI_{\widehat{\mathcal{H}}}(t)}{dt}$ and $\frac{dI_{\mathcal{H}}^{Q^*}(t)}{dt}$. For $\frac{dI_{\widehat{\mathcal{H}}}(t)}{dt}$, we adopt a mean-field description of the corresponding multi-edge dyadic graph. Assuming an infection rate β on this graph, the expression for $\frac{dI_{\widehat{\mathcal{H}}}(t)}{dt}$, analogous to Eq. 10, can be expressed as:

$$\frac{dI_{\widetilde{\mathcal{H}}}(t)}{dt} = \big(1 - I(t)\big) \cdot \big(\langle k_{e_2}\rangle + 2\langle k_{e_3}\rangle\big) \cdot \beta I(t). \tag{42}$$

We proceed to evaluate $\frac{dI_{\mathcal{H}}^{Q^*}(t)}{dt}$. In the case where $Q = Q^*$, the parameters satisfy $\lambda_{2,1}^{2} = \beta$, $\lambda_{3,1}^{3} = \beta/1^{\nu}$, and $\lambda_{3,2}^{3} = 2\beta/2^{\nu}$. Under these assignments, $\frac{dI_{\mathcal{H}}^{Q^*}(t)}{dt}$ follows directly from Eq. 41, and can be formulated as:

$$\frac{dI_{\mathcal{H}}^{Q^*}(t)}{dt}$$
$$= (1 - I(t)) \cdot \left[\langle k_{e_3}\rangle \cdot \left(\lambda_{3,1}^2 \cdot 1^\nu \cdot 2I(t) \cdot (1 - I(t)) + \lambda_{3,2}^2 \cdot 2^\nu \cdot (I(t))^2\right) + \langle k_{e_2}\rangle \cdot \lambda_{2,1}^2 \cdot 1^\nu I(t)\right]$$
$$= (1 - I(t)) \cdot \left[\langle k_{e_3}\rangle \cdot \left(\frac{1}{1^\nu}\beta \cdot 1^\nu \cdot 2I(t) \cdot (1 - I(t)) + \frac{1}{2^\nu}2\beta \cdot 2^\nu \cdot (I(t))^2\right) + \langle k_{e_2}\rangle \cdot \beta \cdot 1^\nu I(t)\right]$$
$$= (1 - I(t)) \cdot \left[\langle k_{e_3}\rangle \cdot \left(2\beta I(t) \cdot (1 - I(t)) + 2\beta \cdot (I(t))^2\right) + \langle k_{e_2}\rangle \cdot \beta I(t)\right]$$
$$= (1 - I(t)) \cdot \left[\langle k_{e_3}\rangle \cdot 2\beta I(t) + \langle k_{e_2}\rangle \cdot \beta I(t)\right]$$
$$= (1 - I(t)) \cdot \left[\langle k_{e_3}\rangle \cdot 2 + \langle k_{e_2}\rangle\right] \cdot \beta I(t).$$

(Eqs. 43-48)

We observe that $\frac{dI_{\mathcal{H}}^{Q^*}(t)}{dt}$ *is equivalent to* $\frac{dI_{\hat{\mathcal{H}}}(t)}{dt}$. *Consequently, within the hypergraph contagion framework, it follows that the quantity* ΔI^* *is equivalent to the sum of* ΔI_1 *and* ΔI_2.

In addition, we have revised previous Supplementary Note 7 (now Supplementary Note 8) to explicitly present the heterogeneous mean-field equations used in our study. Specifically, we have now: (i) Introduced the formulation of the heterogeneous mean-field approach that incorporates the actual degree k_i and 2-simplex count $k_{\Delta,i}$ of each node. (ii) Explained how this approach captures the heterogeneity of node connectivity and its impact on spreading dynamics. (iii) Provided the full set of extended equations governing the infection probability of individual nodes. These revisions provide a clear, self-contained description of our methodology and ensure that the technical details underlying our simulations and theoretical analysis are fully transparent. In the revised version (Supplementary Note 8, page 12), the descriptions have been updated as follows:

Page 12, Supplementary Note 8:

Specifically, we extend the classical mean-field approach by incorporating the actual degree k_i *and 2-simplex count* $k_{\Delta,i}$ *of each node* i, *rather than relying on average degree values. Specifically, the heterogeneous mean-field equation governing the infection probability* $I_i(t)$ *of node* i *reads:*

$$\frac{dI_i}{dt} = \left(1 - I_i(t)\right)\left[k_{\Delta,i}(2\beta I_i(t) + \beta_\Delta (I(t))^2) + k_i \beta I_i(t)\right]. \quad (51)$$

Here, k_i *and* $k_{\Delta,i}$ *denote the number of independent edges and 2-simplexes incident to node* i, *respectively;* β *and* β_Δ *are the infection rates associated with 1-simplex and 2-simplex interactions. This formulation explicitly accounts for the heterogeneity in node connectivity and the nonlinear influence of higher-order structures on the spreading dynamics.*

Minor issues.

1 In the text often the authors use the terms "network dynamics" and "dynamical networks": these terms are misleading because they are generally used to describe temporal networks in which interactions evolve over time. It would be preferable use "dynamics on networks" to avoid misunderstandings. Moreover, the authors discuss the "interplay" of the processes at different orders or the presence of "mutual dependence": I think these terms are misleading since they suggest a coupling of different processes.

Reply: Thank you for the suggestion. We have replaced all instances of "network dynamics" and "dynamical networks" with "dynamics on networks" throughout the manuscript. This revision clarifies that we refer to processes occurring on a fixed network structure, rather than temporal networks with evolving interactions, thereby avoiding potential misunderstandings. The details of these changes are summarized below.

Additionally, to address the concern regarding potentially misleading terms such as "interplay" and "mutual dependence", we have revised these expressions throughout the manuscript. Specifically, we replaced them with more precise terminology (e.g., transformability, mapping) that accurately reflects the focus on the behavior of the dynamics across different network orders, without implying coupling between distinct dynamical processes. Furthermore, explicit definitions of the originally ambiguous terms are provided in the Introduction. The details of these modifications are provided below.

Revisions to "network dynamics"：

Page 1, Abstract:

Recent studies on dynamics on higher-order networks have predominantly focused on intrinsic properties such as bistability and discontinuous phase transitions, while largely overlooking transformability—the ability of dynamics adaptation across different network structures, which fundamentally captures the essence of the dynamical processes.

Focusing on contagion dynamics, we identify and quantify dynamical and structural factors that explain the transformability of dynamics on higher-order networks, uncovering a universal model governed by these factors from the perspective of system disorder.

Characterizing dynamics on networks is pivotal to encoding the evolution of collective behavior [1-3], with contagion dynamics being the most extensively studied due to their wide applications spanning pathogen transmission [4], information diffusion [5, 6], cultural socialization [7], biological reaction [8], etc.

Page 2, Section 1:

Thirdly, these approaches further facilitates the identification of key factors driving the transformability of dynamics on networks, particularly from pairwise to higher-order networks, see Fig. 1c.

Page 2, Section 1:

To the best of our knowledge, this study is the first to offer a comprehensive analysis for the transformability of dynamics on higher-order networks via the lens of system statistical uncertainty.

Page 5, Section 1:

Building on the transformation among dynamics via the infection probability, we further explore factors driving the transformability of dynamics on higher-order networks, particularly focusing on the dynamic transitions between higher-order and pairwise networks.

Page 8, Section 2.2:

Since we have identified and quantified the factors driving the transformability of dynamics on higher-order networks, we extend our analysis to include a broader range of dynamics categories.

Page 11, Section 3:

To conclude, by systematically investigating the transformability of dynamics on higher-order networks, we have shown that structural and dynamical factors are two crucial drivers that account for the transformation of dynamical behaviors between dynamics on higher-order and pairwise networks.

Page 11, Section 3:

These findings provide crucial reflection on the widespread assumption of the necessity of blindly using dynamics on higher-order networks when characterizing real dynamical processes.

Revisions to the term "interplay":

Page 1, Abstract:

Here, we present a holistic analysis framework that bridges the relationships between dynamics in pairwise and higher-order systems, demonstrating that these processes are not independent but can undergo systematic transformations.

Page 2, Caption of Fig.1:

c *The relationship between dynamics on the higher-order network (Υ) and its pairwise counterpart ($\hat{\Upsilon}$).*

e *A unified framework demonstrating the transformation of dynamics across* *different orders ($\Delta\Phi^*$) as governed by the combined contributions of dynamical ($\Delta\Phi_1$) and structural ($\Delta\Phi_2$) factors.*

Page 2, Section 1:

While substantial efforts have been made to understand the dynamics of contagion, ranging from pairwise-based mechanisms to those driven by higher-order interactions [32-34] (see Fig. 1a), these studies have largely overlooked the relationship of dynamical processes across networks of different orders.

Notably, finding such a systematic relationship is fundamental to explain evolutionary principles that govern chaotic dynamics in empirical systems, as well as to uncover driving factors that allow dynamical processes to be viewed through a more nuanced and complex lens [35-37].

Page 4, Caption of Fig.2:

The relationships of dynamics across network representations.

Page 6, Section 2.1:

These results suggest that when the transformable condition between two contagion dynamics becomes more restrictive, the dynamics tend to converge; otherwise, they diverge further, underscoring the complex mapping of dynamics across network orders.

Page 8, Section 2.2:

Through this framework, we disentangle the transformation of dynamics across different network orders into two explicit and additive components}, namely dynamical and structural, thereby enabling the framework's adaptability to a broad range of processes, including contagion and opinion dynamics.

Page 11, Section 3:

Our works has the potential to drive applications across diverse real-world scenarios, as unveiling the transformability of dynamics across diverse network representations is fundamental to explain evolutionary principles that govern chaotic dynamics in empirical systems [37].

Revisions to the term "tranformability", "transformed" and "transformation":

Page 3, Section 1:

In this work, we introduce the concept of transformability, defined as the capability to map contagion dynamics across different network types. When specific conditions are asymptotically approached, the behaviors of dynamics on one network can approximate those on another, a phenomenon we refer to as transformed and the process as transformation.

Revisions to the term "system disorder" (previously referred to as system

instability)：

Page 3, Section 1:

Secondly, the contagion dynamics are governed by the evolution of individual node states (e.g., infection probabilities), which gives rise to disorder at the system level, hereafter referred to as system disorder. To quantify this disorder globally, we employ information entropy, which provides a rigorous measure of the system's statistical uncertainty throughout the process (Fig. 1b).

2.1 In Section 2.3, an α parameter is introduced without specifying its meaning.

Reply: We sincerely thank the reviewer for the comment. Firstly, we have revised Section 2.3 to clarify the extended models for opinion dynamics and to explicitly define the parameter α. In particular, we now describe the extension of both dynamical models on hypergraphs in the Methods section. Specifically, in the proposed DW model, the tolerance parameter is linked to the influence of commonly shared groups (higher-order interactions), with the update rule formulated as:

Page 9, Section 2.3:

We then extend both the two dynamic models in hypergraphs, as detailed in the Methods section. Specifically, in the proposed DW model, the tolerance parameter is linked to the influence of commonly shared groups; accordingly, the update rule is formulated as $\frac{1}{\sum_s |h_s|^\alpha}\left(o_i - o_j\right)^2 \leq \epsilon, (i,j) \in h_s$*. Here, where* $|h_s|$ *denotes the size of hyperedge* h_s*, i.e., the number of nodes it contains.*

Physically, α *is an adjustable parameter controlling the nonlinear scaling of influence from neighboring hyperedges on opinion updates. It modulates how the size of these hyperedges affects their contribution, with its value capturing diminishing or amplifying effects of group size on opinion dynamics. Additionally, we design a multivariate Voter model sharing the consistent bound criterion as the extended DW model to test the persistence of observed phenomena under a distinct update mechanism: while the DW process features continuous mutual convergence, the Voter process involves discrete state adoption without averaging (see Method for details).*

2.2 Moreover, in Fig. 4, which synthetic graph is considered, and for what model parameter values are the simulations conducted?

Reply: We thank the reviewer for this comment. We have clarified in the caption of Fig. R4 (now Fig. 5 in the revised manuscript) that the synthetic hypergraphs were generated using the HyperCL configuration model (with relevant references added in the main text), and we have explicitly specified the parameters used in the simulations.

The revised descriptions and figure are as follows:

Page 10, Section 2.3:

Fig. 5a illustrates the evolution of opinion variance for hypergraphs generated by the HyperCL configuration model [20] and their projected networks, showing a steady decline in opinion dispersion under DW opinion dynamics as node opinions gradually converge with increasing t.

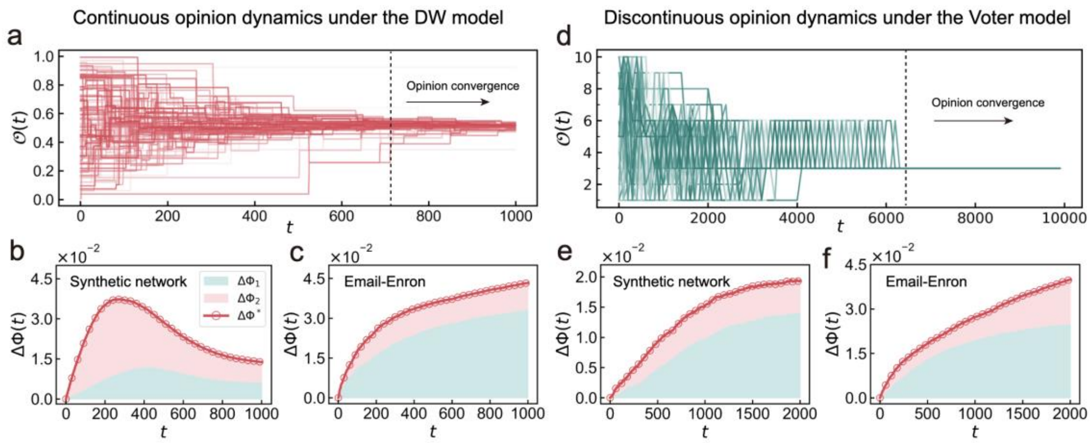

Fig. R4 (Fig. 5 in the revised main text). Validations in DW and Voter opinion dynamics. a *Opinion variations of nodes in* $\mathcal{H}$ *in a simulation of DW model. The initial opinion values are set to follow a uniform distribution. As time progresses, continuous opinions among nodes evolve and eventually converge to a steady state.* ***b-c*** *The relationships among the dynamical uncertainty* $\Delta\Phi_1$*, the structural uncertainty* $\Delta\Phi_2$*, and the total differences of system disorder* ($\Delta\Phi^*$) *underlie the interplay between higher-order and pairwise networks in both synthetic and empirical systems. The bound* c *is set to 0.1 for the synthetic network and 0.003 for the Email-Enron, while the hypergraph DW model parameter* α *is 0.5 and 0.8, respectively. The opinion dynamics are simulated for 1000 time steps.* ***d*** *Opinion variations of nodes in* $\mathcal{H}$ *in a simulation of Voter model. The initial opinion values are distributed uniformly. Over time, discontinuous opinions among nodes evolve and eventually converge to a steady state.* ***e-f*** *The relationships among the dynamical uncertainty* $\Delta\Phi_1$*, the structural uncertainty* $\Delta\Phi_2$*, and the total differences of system disorder* ($\Delta\Phi^*$) *underlie the interplay between higher-order and pairwise networks in both synthetic and empirical systems. We set model parameter* α *to 0.5 in both (e) and (f). The opinion dynamics are simulated for 2000 time steps. Note that the synthetic network in panels (b) and (e), with* $|V| = |E| = 100$*, is generated using HyperCL. Each value of* $\Phi(t)$ *is based on* 10^3 *simulations.*

2.3 In SI Fig. 3, there are inconsistencies between the caption and the plot, in the *colours and descriptions of the panels. Furthermore, what do the colours under the black curves indicate?*

Reply: We sincerely thank the reviewer for this observation. We have updated the caption of Supplementary Fig. 3 to correct inconsistencies in panel colors and descriptions. In addition, we explicitly clarify the meaning of the areas under the curves (i.e., the colored regions beneath the black curves), which highlight the differences between dynamics on higher-order networks and those on their corresponding simple projections. These changes are reflected in the revised figure (Fig. R5).

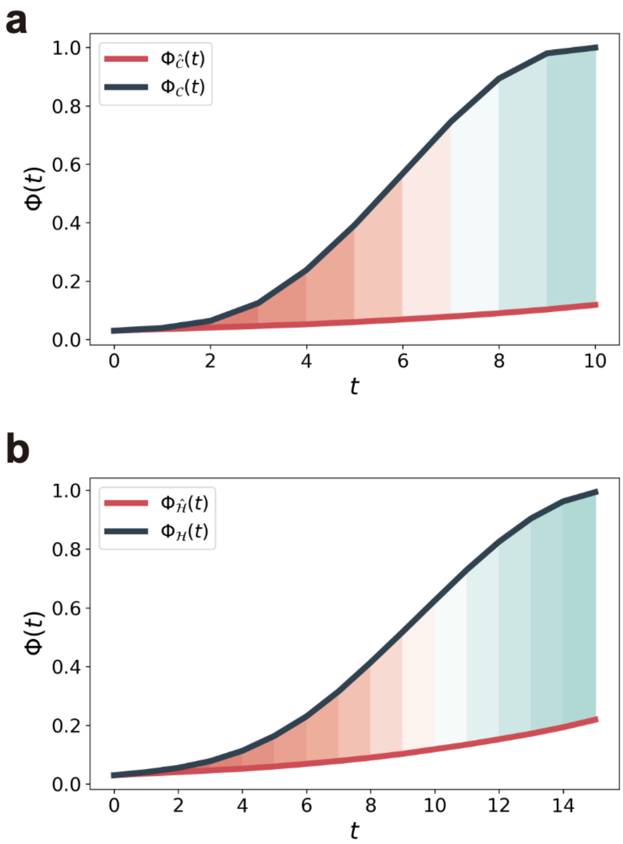

Fig. R5. *Encoding empirical systems with higher-order interactions as dyadic graphs leads to information loss in dynamics. The variance of information entropy Φ during contagion dynamics is analyzed in (**a**) a hypergraph $\mathcal{H}$, (**b**) a simplicial complex $\mathcal{C}$, and their projected simple graphs. Notably, the hypergraph and simplicial complex are derived from real datasets of High-school and Primary-school. As time steps increase, a growing disparity in Φ emerges between dynamics on hypergraphs (black) or simplicial complexes (black) and their projected graphs (red). The shaded area between the black and red curves indicate the variation in entropy change during the dynamics, highlighting the differences between dynamics on higher-order networks and those on their corresponding simple projections. Each time step t represents the average over*

500 simulations of the SI contagion process.

3 In schools datasets, contacts are collected as pairwise interactions. How are the groups defined?

Reply: We thank the reviewer for this question. We have adopted a rigorous definition consistent with the data provider's protocol and widely used in the literature [R1-R2], with references provided in the final section of this response. Specifically, groups are defined as maximal cliques detected within short time windows, which ensures that all individuals in a group are simultaneously interacting and allows the network representation to accurately capture higher-order interactions.

We have updated the manuscript to include a clear definition of group interactions in the school datasets, along with relevant references and information on data availability. The data definition follows the protocol of the data provider and can be accessed at: https://www.cs.cornell.edu/~arb/data/. In the revised version, the data description has been modified as follows:

Page 1, Supplementary Note 1:

The interactions collected by wearable sensors every 20 seconds, aggregating all contacts occurring within each preceding interval. Groups are then defined as maximal cliques detected within these time windows [1].

4 Which configuration model is used? Is the model proposed in [D]?

[D] Iacopini, I., Petri, G., Barrat, A. et al. Simplicial models of social contagion. Nat Commun10, 2485 (2019).

Reply: We thank the reviewer for this question. We have clarified the configuration models used for generating the synthetic networks of hypergraphs and simplicial complexes. Specifically, synthetic simplicial complexes were constructed using the method of [R3] (i.e., [D] provided by the reviewer), while synthetic hypergraphs were generated following the algorithm of [R4]. In addition, Supplementary Note 1 has been updated to reflect these clarifications and provide a detailed description of the construction for all synthetic networks. The relevant modifications are listed below:

Page 2, Supplementary Note 1:

The construction of these synthetic simplicial complexes (referred to as SSC networks) follows a configuration model [4], a widely adopted network generation model in the study of simplicial contagions.

Additionally, we construct a series of hypergraphs to validate our findings in opinion dynamics. These hypergraphs are generated using the HyperCL algorithm [6], with the hyperdegree distribution $\mathcal{P}(k_h) \sim k_h^{-\gamma}$ controlled by the exponent γ [6-8].

Also, in the main text of the manuscript, we highlighted the configuration models for generating different synthetic networks and also provided the related references, details are listed below:

Page 8, Section 2.2:

Here, networks with controlled topologies, including node degrees and 2-simplex degrees, are generated via a configuration model [28].

Page 10, Section 2.3:

Fig. 5a illustrates the evolution of opinion variance for hypergraphs generated by the HyperCL configuration model [20] and their projected networks, showing a steady decline in opinion dispersion under DW opinion dynamics as node opinions gradually converge with increasing t.

5.1 In the SI: Table 2 is unclear because it shows a list of properties but not which network they correspond to: different N and |E|?

Reply: We thank the reviewer for the suggestion. We have revised the caption of Table 2 in Supplementary Note 1 (now presented as Table R1) to clearly indicate the values of N and $|E|$ for each synthetic network. For additional clarity, we have also assigned distinct names to the different synthetic networks, making it explicit which properties correspond to which network.

Furthermore, to improve the clarity of Fig. 2, we have added detailed comments in the figure caption, explaining the unusually high infection rate values (up to 10^{14} and explicitly indicating the values of m and χ on the heatmaps. These modifications ensure that both the table and figure can be interpreted unambiguously.

Table R1 (Table 2 in the revised Supplementary Note 1). *Topological properties of synthetic higher-order networks SSC1–SSC4. $\langle k \rangle$ and $\langle k^* \rangle$ represents the average node degrees with/without excluding binary links contained in simplices. $\langle k_\Delta \rangle$ represents the average number of 2-simplex in the simplicial complex. $\langle C_1 \rangle$ and $\langle C_2 \rangle$ denotes the average clustering coefficient in 1- and 2-hops.*

Synthetic networks	N	$\|E\|$	$\langle k^* \rangle$	$\langle k \rangle$	$\langle k_\Delta \rangle$	$\langle C_1 \rangle$	$\langle C_2 \rangle$
SSC1	100	208	8	10	3	0.2325	0.2020
SSC2	100	256	10	12	4	0.1847	0.1762
SSC3	500	2170	15	10	5	0.2009	0.2020
SSC4	2000	9403	20	4	8	0.0552	0.0516

5.2 Fig. 2 is unclear and more comments should be added to describe it: why the infection rate reach values of 10^14? It would be better to indicate the values of m and X on the heatmaps.

In addition, we have added detailed explanations to clarify Fig. 2 in the Supplementary Information (now shown as Fig. R6). Specifically, we explain that Fig. 2 in the Supplementary Information depicts the combination number obtained from $\mathcal{L}$, which corresponds to the coefficient of β in the mapping from contagion dynamics on hypergraphs to dyadic graphs (i.e., this mapping is quantified by $\mathcal{L}(m, \chi, \kappa) \cdot \beta$). In our figures, the hyperedge size m is considered up to its maximum value of 100. For each hyperedge, we take into account all possible infection numbers ranging from 1 to 100. Due to the combinatorial computation, when m, χ and κ take large values, the coefficient $\mathcal{L}$ can become extremely large, which explains why the infection rate reaches values on the order of 10^{14}.

Moreover, following the reviewer's valuable suggestion, we have updated Figs. 2a–c in Supplementary Note 3 (now presented as Figs. R6a-c) by explicitly indicating the values of m and χ on the heatmaps, which we believe makes the figure clearer and more informative.

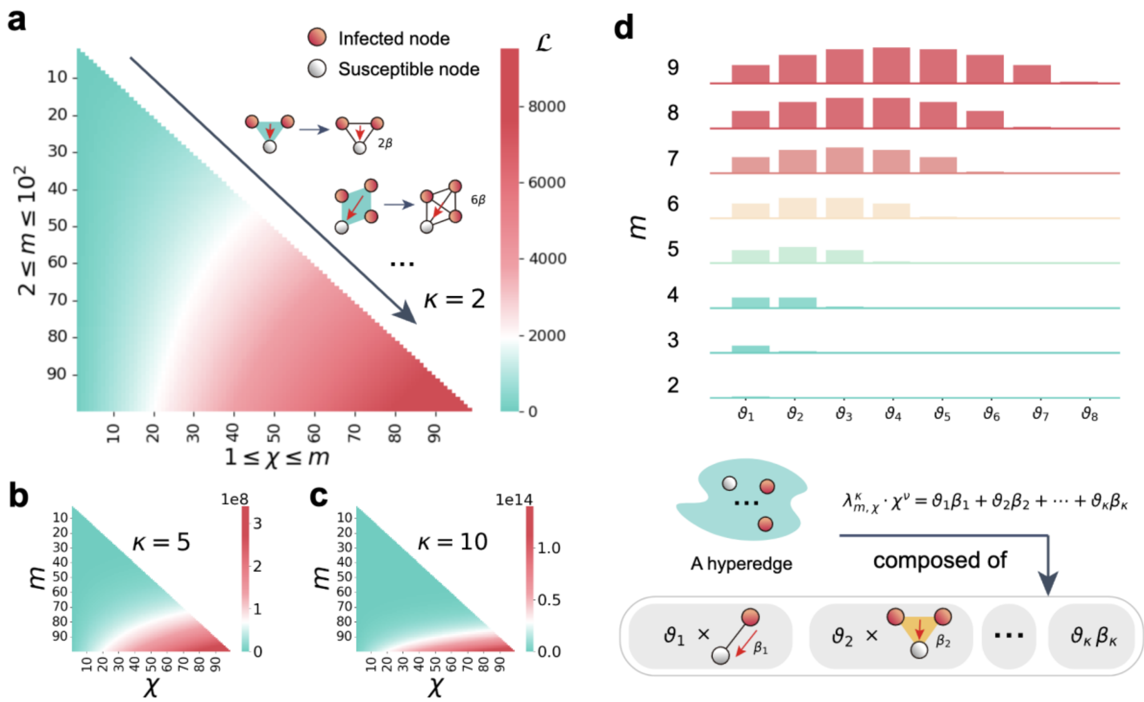

Fig. R6. *Interrelationships among dynamics through infection rates.* ***a*** *Infection rates when contagion on hypergraphs is mapped onto dyadic graphs. This mapping is quantified by the term $\mathcal{L}(m, \chi, \kappa)$, which denotes the infection rate experienced by an S-state node when dynamics within an m-sized hyperedge of the hypergraph are projected onto a dyadic graph. Here, $\mathcal{L}(m, \chi, \kappa) = \sum_{a=\tau}^{\tau^*} a \cdot$*

$\binom{\chi}{a}\binom{m-\chi-1}{\kappa-a}$, derived from C2. $\lambda_{m,\chi}^{\kappa}\cdot\chi^{\nu}$ corresponds to the infection rate in an m-sized hypergraph with mapping ratio κ, containing χ I-state nodes. ***a*** *illustrates the variation of $\mathcal{L}(m,\chi,\kappa=2)$ as m and χ change, while* ***b*** *and* ***c*** *show corresponding results for $\kappa=5$ and $\kappa=10$, respectively. The analysis reveals that as κ increases, χ becomes the dominant factor influencing the infection rate relationship between hypergraph and dyadic graph dynamics, establishing a clear connection between complex and simple contagion processes.* ***d*** *The relationships of infection rates between dynamics on hypergraphs and simplicial complexes. The plot decomposes the contributions from simplices of varying orders within hyperedges of size $m = 2$ to 9, with $\kappa=8$ and $\chi=m-1$. The coefficient ϑ_{δ} quantifies the contribution of a δ-simplex (infection rate β_{δ}) to the S-state node.*

Response to the comments of Reviewer #2

Reviewer #2 (Remarks to the Author):

The article, "Transformability of Higher-order Network Dynamics" explores when hypergraph dynamics can be mapped ("transformed" in the parlance of the article) to pairwise networks, when hypergraph dynamics can be mapped to dynamics on a simplicial complex, and when dynamics on a simplicial complex can be mapped to pairwise network dynamics. The manuscript treats this as a classification problem and determines parameter regimes for which both processes are indistinguishable, and thus, the dynamics are equivalent. The manuscript derives mathematical conditions for when these dynamics are interchangeable and validates these predictions with numerical simulations. Overall, I find this manuscript interesting and potentially valuable to the higher-order and pairwise network science community. Most of my comments on the manuscript are related to its lack of clarity. Some of the mathematical details are not sufficiently described and jargon and inadequately described terminology detracts from the paper's narrative. That being said, I think with an extensive revision, that the paper would be improved greatly, and I would be able to more accurately determine the merit of this piece. Some more detailed comments and questions:

Reply: We appreciate the reviewer's valuable comments and have carefully considered them. Our responses to address each point are provided below.

1 The in-text references don't seem to correspond to the articles in the bibliography. Is the numbering off somehow? As one example: In the introduction, the manuscript states "Nowadays, higher-order networks have become foundational tools for studying contagion dynamics [22–24]" and navigating to the bibliography, Refs. 22-24 are:

[22] "How do hyperedges overlap in real-world hypergraphs?" (for which the formattingseems off...)

[23] "Networks beyond pairwise interactions: Structure and dynamics."

[24] "Higher-order interactions shape collective dynamics differently in hypergraphs and. simplicial complexes."

Of these, only the last reference seems directly relevant, although the second one is relevant in a very general sense. I didn't exhaustively check the references, but I would suggest a double-check on all the references.

[Ref.1] Rachith Aiyappa et al., Emergence of simple and complex contagion dynamics from weighted belief networks. Sci. Adv. 10, eadh4439 (2024). DOI: 10.1126/sciadv.adh4439: The authors show that including belief networks on a pairwise network can lead to both simple and complex contagions.

[Ref.2] Leonie Neuhäuser, Andrew Mellor, and Renaud Lambiotte, Multibody interactions

and nonlinear consensus dynamics on networked systems, Phys. Rev. E 101, 032310 DOI: https://doi.org/10.1103/PhysRevE.101.032310: The authors show that "higher-order" linear dynamics are always reducible to pairwise dynamics.

Reply: We thank the reviewer for this suggestion. We have carefully checked and revised previously unmatched references in the updated manuscript to ensure that all in-text citations correspond correctly to the bibliography and that each reference accurately reflects the cited content.

First, we have modified and added relevant references ([15–25] in the revised manuscript, presented as [R5]–[R15] at the end of this response) to support the discussion of hypergraphs, simplicial complexes, and contagion dynamics in the Introduction. For example, the revised text now reads:

Page 1, Section 1:

The prevalence of group interactions in real-world systems has led to the emergence of higher-order networks [15-17], such as hypergraphs [18-20] and simplicial complexes [21-23], as foundational tools for studying contagion dynamics [24, 25], which overcome the limitations of traditional models.

Second, we updated references ([26–29], here presented as [R16]–[R19]) to support studies of dynamics on higher-order networks via diverse propagation pathways:

Page 2, Section 1:

First, higher-order networks effectively represent multifaceted interactions among nodes (i.e., higher-order interactions) [26, 27], allowing for diverse propagation pathways [28, 29].

In addition, we have carefully checked and readjusted references [1–8] throughout the manuscript. The modifications are as follows:

Page 1, Section 1:

Characterizing dynamics on networks is pivotal to encoding the evolution of collective behaviors [1-3], with contagion dynamics being the most extensively studied due to their wide applications spanning pathogen transmission [4], information diffusion [5, 6], cultural socialization [7], biological reaction [8], etc.

Moreover, we have incorporated the reviewer-suggested references ([Ref.1] and [Ref.2], now [35] and [36] in the revised manuscript, presented as [R20]–[R21]) into the relevant sections of the main text:

Page 2, Section 1:

Notably, finding such a systematic relationship is fundamental to explain *evolutionary principles that govern chaotic dynamics in empirical systems, as well as to uncover driving factors that allow dynamical processes to be viewed through a more nuanced and complex lens [35-37].*

2.1 Typographical errors: In the abstract: "interplays" should be "interplay".

Reply: Thanks for the suggestion. Firstly, we have revised these expressions throughout the manuscript to address the misleading terms such as "interplay". Specifically, we replaced them with more precise terminology (e.g., transformability, mapping) that reflects the behavior of the dynamics across different network representations, without implying coupling between distinct dynamical processes. The detailed revisions are presented as follows:

Page 1, Abstract:

Here, we present a holistic analysis framework that bridges the relationships between dynamics in pairwise and higher-order systems, demonstrating that these processes are not independent but can undergo systematic transformations.

Page 2, Caption of Fig. 1:

c *The relationship between dynamics on the higher-order network (Υ) and its pairwise counterpart ($\hat{\Upsilon}$).*

e *A unified framework demonstrating the transformation of dynamics across different orders ($\Delta\Phi^*$) as governed by the combined contributions of dynamical ($\Delta\Phi_1$) and structural ($\Delta\Phi_2$) factors.*

Page 2, Section 1:

While substantial efforts have been made to understand the dynamics of contagion, ranging from pairwise-based mechanisms to those driven by higher-order interactions [32-34] (see Fig. 1a), these studies have largely overlooked the relationship of dynamical processes across networks of different orders.

Notably, finding such a systematic relationship is fundamental to explain evolutionary principles that govern chaotic dynamics in empirical systems, as well as to uncover driving factors that allow dynamical processes to be viewed through a more nuanced and complex lens [35-37].

Page 4, Caption of Fig. 2:

The relationships of dynamics across network representations.

Page 6, Section 2.1:

These results suggest that when the transformable condition between two contagion dynamics becomes more restrictive, the dynamics tend to converge; otherwise, they diverge further, underscoring the complex mapping of dynamics across *network orders.*

Page 8, Section 2.2:

Through this framework, we disentangle the transformation of dynamics across different network orders into two explicit and additive components, namely dynamical and structural, thereby enabling the framework's adaptability to a broad range of processes, including contagion and opinion dynamics.

Page 11, Section 3:

Our works has the potential to drive applications across diverse real-world scenarios, as unveiling the transformability of dynamics across diverse network representations is fundamental to explain evolutionary principles that govern chaotic dynamics in empirical systems [37].

2.2 In the introduction: I don't believe that "examplied" is a word.

Reply: Thanks for this comment. In response, the term "examplied" in the Introduction has been replaced with "such as". The updated sentence reads:

Page 1, Section 1:

The prevalence of group interactions in real-world systems has led to the emergence of higher-order networks [15-17], such as hypergraphs [18-20] and simplicial complexes [21-23], as foundational tools for studying contagion dynamics [24, 25], which overcome the limitations of traditional models.

2.3 There are numerous punctuation errors including missing commas, spaces prior to. commas, etc.

Reply: Thanks for your suggestion. We carefully re-checked the entire manuscript and corrected all punctuation errors, including missing commas, misplaced spaces, and the positioning of references. For clarity, we provide several representative corrections below:

In the Introduction, we corrected the punctuation errors, and the sentence has been revised as follows:

Page 1, Section 1:

Characterizing dynamics on networks is pivotal to encoding the evolution of collective behavior [1-3], with contagion dynamics being the most extensively studied due to their wide applications spanning pathogen transmission [4], information diffusion [5, 6], cultural socialization [7], biological reaction [8], etc.

Also, we corrected the spacing before commas and revised the text to:

Page 2, Section 1:

First, higher-order networks effectively represent multifaceted interactions among nodes, i.e., higher-order interactions [26, 27], allowing for diverse propagation pathways [28, 29].

In Section 2.2, we have corrected the comma errors in the description, which now reads:

Page 6, Section 2.2:

To explore the contributing factors, we first obtain the information entropy Φ from $\bar{I}(t)$ for contagion dynamics on both higher-order and pairwise networks (the first plot of Fig. 1c, see detailed information in the Supplementary Information), and then calculate the entropy differences between these two curves (represented as $\Delta\Phi^*$ in grey in the second plot of Fig. 1c).

2.4 Reword "between individual neighbors." to "with a single neighbor."

Reply: We sincerely thank the reviewer for this suggestion. We have thoroughly reviewed the manuscript for grammatical and punctuation errors and have revised all identified issues. In particular, the phrase "between individual neighbors." has been updated to "with a single neighbor." in the Introduction:

These paradigms, however, are largely based on pairwise interactions (Fig. 1a), where the state of a node is dictated by interactions with a single neighbor.

3 In the introduction and the abstract, the terms "transformable" and "inter-transformed" are used without explicitly explaining what these terms mean. I would add a sentence or two of introduction. Later, in Section 2.3, the manuscript mentions "generalizability". Is this the same thing?

Reply: Thanks for your suggestion. We have added explicit definitions of "transformability" and clarified its distinction from "generalizability" in the Introduction. Specifically, we now introduce transformability as follows:

Page 6, Section 2.2:

In this work, we introduce the concept of transformability, defined as the capability to map contagion dynamics across different network types. When specific conditions are asymptotically approached, the behaviors of dynamics on one network can approximate those on another, a phenomenon we refer to as transformed and the process as transformation.

Furthermore, by investigating the structural and dynamical components that drive the transformations of dynamics between higher-order networks and pairwise graphs, we proposed a structural-dynamical decomposition scheme. The term generalizability refers to the ability of this scheme to extend beyond contagion dynamics, capturing analogous transformations in other dynamical processes such as opinion dynamics. The revised text now reads:

Page 3, Section 1:

Notably, we show that the structural factor (i.e., the presence of multiple contagion contacts within higher-order interactions) and dynamical factor (i.e., the nonlinear impact induced by contagion processes) serve as two independent drivers governing the transformation between the dynamics on higher-order and pairwise networks. This insight allows us to propose a "structural-dynamical" decomposition scheme to capture the transformation.

Finally, we validate the generalizability of the proposed unified scheme in the context of opinion dynamics [38-40], showcasing its robustness and applicability across a broad spectrum of dynamical systems (Fig. 1d).

4 This sentence is filled with jargon and imprecision: "Secondly, as the dynamical process inherently reflects the variations of node states within a system, which can be characterized through the evolution of system instability, we naturally leverage information entropy to globally quantify the evolution of instability generated throughout these contagion processes." What do "reflect" and "variations" mean in this context? I would say that the dynamical process determines node state transitions; is that what this clause means? What does "evolution of system instability" mean? Is this saying that the fixed points and their stabilities are changing in time?

Reply: We thank the reviewer for this suggestion. We have revised the relevant text to clarify the relationship between the dynamical process and node state transitions, as well as to define the concept of system disorder (previously referred to as system instability) more precisely. As suggested, the dynamical process here refers to the mechanism that determines temporal transitions of node states.

Specifically, we now define system disorder as the temporal progression of uncertainty within the system, capturing both the magnitude and diversity of instabilities that arise during contagion processes. To quantify this, we employ information entropy as a global indicator. The revised text in the manuscript reads:

Page 3, Section 1:

Secondly, the contagion dynamics are governed by the evolution of individual node states (e.g., infection probabilities), which gives rise to disorder at the system level, *hereafter referred to as system disorder. To quantify this disorder globally, we employ information entropy, which provides a rigorous measure of the system's statistical uncertainty throughout the process (Fig. 1b).*

Additionally, we have updated Methods Section 4.3 to provide a detailed description of the indicators used to measure system disorder.

5 The introduction starts with a broad overview of higher-order dynamics and offers a nice overview of current modeling limitations, but the introduction should be more grounded in the framework that this manuscript introduces. Specifically, the last paragraph of the introduction is filled with technical jargon (and, as I note above, imprecision) and a lack of overview into what it is that this manuscript accomplishes.

Reply: Thank you for your suggestion. To enhance readability and better emphasize the key points, we have revised the last paragraph of the Introduction by removing confusing technical terms and explicitly highlighting the goals and contributions of our work.

Specifically, our study aims to systematically identify the key factors governing the mapping of dynamics between higher-order networks and pairwise graphs, uncover and decompose the underlying driving components, and propose a versatile structural-dynamical scheme to capture these transformations. The contributions are organized into three parts: (i) Establishing systematic conditions for mapping dynamics between higher-order networks and graphs; (ii) Identifying the driving factors of these transformations and proposing a structural-dynamical scheme to capture them; (iii) Demonstrating the applicability of the structural-dynamical scheme across both contagion and opinion dynamics. The revised paragraph in the manuscript now reads as follows:

Page 3, Section 1:

In this work, we introduce the concept of transformability, defined as the capability to map contagion dynamics across different network types. When specific conditions are asymptotically approached, the behaviors of dynamics on one network can approximate those on another, a phenomenon we refer to as transformed and the process as transformation. Our objective is to systematically identify the key factors governing such transformations, uncover and decompose the underlying drivers, and propose a versatile scheme to capture these transformations.

Firstly, we develop a theoretical framework that establishes systematic criteria for mapping contagion dynamics between pairwise and higher-order networks. This *formulation reveals that seemingly distinct dynamical processes are not isolated but can be mathematically mapped onto one another through well-defined transformation rules.*

Secondly, the contagion dynamics are governed by the evolution of individual node states (e.g., infection probabilities), which gives rise to disorder at the system level, hereafter referred to as system disorder. To quantify this disorder globally, we employ information entropy, which provides a rigorous measure of the system's statistical uncertainty throughout the process (Fig. 1b).

Thirdly, this approach further facilitates the identification of key factors driving the transformability, particularly from pairwise to higher-order networks, see Fig. 1c.

Notably, we show that the structural factor (i.e., the presence of multiple contagion contacts within higher-order interactions) and dynamical factor (i.e., the nonlinear impact induced by contagion processes) serve as two independent drivers governing the transformation between the dynamics on higher-order and pairwise networks. This insight allows us to propose a "structural-dynamical" decomposition scheme to capture the transformation.

Finally, we validate the generalizability of the proposed unified scheme in the context of opinion dynamics [38-40], showcasing its robustness and applicability across a broad spectrum of dynamical systems (Fig. 1d).

To the best of our knowledge, this study is the first to offer a comprehensive analysis for the transformability of dynamics on higher-order networks via the lens of system's statistical uncertainty. Moreover, we provide a foundational understanding of the roles played by both structural and dynamical factors in dynamic transformations, thereby shedding light on the unique characteristics of higher-order dynamical systems.

6 In Fig. 2, the caption uses notation and terminology that is not introduced until later in the paper ($kappa$, for example). In addition, I think that more description in both the figure and the caption would help.

Reply: Thank you for your suggestion. Firstly, we have revised Fig. 2 (presented here as Fig. R7) and its caption by explicitly introducing and defining all notations used in the figure, including λ, κ, m and χ.

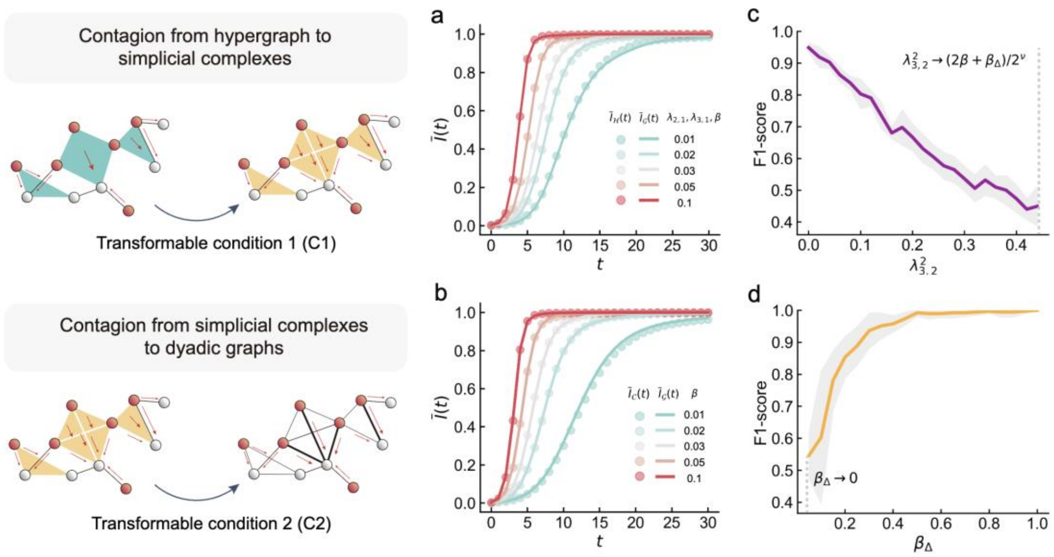

Fig. R7. The relationships between dynamic processes. a *Average infection density $\bar{I}(t)$ for contagion dynamics on a hypergraph and its projected simplicial complex, based on an empirical high-school social network. For the hypergraph (dots), $\lambda_{2,1} = \lambda_{3,1} = \beta$, $\lambda_{3,2} = (2\beta + \beta_\Delta)/2^\nu$; for the simplicial complex (lines), $\beta_\Delta = 0.5$. β varies from 0.005 to 0.1, with $\kappa = 2$.* ***b*** *Comparison of $\bar{I}(t)$ for dynamics on simplicial complex (dots) and those on projected dyadic graph (lines). Results are averaged over 500 simulations with $\mathcal{T} = 30$.* ***c, d*** *F1-score variation as the system approaches critical states C1 (**c**) and C2 (**d**). Lower F1-scores in **c** indicate reduced accuracy in distinguishing hypergraph-based contagion, while higher F1-scores in **d** reflect improved classification of simplicial complex dynamics. Note that the $\lambda^\kappa_{m,\chi}$ represents the basic infection rate isolated by hyperedge size m, the number of infection nodes in the hyperedge χ and with the mapping ratio κ, see Methods for details. The SVM classifier uses node degree and infection order features from simulations with $\lambda = 0.04, \nu = 1$ (hypergraphs) and $\beta = 0.04, \beta_\Delta = 0.8$ (simplicial complexes). Results are averaged over 10^3 runs with $\mathcal{T} = 50$.*

To enhance the clarity and readability of the manuscript, we have included descriptions of the mapping ratio in both the main text and the Methods section. The details of these revisions are as follows:

Page 5, Section 1:

We then determine the transformable conditions and show that the SI process on any hypergraph, with hyperedges of arbitrary size m and an arbitrary mapping ratio κ, where restricts hyperedges larger than $\kappa + 1$ to subsets of size at most $\kappa + 1$, and yields a κ-simplicial complex with $max(\delta) = \kappa$ (see Methods for details), can be consistent with contagion process on the simplicial complex representation.

Page 12, Section 4.1:

Moreover, another key projection maps a hypergraph to its corresponding simplicial complex with a mapping ratio κ [54]. This process compresses hyperedges larger than $\kappa+1$ into subsets of size at most $\kappa+1$, yielding a κ-simplicial complex. As a result, the maximum order δ of simplices in the projected structure is constrained to κ, ensuring that $max(\delta)=\kappa$.

7 When defining the infection rate as χ^ν, I think a reference to Ref. 3 in my list of relevant references would be appropriate (or Ref. [29] in the manuscript). Also: what does the "mapping ratio" mean?
[Ref.3] Guillaume St-Onge, Vincent Thibeault, Antoine Allard, Louis J. Dubé, and Laurent Hébert-Dufresne, Social Confinement and Mesoscopic Localization of Epidemics on Networks. Phys. Rev. Lett. 126, 098301 DOI: https://doi.org/10.1103/PhysRevLett.126.098301

Reply: Thank you for your suggestion.

Firstly, we have added the relevant reference ([41] in the manuscript, corresponding to [Ref. 3] in the reviewer's list) when defining the infection rate. The revised description now reads:

Page 5, Section 2.1:

For the contagion dynamics on hypergraphs, we isolate the effects of higher-order interactions by defining $\lambda\cdot\chi^{\nu}$ as the infection rate within an m-sized hyperedge containing χ nodes in the infected (I) state [41].

Secondly, we have clarified the concept of the mapping ratio. In our study, the mapping ratio κ governs the projection of a hypergraph onto a simplicial complex: hyperedges larger than $\kappa+1$ are decomposed into subsets of size at most $\kappa+1$, resulting in a κ-simplicial complex with maximum simplex order $max(\delta)=\kappa$. This definition ensures a controlled reduction of higher-order interactions while preserving key structural features.

To incorporate this definition, we have revised both the main text and the Methods section. In the main text, we now state:

Page 5, Section 2.1:

We then determine the transformable conditions and show that the SI process on any hypergraph, with hyperedges of arbitrary size m and an arbitrary mapping ratio κ, where restricts hyperedges larger than $\kappa+1$ to subsets of size at most $\kappa+1$, and yields a κ-simplicial complex with $max(\delta)=\kappa$ (see Methods for details), can be consistent with contagion process on the simplicial complex representation.

Additionally, in the Methods section, we have provided additional details:

Page 12, Section 4.1:

Moreover, another key projection maps a hypergraph to its corresponding simplicial complex with a mapping ratio κ *[54]. This process compresses hyperedges larger than* $\kappa+1$ *into subsets of size at most* $\kappa+1$*, yielding a* κ*-simplicial complex. As a result, the maximum order* δ *of simplices in the projected structure is constrained to* κ*, ensuring that* $max(\delta)=\kappa$*.*

8 In Fig. 2, the mention of a "projected simplicial complex" reminded me of an "induced simplicial complex" introduced in Ref. 4 in the list below.

[Ref. 4] Landry, N.W., Young, JG. & Eikmeier, N. The simpliciality of higher-order networks. EPJ Data Sci. 13, 17 (2024).

Reply: Thank you for your suggestion. We thank the reviewer for pointing out the connection to the concept of an *induced simplicial complex* in [Ref. 4]. In fact, our projected simplicial complex can be viewed as a more general and abstract construction. The induced simplicial complex corresponds to the special case where all hyperedges are fully retained. In contrast, our framework introduces a mapping ratio κ, which systematically constrains hyperedges larger than $\kappa+1$ to subsets of size at most $\kappa+1$, yielding a κ-simplicial complex with maximum simplex order $max(\delta)=\kappa$.

This abstraction allows us to flexibly control the maximum order of simplices while preserving essential higher-order structure. It thus provides a physically motivated, tunable projection that can capture the effects of higher-order interactions in a controlled manner, enabling a consistent comparison of dynamics between hypergraphs and their simplicial complex representations (see Methods for details).

Besides, we have incorporated the reference (i.e., [Ref. 4]) suggested by the reviewer when introducing such structure of simplicial complexes in the main text. This citation now appears in Section 4.1 (page 12).

Page 12, Section 4.1:

Moreover, another key projection maps a hypergraph to its corresponding simplicial complex with a mapping ratio κ *[54]. This process compresses hyperedges larger than* $\kappa+1$ *into subsets of size at most* $\kappa+1$*, yielding a* κ*-simplicial complex. As a result, the maximum order* δ *of simplices in the projected structure is constrained to* κ*, ensuring that* $max(\delta)=\kappa$*.*

These clarifications are now reflected in the main text, Methods section, and figure captions, highlighting both the generality of the construction and its connection to the traditional induced simplicial complex.

9 In Fig. 1(c), the x-label is chopped off. Consider using tight_layout() in pyplot.

Reply: Thank you for your suggestion. We clarify that Fig. 1c is an illustration highlighting the differences in entropy between dynamics on higher-order networks and their corresponding graphs. To address the issue, we have re-adjusted the figure layout to ensure that the x-label is fully visible, while preserving the experimental curves (see Fig. R8).

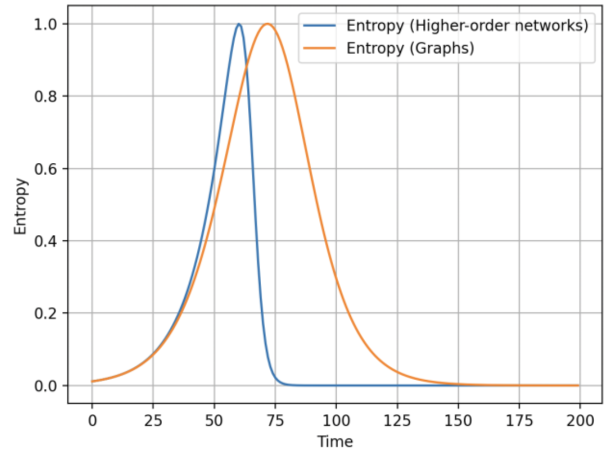

Fig. R8. Temporal evolution of entropy. *The curves show entropy changes computed from the mean-field solutions for contagion dynamics on simplicial complexes and on graphs, respectively. The simplicial complexes consist of* $N = 1000$ *nodes. The infection rates for 1-simplices and 2-simplices are set to* 0.1 *and* 0.3*, respectively, and the dynamics are simulated over* 200 *time steps.*

The updated version of the left panel in Fig. 1(c) is shown in Fig. R9.

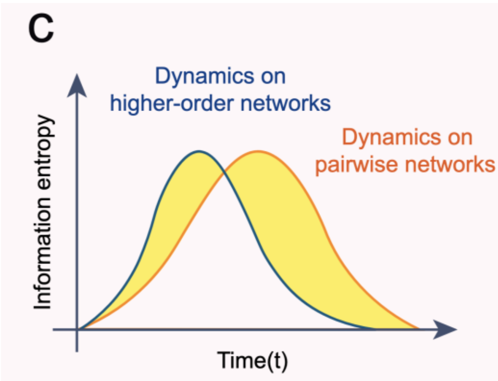

Fig. R9. *Updated illustration of the left panel of Fig.1c, showing the differences in entropy between dynamics on higher-order networks and corresponding graphs. The figure layout has been adjusted to ensure full visibility of all axis labels and features.*

10 Why not distinguish hypergraphs from graphs in Fig. 2 and why not derive an *additional condition, similar to C1 and C2? Especially since this is illustrated in Fig. 1. In my opinion, this is just as important, if not more, than the other comparisons.*

Reply: Thanks for your suggestion. To address this concern, we emphasize the role of Condition 3 (C3), which is specifically designed to characterize the distinction between dynamics on hypergraphs and their corresponding projected graphs. In particular, we have conducted additional experiments to validate this condition. As shown in the newly added Fig. R10, when C3 is satisfied, the dynamics on hypergraphs and graphs become equivalent. Indeed, C3 can be regarded as a combination of the conditions in C1 and C2. However, due to the involvement of multiple parameters in C3, its distinguishing capacity is less straightforward to visualize. To overcome this, we provide a more detailed analysis in Fig. 4a of revised manuscript, as shown in Fig. R1. This figure illustrates how the dynamical behavior on hypergraphs gradually approaches that on graphs under different parameter regimes. The white line in Fig. R1 marks the parameter region where the two dynamics are nearly indistinguishable. Conversely, as the system deviates further from this line, the difference between the two types of dynamics becomes increasingly pronounced.

For clarity, we have now explicitly described C3 in the manuscript as follows:

Page 5, Section 2.1:

Combining Eq. 2 with the condition defined as $\beta_\delta = 0$ for $\delta > 1$ (Condition 2, C2), the contagion dynamics on $\mathcal{H}$ become equivalent to those on its projected dyadic graph with multiple edges when the following condition (Condition 3, C3) is satisfied:

$$\lambda_{m,\chi}^{\kappa} = \frac{1}{\chi^{\nu}} \sum_{a=\tau}^{\tau^*} a \cdot \binom{\chi}{a} \binom{m-\chi-1}{\kappa-a} \beta. \tag{3}$$

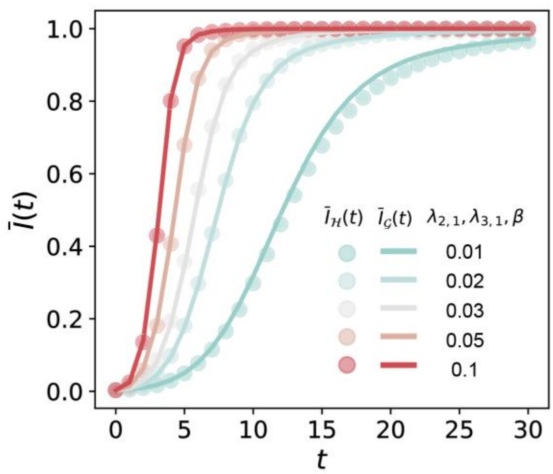

Fig. R10. *The interplay between dynamic processes on hypergraphs and those on graphs.* ***a*** *Average infection density $\bar{I}(t)$ for contagion dynamics on a hypergraph* *and its projected simplicial complex, based on an empirical high-school social network. For the hypergraph (dots),* $\lambda_{2,1} = \lambda_{3,1} = \beta, \lambda_{3,2} = 2\beta/2^{\nu}$*; for the graph (lines),* β *varies from* 0.005 *to* 0.1*, with* $\nu = 1$ *and* $\kappa = 2$*.*

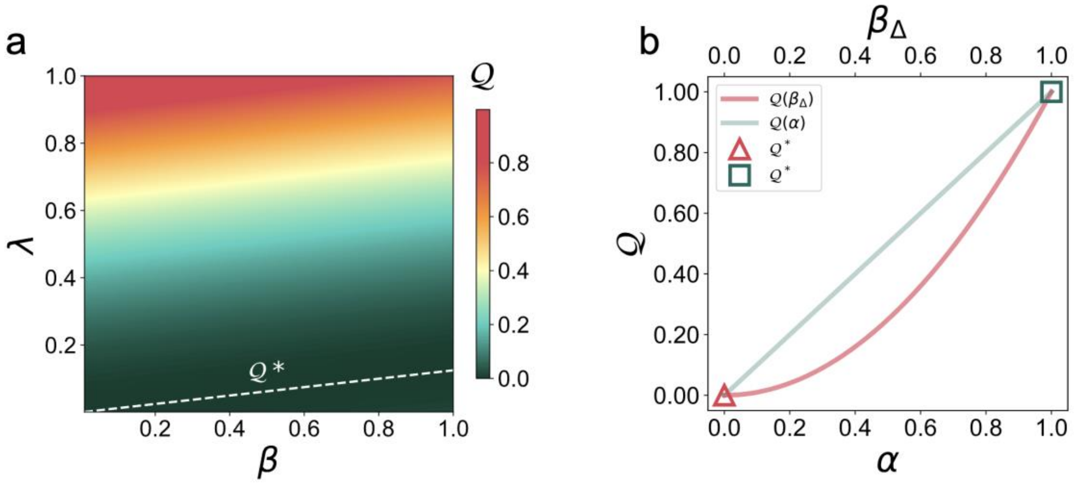

Fig.R1. (Fig. 4 in the revised manuscript) *Q^* in dynamics on hypergraphs and simplicial complexes.* ***a*** *Variation of Q with respect to λ and β in contagion dynamics on hypergraphs ($I_{\Upsilon=\mathcal{H}}$) with $m = 3$ and $\chi = 2$. The dashed line indicates the condition $Q = Q^*$.* ***b*** *Variation of Q with respect to β_Δ in contagion dynamics on simplicial complexes (red line), where the red triangle denotes $Q = Q^*$. The green line shows Q for two opinion dynamics on hypergraphs, with the green square indicating Q^*.*

11 Equations (2) and (3) seem fundamental to the message of the paper. Yet there is no build-up to the presentation of these conditions, all derivation is relegated to Supplementary Note 4, and there is hardly any discussion of the intuitive interpretation of these results.

Reply: Thank you for your suggestion. In response, we have enhanced the presentation of Eqs 2 and 3 in the Methods section by including the essential conceptual build-up. Specifically, we have incorporated the core derivations of conditions C1–C3 in subsection 4.2.3 of the Methods, which were previously only provided in Supplementary Note 4. Moreover, we have added a detailed discussion on the intuitive interpretation of these results. The corresponding modifications are highlighted in the revised manuscript as follows:

Page 14, Section 4.2.3:

Transformation conditions of dynamics

To establish the transformation conditions of dynamical processes across different network representations, we derive the infection rate by exploiting the infection probabilities defined on each dynamical process. We first examine the mapping of *dynamics between hypergraphs and simplicial complexes. The resulting conditions naturally divide into two regimes: (i)* $\kappa < m$, *and (ii)* $\kappa \geq m$. *We analyze the behavior of* $\lambda^{\kappa}_{m,\chi}$ *in each case separately and subsequently integrate the findings into a unified framework. The derivation is provided in the Supplementary Information.*

In the regime $\kappa < m$, *an* m*-sized hyperedge is first decomposed into* κ*-simplices. Let* χ *denote the number of infected nodes within the hyperedge. The infection rate associated with a* κ*-simplex containing* a *infected nodes (where* a *is the number of I-state nodes in such simplex) is then given by* $\sum_{b=1}^{a}\binom{a}{b}\beta_b$, *where* β_b *denotes the infection probability mediated by* b *infected neighbors. Accordingly, the effective infection rate for a focal node* i *can be expressed as:*

$$\lambda^{\kappa}_{m,\chi}\cdot\chi^{\nu} = \sum_{a=max(1,\kappa+1-(m-\chi))}^{min(\kappa,\chi)} \binom{\chi}{a}\binom{m-\chi-1}{\kappa-a}\sum_{\mathrm{b}=1}^{a}\binom{a}{b}\beta_{\mathrm{b}}. \tag{14}$$

For the second regime, where $\kappa \geq m$, *the hyperedge can be treated directly without further decomposition. In this case, the effective infection rate acting on a susceptible node* i *that belongs to the* m*-hyperedge is given by:*

$$\lambda^{\kappa}_{m,\chi}\cdot\chi^{\nu} = \sum_{a=1}^{\chi}\binom{\chi}{a}\beta_a. \tag{15}$$

By merging the results from Eqs. 14 and 15, we obtain a single compact expression that holds across both regimes, further details are provided in the Supplementary Information. To this end, we introduce the auxiliary quantities $\tau = max\big(1,\kappa+1-(m-\chi)\big)$ *and* $\tau^{*} = min(\kappa,\chi)$, *which capture the admissible ranges of contributions. The consolidated infection rate can then be expressed as:*

$$\lambda^{\kappa}_{m,\chi} = \frac{1}{\chi^{\nu}}\sum_{a=\tau}^{\tau^{*}}\binom{\chi}{a}\binom{m-\chi-1}{\kappa-a}\sum_{b=1}^{a}\binom{a}{b}\beta_b. \tag{16}$$

Building on this framework, we derive the generalized condition governing the coupling of dynamics between hypergraphs and simplicial complexes. In addition, the transformability condition for mapping hypergraph dynamics onto its dyadic multi-edge projection arises when $\beta_{\delta} = 0$ *for all* $\delta > 1$, *and takes the form:*

$$\lambda^{\kappa}_{m,\chi} = \frac{1}{\chi^{\nu}}\sum_{a=\tau}^{\tau^{*}} a\cdot\binom{\chi}{a}\binom{m-\chi-1}{\kappa-a}\beta. \tag{17}$$

Then, the generalized conditions for the coupling across various dynamics are established. These expressions can be understood as the conditions that govern the transformation of dynamics on a hypergraph to simplicial complexes or their multi-edge graph projections. They correspond to a weighted aggregation of all admissible contributions from interacting nodes or simplices. Furthermore, the transformation conditions for mapping simplicial complexes onto their graph projections effectively eliminate the nonlinear contributions arising from contagion at the level of higher-

order simplices, thereby enabling a simplified representation of the dynamics.

12 The manuscript states that "we classify dynamics using a model of Support Vector Machine", but more information is needed to reproduce the results of this paper. I assume that the population-level time series (not nodal timeseries) are fed into the SVM? How was the number of time steps determined?

Reply: Thank you for your suggestion. To clarify, the input to the Support Vector Machine (SVM) classifier consists of population-level time series features, which summarize the collective progression of contagion rather than individual node trajectories. This choice ensures that the classifier captures macroscopic patterns of the dynamics while reducing variability from single-node fluctuations. Each contagion type was simulated 1000 times, with each simulation lasting $T = 50$ discrete steps, which provides a sufficiently time window to capture the early and intermediate stages of contagion spread for the purpose of classification. Details of the updated description in the Methods Section in the manuscript are as follows:

Page 15, Section 4.2.4:

We classified contagion dynamics using a Support Vector Machine (SVM) with an RBF kernel. For each contagion type, 1000 *independent simulations were performed, each lasting* $T = 50$ *discrete steps. At each step, we identified the newly infected nodes and computed their mean degree and mean clustering coefficient (the latter derived from the restricted hypergraph). These values formed two time series, and the infection time sequence recorded the steps at which new infections occurred.*

Because simulations can saturate before T*, sequence lengths varied. All sequences were zero-padded to the maximum observed length and concatenated into a single feature vector per simulation. The population-level resulting vectors (*1000 *per contagion type) formed the training set for the SVM. Test sets were generated from independent simulations and processed identically, ensuring consistent feature construction for prediction.*

In the main text, we have updated the relevant description and refer to the Methods section for further details to enhance clarity and readability.

In addition, to numerically test the progressive effect of proposed conditions on the transformation between contagion dynamics, we classify dynamics using a model of Support Vector Machine (SVM). The classification is based on the correlation between the node degree and infection order [31], see Methods.

13 Overall, I thought that the way sections 2.2 and 2.3 were written felt like an abrupt shift from the prior section. I think that they should be re-written to better motivate *why these sections are important to the paper.*

Reply: Thank you for your suggestion. We have revised Sections 2.2 and 2.3 to improve the flow from the preceding section and to better motivate the importance of these analyses. The main updates in the revised manuscript are summarized below:

Page 6, Section 2.2:

Building on the transformation among dynamics via the infection probability, we aim to uncover the underlying factors that drive the transformability of dynamics on higher-order networks, particularly focusing on the dynamic transitions between higher-order and pairwise networks. While the preceding section established the fundamental framework for capturing local infection probabilities, a deeper understanding requires moving beyond node-level descriptions to examine the system-wide behavior of network dynamics. To this end, we advance from a localized perspective, centered on individual node states, to a holistic perspective that captures the systemic evolution of node states at the global scale. To quantify this global behavior, we employ information entropy, which effectively captures system disorder arising from the diversity of node states during the dynamic process (Fig. 1b, see Methods for details). By leveraging entropy, we can identify and quantify the key factors governing dynamic transformations, thereby constructing a comprehensive scheme to unravel the distinctions between higher-order and pairwise network dynamics.

Page 8, Section 2.3:

To assess generalizability, i.e., the broader relevance and robustness of the proposed framework, it is essential to examine its applicability beyond contagion processes, encompassing diverse types of dynamics and network domains. Accordingly, we extend our analysis to a representative class of dynamics distinct from contagion processes. Specifically, we consider opinion dynamics models, which capture how individual opinions evolve, propagate, and stabilize within complex networks. For illustration, consider a social network of friends debating their coffee preferences (Fig. 1e). Each individual initially holds one of three opinions, positive (POS), negative (NEG), or neutral (NEU), representing enthusiasm, aversion, or indifference. Through social communications, these opinions evolve as individuals influence one another, for instance, a coffee enthusiast may persuade an opponent or moderate their own stance toward neutrality. Building on the proposed unified framework, we validate its applicability to both continuous and discontinuous opinion dynamics, specifically employing the Deffuant–Weisbuch (DW) model [42, 43] and the Voter model [44]. This extension demonstrates the framework's versatility in capturing the structural and dynamical distinctions across diverse networked processes.

14.1 The section title "A unified framework from the perspective of system instability" is a confusing title. First, how is it unified? That could be spelled out more clearly. Second, there are many mentions of "system instability" in the manuscript. As a dynamical systems person, I would use this to refer to equilibria and their stability, but the manuscript seems (?) to be using this to refer to "avalanche-like" behavior, where the system accelerates toward complete infection.

Reply: Thank you for your suggestion. Firstly, we have renamed it to "A structural-dynamical decomposition scheme via system disorder". This emphasizes that the framework is unified in the sense that it systematically captures the transformation of dynamics between higher-order networks and graphs by decomposing the structural and dynamical components, which act as the two driving factors governing these transformations.

Regarding the previous term "system instability", we have replaced it with "system disorder." In our study, we use it to quantify the temporal evolution of uncertainty and variability in node states during contagion processes, rather than the traditional notion of equilibria in dynamical systems. We clarified the concept in the Introduction, details are as follows:

Page 3, Section 1:

Secondly, the contagion dynamics are governed by the evolution of individual node states (e.g., infection probabilities), which gives rise to disorder at the system level, hereafter referred to as system disorder. To quantify this disorder globally, we employ information entropy, which provides a rigorous measure of the system's statistical uncertainty throughout the process (Fig. 1b).

Additionally, we give the explicit expressions to evaluate the system disorder in the Methods section.

14.2 In Eq. (4), I am unclear how this would scale with maximum edge size.

Reply: We thank the reviewer for pointing out this issue. For Eq. 4, we examined the behavior of Q in hypergraph contagion dynamics under varying edge sizes m. As shown in the experimental results in Fig. R11, we observe that, with other parameters fixed, increasing m leads to noticeable transitions in the value of Q. However, these transitions are less pronounced than the ones induced by changes in λ. The revisions are as follows:

Page 8, Supplementary Note 5:

Supplementary Note 5: Q VALUES UNDER THE EFFECT OF DIFFERENT EDGE SIZE m

To investigate how $\mathcal{Q}$ changes in hypergraph contagion ($I_{\Upsilon=\mathcal{H}}$) under varying hyperedge sizes, we evaluate $\mathcal{Q}$ for different values of m (see Fig.3 a–b). We observe that, for a fixed χ, the $\mathcal{Q}$ value decreases as m increases due to variations in λ. Moreover, larger values of κ further amplify this effect. Notably, when χ is fixed, larger m can increase the scale coefficient in $\mathcal{Q}$ (i.e., $\sum_{a=\tau}^{\tau^*} a \cdot \binom{\chi}{a}\binom{m-\chi-1}{\kappa-a}$), which directly affects such coefficient. Detailed derivations of this scale coefficient are provided in Supplementary Note 3.

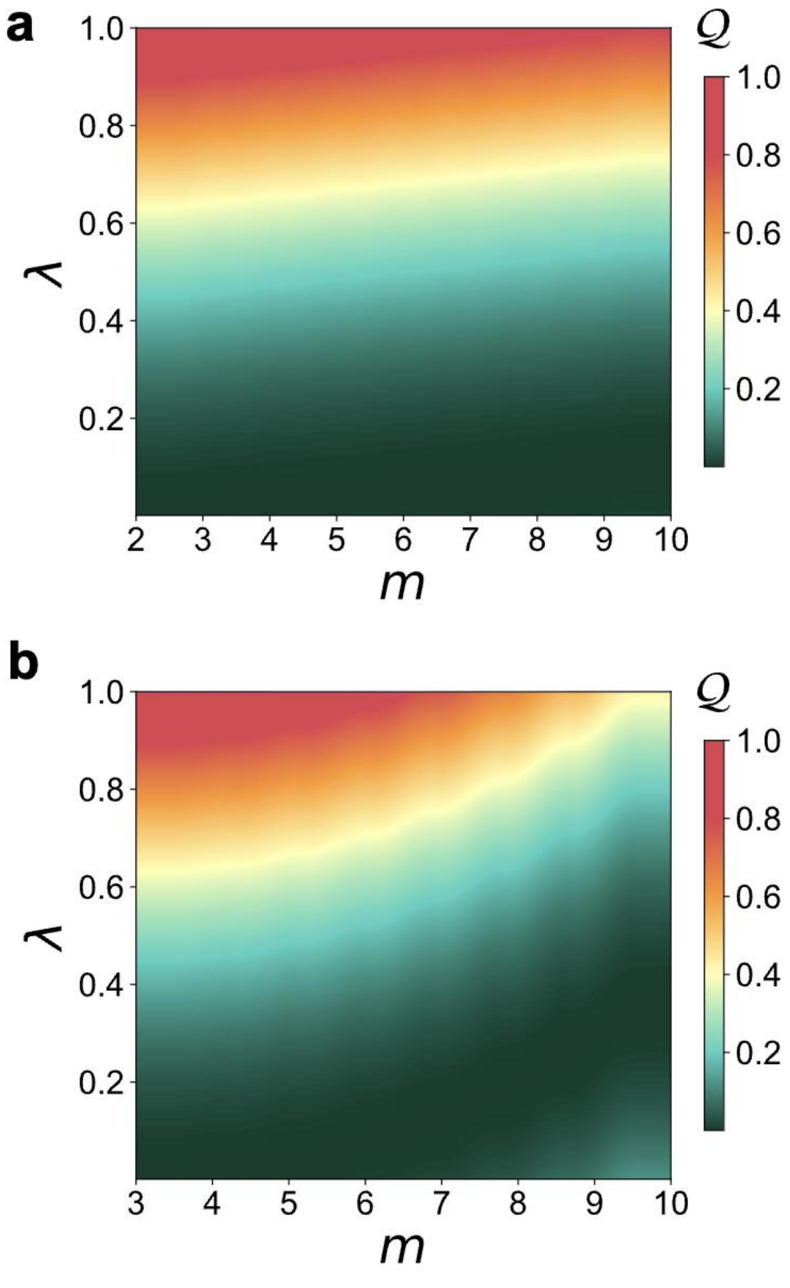

Fig.R11. *$\mathcal{Q}$ in dynamics on hypergraphs and simplicial complexes. Variation of $\mathcal{Q}$ with respect to λ and m in hypergraph contagion dynamics ($I_{\Upsilon=\mathcal{H}}$) for fixed parameters $\chi = 2$, $\beta = 0.1$, and $\nu = 4$: (**a**) $\kappa = 2$ and (**b**) $\kappa = 3$.*

Page 5, Supplementary Note 3:

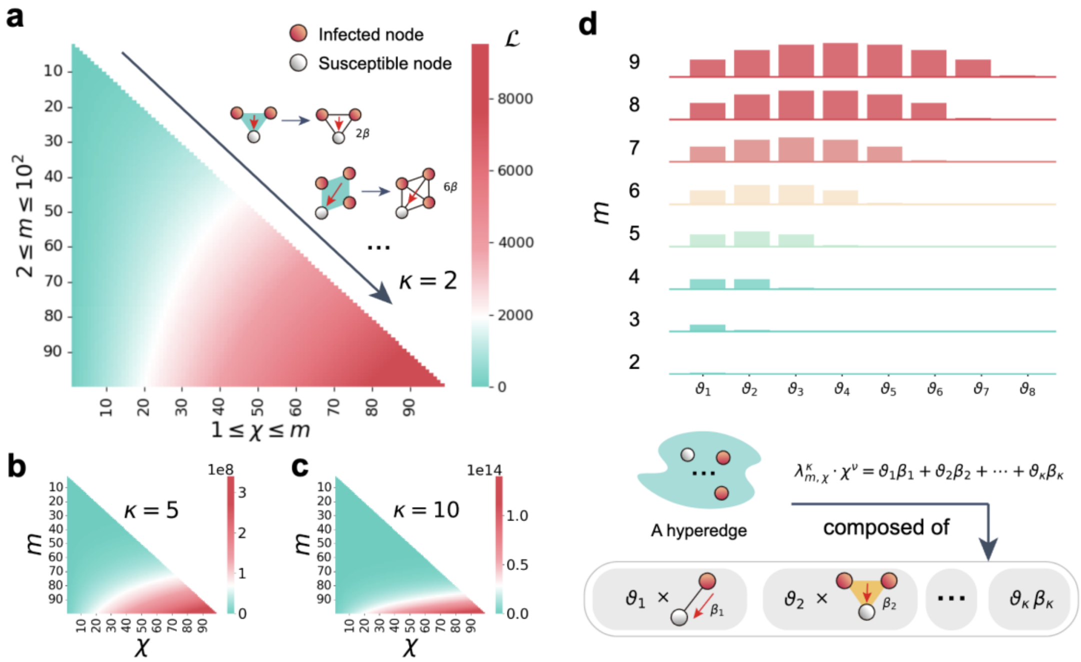

Fig. R6. *Interrelationships among dynamics through infection rates.* ***a*** *Infection rates when contagion on hypergraphs is mapped onto dyadic graphs. This mapping is quantified by the term* $\mathcal{L}(m,\chi,\kappa)$, *which denotes the infection rate experienced by an S-state node when dynamics within an* m*-sized hyperedge of the hypergraph are projected onto a dyadic graph. Here,* $\mathcal{L}(m,\chi,\kappa) = \sum_{a=\tau}^{\tau^*} a \cdot \binom{\chi}{a}\binom{m-\chi-1}{\kappa-a}$, *derived from C2.* $\lambda^{\kappa}_{m,\chi} \cdot \chi^{\nu}$ *corresponds to the infection rate in an* m*-sized hypergraph with mapping ratio* κ, *containing* χ *I-state nodes.* ***a*** *illustrates the variation of* $\mathcal{L}(m,\chi,\kappa=2)$ *as* m *and* χ *change, while* ***b*** *and* ***c*** *show corresponding results for* $\kappa = 5$ *and* $\kappa = 10$, *respectively. The analysis reveals that as* κ *increases,* χ *becomes the dominant factor influencing the infection rate relationship between hypergraph and dyadic graph dynamics, establishing a clear connection between complex and simple contagion processes.* ***d*** *The relationships of infection rates between dynamics on hypergraphs and simplicial complexes. The plot decomposes the contributions from simplices of varying orders within hyperedges of size* $m = 2$ *to* 9, *with* $\kappa = 8$ *and* $\chi = m - 1$. *The coefficient* ϑ_δ *quantifies the contribution of a* δ*-simplex (infection rate* β_δ*) to the S-state node.*

14.3 Also I found the notation of condition C2 confusing, following Eqs. (2) and (4) ($\beta\_\delta=0(\delta>1)$ and $\beta\_\delta^2(\delta>1)$).

Reply: We sincerely thank the reviewer for this comment. Regarding condition C2, we have clarified the notation in the revised manuscript: $\beta_\Delta = 0$ for $\delta > 1$

indicates that interactions beyond pairwise are excluded, whereas $\beta_{\Delta}^{2}(\delta > 1)$ denotes the nonlinear infection contribution from higher-order interactions. The updated description now makes these distinctions explicit following Eqs. (2) and (4). The revised version is as follows:

Page 5, Section 2.1:

Combining Eq. 2 with the condition defined as $\beta_\delta = 0$ for $\delta > 1$ (Condition 2, C2), the contagion dynamics on $\mathcal{H}$ become equivalent to those on its projected dyadic graph with multiple edges when the following condition (Condition 3, C3) is satisfied.

15 More details need to be shared about the entropy. Is this computed on the population average or on a node-by-node basis? How do you deal with continuous nodal states (binning, etc.)?

Reply: We thank the reviewer for this comment. To clarify, the information entropy $\Phi(\mathrm{t})$ is calculated from the population-level state at each time step. Specifically, using the SI model as an example, we first compute the fractions of susceptible and infected nodes across the entire population and then evaluate the entropy based on these fractions. This population-level entropy provides a macroscopic measure of the overall uncertainty or heterogeneity in the system, without relying on node-by-node tracking, and is consistent with the standard definition of information entropy applied to the distribution of states. Since the SI model has binary nodal states (S or I), no further binning or discretization is required. This approach captures the collective dynamics of contagion spread while reducing variability from individual nodes. The revised version is presented as follows:

Page 16, Section 4.3:

Consequently, the system disorder at time t in the dynamics is quantified using the population-level fractions of susceptible and infected nodes via the information entropy $\Phi(t)$ as follows:

$$\Phi(t) = -\mathbf{p}_{\mathrm{S}}(t)\log_2 \mathbf{p}_{\mathrm{S}}(t) - \mathbf{p}_{\mathrm{I}}(t)\log_2 \mathbf{p}_{\mathrm{I}}(t). \quad (22)$$

$$= -\big(1-\mathbf{p}_{\mathrm{I}}(t)\big)\log_2\big(1-\mathbf{p}_{\mathrm{I}}(t)\big) - \mathbf{p}_{\mathrm{I}}(t)\log_2 \mathbf{p}_{\mathrm{I}}(t) \quad (23)$$

Note that, this approach uses the population-average state rather than computing entropy node-by-node. Since the SI model has binary nodal states (S or I), no further binning or discretization is needed; the entropy naturally captures the diversity of the population-level node states. The entropy $\Phi(t)$ reflects the overall uncertainty or heterogeneity of the epidemic at the population level. Specifically, a high entropy indicates that the population is roughly evenly split between susceptible and infected individuals, corresponding to a rapidly spreading or unpredictable epidemic, where *infection events are diverse and widespread. Conversely, a low entropy means most individuals are in the same state (mostly susceptible or mostly infected), representing a controlled or saturated epidemic, where the outbreak has stabilized.*

16 Where does Q show up in the results? I understand that Q just indicates the system state, but I don't understand why it's introduced and then in Fig. 3, for example, it's never used.

Reply: Thank you for your suggestion. We thank the reviewer for this insightful comment. The quantity Q is introduced to capture the system state in a way that allows us to assess whether the dynamics can be decomposed into structural and dynamical components. Specifically, the existence of a fixed point $Q = Q^*$ determines the feasibility of such a decomposition. In the revised manuscript, we analyze the behavior of Q in both hypergraph and simplicial complex contagion dynamics, and we further discuss the conditions for the existence of $Q = Q^*$ under different parameter regimes, as illustrated in Fig. 4 (shown in Fig. R1). Details of these analyses have been added to clarify the role of Q in our results.

Page 8, Section 2.2:

Q^* as a criterion for dynamic transformation. *The feasibility of decomposition into structural and dynamical components critically depends on the value of Q^*. As shown in Fig. 4a–b, sufficiently small values of λ (e.g., $\lambda \ll \beta$ when $\beta_\Delta = 0$) enable contagion dynamics on hypergraphs to be mapped onto equivalent dynamics on projected multi-edge dyadic graphs, thereby allowing decomposition. In contrast, when $\lambda > 0.2$, no valid mapping β exists, and the decomposition becomes infeasible. A similar condition arises in simplicial complexes, where $\beta_\Delta = 0$ determines whether decomposition is attainable. These results highlight a fundamental finding, i.e., the existence of Q^* is not guaranteed universally but is restricted to specific parameter regimes. Consequently, the applicability of our framework depends on whether the underlying dynamics fall within these regimes. This observation underscores the importance of Q^* not only as a technical requirement, but also as a critical criterion delineating when higher-order contagion processes can, or cannot, be faithfully reduced to lower-order representations.*

17 In plots 3(c) and (d), $\phi1$ and $\phi2$ should be ϕ_1 and ϕ_2 respectively.

Reply: Thank you for your suggestion. We have corrected the labels in Fig.3c and d, changing $\phi 1$ and $\phi 2$ to ϕ_1 and ϕ_2, respectively, in the updated manuscript (see

Fig.R3).

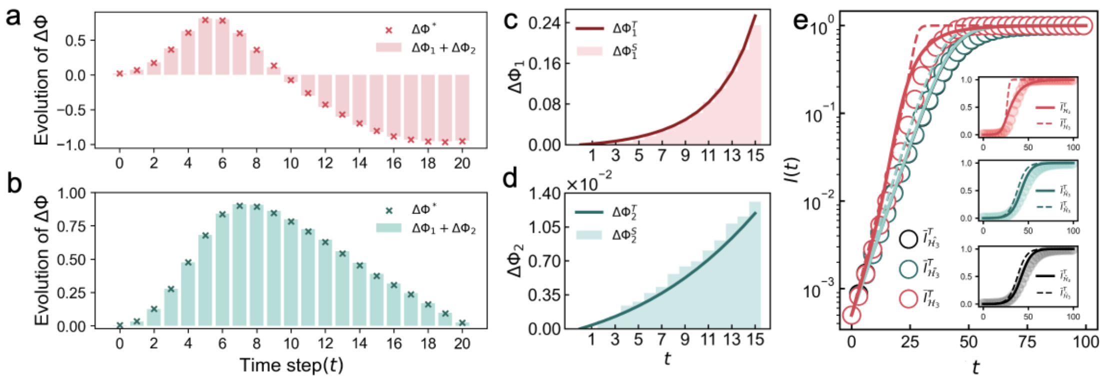

Fig.R3. (Fig. 3 in the revised main text). Identification and quantification of contributing factors in contagion dynamics. a-b *Temporal evaluation of $\Delta\Phi_1(t)+\Delta\Phi_2(t)$ in SI contagion processes simulated on real-world datasets of primary school and high school interactions. In* ***a****, $\Delta\Phi_1(t)$ is calculated as $\Delta\Phi_1(t)=\Phi^{\mathcal{Q}}(t)-\Phi^{\mathcal{Q}^*}(t)$, with $\mathcal{Q}(\lambda=0.005,\nu=4)$ and $\mathcal{Q}^*(\nu=1)$, where λ satisfies Eq.3 for $\mathcal{Q}^*$. $\Delta\Phi_2(t)$ is derived as $\Phi_{\widehat{\mathcal{H}}}(t)-\Phi_{\widetilde{\mathcal{H}}}(t)$. In* ***b****, for the simplicial complex $\mathcal{C}$, $\Delta\Phi_1(t)$ is evaluated by setting $\mathcal{Q}(\beta_\Delta=0.9)$ and $\mathcal{Q}^*(\beta_\Delta=0)$, while $\Delta\Phi_2(t)$ is calculated similarly to* ***a****. The total entropy difference, $\Delta\Phi^*$ (dotted line), closely matches the sum of $\Delta\Phi_1(t)$ (dark-colored bars) and $\Delta\Phi_2(t)$ (light-colored bars) over time. Note that, for clarity, $\Delta\Phi^*$ (scatter points marked with "×") is compared with the sum of $\Delta\Phi_1$ and $\Delta\Phi_2$ (shown as bars). Results are averaged over 500 independent simulations.* ***c-d*** *Comparison of theoretical predictions ($\Delta\Phi^T$, solid lines) from the SI model with simulation results ($\Delta\Phi^S$, bars) for $\Delta\Phi_1(t)$ and $\Delta\Phi_2(t)$. Strong agreement is observed between theory and simulation.* ***e*** *Comparison of quantitative evaluation of the mean infection density $\bar{I}(t)$ between the original and the refined models. Theoretical predictions $\bar{I}^T(t)$ (solid lines) align closely with simulation results $\bar{I}^S(t)$ (dots), as shown for simplicial complexes $\bar{I}_{\mathcal{H}_3}(t)$, projected multi-edge graphs $\bar{I}_{\widehat{\mathcal{H}}_3}(t)$, and simple graphs $\bar{I}_{\widetilde{\mathcal{H}}_3}(t)$. The inset presents the non-logarithmic results of $\bar{I}(t)$ with error bars. Note that the simplicial complexes utilized here are shown in SSC networks in Supplementary in detail. Simulation of contagion dynamics are over 500 independent Monte Carlo realizations. The mean-field solutions for $\bar{I}_{\mathcal{H}_3}(t)$ are obtained by numerically integrating the corresponding differential equations using the LSODA algorithm.*

18 In Section 2.3, the manuscript stated, "The scattered points, aligned along the diagonal, highlight the generalizability and robustness of our unified framework *and delineate the transitions in dynamical behavior." I must have missed this, because this is not clear to me.*

Reply: Thank you for your suggestion. We have revised the descriptions in Section 2.3 to clarify the statement regarding the scattered points. Specifically, we have elaborated on how the alignment of points along the diagonal reflects the consistent behavior of the dynamics across different network representations, highlighting the robustness of the proposed scheme in the opinion dynamics. The updated text provides a clearer explanation of these observations.

Page 11, Section 2.3:

We find that our proposed "structural–dynamical" scheme is validated in opinion dynamics through the consistency between $\Delta\ddot{\Phi}^*$ *and* $\Delta\ddot{\Phi}_1 + \Delta\ddot{\Phi}_2$ *In our scatter plots, this consistency manifests as points lying close to the diagonal, indicating that the dynamic transformation from higher-order networks to pairwise networks can be decomposed into structural and dynamical contributions, which can be theoretically predicted. This finding holds across both synthetic networks with different topologies and empirical higher-order networks from diverse domains, including online (Email-Enron) and offline social (High-School and Primary-School) and biological systems (NDC-classes-full). This reflects the robustness and the generalizability of the proposed scheme.*

19 I found the notation very hard to follow, relying on tildes, umlauts, hats, with non-intuitive (and sometimes inconsistent letters. The scripts on the letters made it more challenging to read.

Reply: Thank you for your suggestion. To improve clarity and enhance readability, we have carefully revised the manuscript and added a dedicated table that summarizes and explains the core parameters and symbols used throughout the paper. This table is now included as Table 1 in the revised manuscript (also provided as Table R2 in the response file). We hope that this addition will make the notation more intuitive and consistent, thereby facilitating better understanding for readers.

Table R2. (Table 1 in the revised manuscript) *Description of parameters and notations used in this study.*

Param.	Description
Υ	Higher-order networks (hypergraphs or simplicial complexes)
$\tilde{\Upsilon}$	Multi-edge dyadic graph projected by the higher-order network Υ.
$\hat{\Upsilon}$	Simple dyadic graph projected by the higher-order network Υ.
$\mathcal{H}$	Hypergraph
$\mathcal{C}$	Simplicial complexes
$\mathcal{G}$	Dyadic graph
β	Infection rate of 1-simplex
β_Δ	Infection rate of 2-simplex
δ	The order of simplexes
λ	Basic infection rate in hypergraphs
ν	Nonlinear scaling of the infection rate in hypergraphs
κ	Mapping ratio for the projection from hypergraph to simplicial complexes
m	Hyperedge size
χ	The number of infection nodes in a hyperedge
$o_i(t)$	Opinion of node i at time step t
α	Scaling factor for the influence of hyperedge size on opinion dynamics.
$\Phi(t)$	System disorder at time step t
$\mathcal{Q}$	Measure of system state

20 Releasing a public GitHub and/or Zenodo repository would make the results in the manuscript more reproducible and I strongly recommend that one be released with the revision.

Reply: Thank you for your suggestion. We have made the data used in this study publicly available, and the corresponding codes have been deposited at the following website: *https://github.com/DDMXIE/transformability-of-dynamics*. In addition, we have included a statement regarding code availability in the revised manuscript, which is now placed immediately before the References section. Specifically, the code availability statement in the revised manuscript reads as follows:

Code availability statement

The codes of our work are available on:
https://github.com/DDMXIE/transformability-of-dynamics.

References

[R1] Chodrow P S, Veldt N, Benson A R. Generative hypergraph clustering: From blockmodels to modularity[J]. Science Advances, 2021, 7(28): eabh1303.

[R2] Mastrandrea R, Fournet J, Barrat A. Contact patterns in a high school: a comparison between data collected using wearable sensors, contact diaries and friendship surveys[J]. PloS one, 2015, 10(9): e0136497.

[R3] Iacopini I, Petri G, Barrat A, et al. Simplicial models of social contagion[J]. Nature communications, 2019, 10(1): 2485.

[R4] Lee G, Choe M, Shin K. How do hyperedges overlap in real-world hypergraphs?-

patterns, measures, and generators[C]//Proceedings of the web conference 2021. 2021: 3396-3407.

[R5] Boccaletti, S., De Lellis, P., Del Genio, C., Alfaro-Bittner, K., Criado, R., Jalan, S. & Romance, M. The structure and dynamics of networks with higher order interactions. Phys. Rep. 1018, 1–64 (2023).

[R6] Horsevad, N., Mateo, D., Kooij, R. E., Barrat, A. & Bouffanais, R. Transition from simple to complex contagion in collective decision-making. Nat. Commun. 13, 1442 (2022).

[R7] Malizia, F., Lamata-Ot´ın, S., Frasca, M., Latora, V. & G´omez-Garde˜nes, J. Hyperedge overlap drives explosive transitions in systems with higher-order interactions. Nat. Commun. 16, 555 (2025).

[R8] Contisciani, M., Battiston, F. & De Bacco, C. Inference of hyperedges and overlapping communities in hypergraphs. Nat. Commun. 13, 7229 (2022).

[R9] Badalyan, A., Ruggeri, N. & De Bacco, C. Structure and inference in hypergraphs with node attributes. Nat. Commun. 15, 7073 (2024).

[R10] Lee, G., Choe, M. & Shin, K. How do hyperedges overlap in real-world hypergraphs?-patterns, measures, and generators in Proc. Web Conf. 2021 (2021), 3396–3407.

[R11] Gambuzza, L. V., Di Patti, F., Gallo, L., Lepri, S., Romance, M., Criado, R., Frasca, M., Latora, V. & Boccaletti, S. Stability of synchronization in simplicial complexes. Nat. Commun. 12, 1255 (2021).

[R12] Ghorbanchian, R., Restrepo, J. G., Torres, J. J. & Bianconi, G. Higher-order simplicial synchronization of coupled topological signals. Commun. Phys. 4, 120 (2021).

[R13] Battiston, F., Cencetti, G., Iacopini, I., Latora, V., Lucas, M., Patania, A., Young, J.-G. & Petri, G. Networks beyond pairwise interactions: Structure and dynamics. Phys. Rep. 874, 1–92 (2020).

[R14] Zhang, Y., Lucas, M. & Battiston, F. Higher-order interactions shape collective dynamics differently in hypergraphs and simplicial complexes. Nat. Commun. 14, 1605 (2023).

[R15] Ferraz de Arruda, G., Aleta, A. & Moreno, Y. Contagion dynamics on higher-order networks. Nature Reviews Physics, 1–15 (2024).

[R16] Barash, V., Cameron, C. & Macy, M. Critical phenomena in complex contagions. Soc. Netw. 34, 451–461 (2012).

[R17] Barrat, A., Ferraz de Arruda, G., Iacopini, I. & Moreno, Y. in Higher-order systems 329–346 (Springer, 2022).

[R18] Iacopini, I., Petri, G., Barrat, A. & Latora, V. Simplicial models of social contagion. Nat. Commun. 10, 2485 (2019).

[R19] Jhun, B., Jo, M. & Kahng, B. Simplicial SIS model in scale-free uniform hypergraph. Journal of Statistical Mechanics: Theory and Experiment 2019, 123207 (2019).

[R20] Aiyappa, R., Flammini, A. & Ahn, Y.-Y. Emergence of simple and complex contagion dynamics from weighted belief networks. Science advances 10, eadh4439 (2024).

[R21] Neuh¨auser, L., Mellor, A. & Lambiotte, R. Multibody interactions and nonlinear consensus dynamics on networked systems. Physical Review E 101, 032310 (2020).

Article title: Transformability of Dynamics on Higher-order Networks
Manuscript Number: COMMSPHYS-25-1130B

Response to editors

Comments to the Author:

Your manuscript titled "Transformability of Dynamics on Higher-order Networks" has now been seen again by 2 referees. You will see from their comments below that some important points, raised by Reviewer 1, still need to addressed. We are interested in the possibility of publishing your study in Communications Physics, but would like to consider your response to these concerns in the form of a revised manuscript before we make a final decision on publication. We therefore invite you to revise and resubmit your manuscript, taking into account the points raised. Please highlight all changes in the manuscript text file.

Reply: We would like to thank editors for their time on our manuscript. Following the comments given by the reviewers, we carefully revised the manuscript. All the revisions are marked in red in the updated manuscript.

Response to the comments of Reviewer #1

Reviewer #1 (Remarks to the Author):

During this revision phase, the authors have made a wide set of modifications to the original version of the paper. I appreciate the attention they paid to the reviewers' suggestions.

I consider the paper significantly improved in terms of clarity and structure. However, I'm not fully satisfied by the modifications and I still have some major and minor concerns that the authors should address before considering the paper for publication in Communication Physics. I detail my concerns below.

Reply: We sincerely thank the reviewer for their insightful comments. Below, we provide detailed responses addressing each of the concerns.

Major issues.

1 Fig. 4 is obtained for a specific value of m and of X: what if they are changed? For example, if the size of interactions is larger? Or with a larger number of infected? Moreover, these results are obtained for a specific structure? If yes, which one (it's not specified in the caption)? The existence of Q^* should be investigated in more details and overall for different m and X: what if Q^* exists for m=3 but not for m=4? It's easier to satisfy the condition for smaller m? And for smaller X? And what is the role of the structure underlying the process? For example, Fig. 3 of SI already partially goes in this direction: for that Fig. what would be Q^*?

Reply: We sincerely thank the reviewer for the comments. We acknowledge that the previous Fig. 4 considered a specific (m, χ) pair and did not fully clarify the generality of our results.

In response to the concern, we have made three main improvements in the revised manuscript. First, we have provided a clarified description of (m, χ) in the transformable conditions, including a detailed explanation of λ as introduced earlier. Second, we have revised and clarified the description of Q^* in hypergraph contagion. Third, we have analyzed the behavior of Q^* under variations of m and χ, updated Fig. 4 accordingly, and incorporated several new findings in the revised manuscript.

Specifically, in Section 2.1, we clarified that the transformable conditions (Eq. 2 and Eq. 3, C1 and C3) are not restricted to a specific structure nor to a single (m, χ) pair. These conditions hold for all (m, χ) pairs observed during the contagion process in the general hypergraph setting. We carefully re-verified the condition and reformulated it as a piecewise function to more clearly express the criteria.

Building on this, in Section 2.2 we have explicitly revised the description of Q^* for hypergraph contagion dynamics by formally defining the component $q_{m,\chi}^{\kappa}$. For a fixed mapping ratio κ, Q^* is satisfied if and only if $q_{m,\chi}^{\kappa} = 0$ for all (m, χ) observed during the contagion process, denoted as $\left(q^{\kappa}_{m,\chi}\right)^{*}$.

Guided by the analysis of $q^{\kappa}_{m,\chi}$ in Fig. 3 of the Supplementary Information, which illustrates the scale of $q^{\kappa}_{m,\chi}$ across different m values, we conducted additional experiments to systematically investigate the existence of $\left(q^{\kappa}_{m,\chi}\right)^{*}$ across different values of m and χ, and updated the original Fig. 4 accordingly (see Fig. R1 in this response). To quantitatively capture the difficulty of decomposition, we defined $\Lambda_{m,\chi}$ as the permissible range of $\lambda_{m,\chi}$ for which $\left(q^{\kappa}_{m,\chi}\right)^{*}$ holds, while keeping κ fixed. The results shown in Fig. R1d are derived from the analysis of Eq. 4 in the manuscript. While this figure illustrates the case in which the maximum hyperedge size is less than 10, the underlying principle captured by Fig. R1d and Eq. 4 can be extended to hypergraphs with larger hyperedges and broader structural heterogeneity. Our results show that as m increases, the number of (m,χ) conditions that can be satisfied grows, and as χ increases, $\Lambda_{m,\chi}$ correspondingly shrinks. This indicates that achieving Q^{*} can become increasingly restrictive in hypergraphs with larger hyperedges, particularly when large hyperedges frequently contain higher numbers of infected nodes during the contagion process.

In addition, we have further reviewed and updated other relevant descriptions throughout the manuscript, with the revisions indicated in red in the revised version.

The specific revisions implemented in the manuscript are detailed below.

Page 5, Section 2.1:

We denote by $\chi = \chi_h(t)$ *the number of I-state nodes in each hyperedge* $h\,(h \in \mathcal{E}_i)$ *adjacent to the S-state node* i *at time* t*, where* $\mathcal{E}_i$ *is the set of hyperedges incident to* i*. In most formulations of contagion dynamics on hypergraphs,* λ *is assumed to be a uniform basic infection rate across all hyperedges and time steps. To explore the relationship between dynamics on hypergraphs and simplicial complexes in depth, in this study, we relax this assumption and consider that* λ *need not be uniform across all hyperedges, but may take distinct values for hyperedges with different size* m *and number of infected nodes* χ *at different time steps. This parametrization provides a flexible yet controlled framework for systematically comparing different contagion dynamics and for elucidating their potential equivalence.*

Page 5, Section 2.1:

We find that, for all combinations of (m,χ) *observed during the contagion process on hypergraph (here, we denote* $\mathcal{Z}$ *as the set of distinct* (m,χ) *pairs observed during the process), the consistency between two dynamical processes is ensured when* $\lambda^{\kappa}_{m,\chi}$ *and* β_{δ} *satisfy a specific relationship. Specifically, this consistency holds under the following condition (Condition 1, C1):*

$$\lambda_{m,\chi}^{\kappa} = \frac{1}{\chi^{\nu}} \begin{cases} \sum_{a=\tau}^{\tau^*} \binom{\chi}{a} \binom{m-\chi-1}{\kappa-a} \sum_{b=1}^{a} \binom{a}{b} \beta_b, & \kappa < m, \\ \sum_{a=1}^{\chi} \binom{\chi}{a} \beta_a, & \kappa \geq m. \end{cases} \quad \forall (m,\chi) \in \mathcal{Z}, \tag{2}$$

where $\tau = max(1, \kappa + 1 - (m - \chi))$ and $\tau^* = min(\kappa, \chi)$. We note that this equation does not prescribe λ as a functional form of m and χ. Instead, it identifies the circumstance under which the two dynamical processes coincide, with the parameters m and χ serving as the key quantities that reconcile their difference. We note that the proposed formulation is flexible, the case $\nu = 1$ corresponds merely to the linear limit, serving as a special instance within this general framework. Further details regarding the dynamic transformation can be found in the Supplementary Information. Combining Eq. 2 with the condition defined as $\beta_\delta = 0$ for $\delta > 1$ (Condition 2, C2), the contagion dynamics on $\mathcal{H}$ become equivalent to those on its projected dyadic graph with multiple edges when the following condition (Condition 3, C3) is satisfied:

$$\lambda_{m,\chi}^{\kappa} = \beta \begin{cases} \chi^{-\nu} \sum_{a=\tau}^{\tau^*} a \binom{\chi}{a} \binom{m-\chi-1}{\kappa-a}, & \kappa < m, \\ \chi^{1-\nu}, & \kappa \geq m. \end{cases} \quad \forall (m,\chi) \in \mathcal{Z}. \tag{3}$$

Page 7, Section 2.2:

For the dynamical factor, in order to explicitly characterize the nonlinearity inherent in node infections, we introduce the measure Q, defined as:

$$Q = \mathcal{A} \cdot \mathbb{I}_{\Upsilon=\mathcal{H}} + \mathcal{B} \cdot \mathbb{I}_{\Upsilon=\mathcal{C}}, \tag{4}$$

where $\mathcal{A} = \sum_{(m,\chi)\in\mathcal{Z}} q_{m,\chi}^{\kappa}$ and $\mathcal{B} = \beta_\delta^2(\delta > 1)$. Here, $\mathbb{I}$ is an indicator function, where $\mathbb{I}_{\Upsilon=\mathcal{H}}$ equals 1 if the system Υ is a hypergraph and 0 if it is a simplicial complex. The component $q_{m,\chi}^{\kappa}$ is defined as $q_{m,\chi}^{\kappa} = [\lambda_{m,\chi}^{\kappa} - \beta(\mathbb{I}_{\kappa<m}\, \chi^{-\nu} \sum_{a=\tau}^{\tau^*} a\binom{\chi}{a}\binom{m-\chi-1}{\kappa-a}) + \mathbb{I}_{\kappa\geq m}\, \chi^{1-\nu})]^2$.

The measure of Q thus indicates the degree of restrictiveness associated with the proposed transformable conditions. Specifically, when C2 (or C3) is satisfied for dynamics on a hypergraph (or a simplicial complex), the measure reduces to $Q = 0$. In such cases, we denote Q as Q^* for clarity.

Notably, when the indicator $\mathbb{I}_{\Upsilon=\mathcal{H}} = 1$ and κ is fixed, the condition Q^* is fulfilled if $q_{m,\chi}^{\kappa} = 0$ for all $(m,\chi) \in \mathcal{Z}$, which we denote as $(q_{m,\chi}^{\kappa})^*$.

Pages 8-9, Section 2.2:

Q^* as a criterion for dynamic transformation. *The feasibility of decomposition into structural and dynamical components critically depends on the value of Q^*. For contagion dynamics on hypergraphs, achieving Q^* requires that $q_{m,\chi}^{\kappa} = 0$ for all observed $(m,\chi) \in \mathcal{Z}$. Here, we fix $\kappa = 2$ as a representative scenario and perform the* *subsequent analysis. Since* κ *is fixed throughout, we henceforth denote* $\lambda_{m,\chi}^{\kappa}$ *and* $q_{m,\chi}^{\kappa}$ *by* $\lambda_{m,\chi}$ *and* $q_{m,\chi}$*, respectively (and* $\left(q_{m,\chi}^{\kappa}\right)^{*}$ *by* $q_{m,\chi}^{*}$*) for brevity. To evaluate when condition of* Q^{*} *can be satisfied, we systematically investigate* $q_{m,\chi}^{*}$ *across across a broad range of hyperedge sizes* m *and numbers of infected nodes* χ *within the hyperedges. As shown in Fig. 4a–c, when the interaction size is small (*$m = 2$*) and the number of infected nodes is low (*$\chi = 1$*), the admissible interval of* $\lambda_{m,\chi}$ *that allowing a mapping between contagion on a hypergraph and that on its projected multi-edge representation remains relatively broad, which in turn promotes decomposition. However, for* $(m, \chi) = (3,2)$ *or* $(4,3)$*, the feasible domain of* $\lambda_{m,\chi}$ *rapidly contracts. This narrowing indicates that, larger group interactions or denser local infection levels may impose stricter constraints on the existence of a valid mapping between hypergraph contagion and that on multi-edge dyadic graphs, thus reducing the feasibility of decomposition. For instance, Fig. 4b shows that when* $\lambda_{3,2} > 0.2$*, no valid mapping exists, and decomposition becomes infeasible.*

To quantitatively capture the difficulty of decomposition, we define $\Lambda_{m,\chi}$ *as the permissible range of* $\lambda_{m,\chi}$ *for which* $q_{m,\chi}^{*}$ *holds. The analysis in Fig. 4d demonstrates that the diversity of* $\Lambda_{m,\chi}$ *increases with larger hyperedges, while the values of* $\Lambda_{m,\chi}$ *systematically shrink as* χ *increases, imposing stricter constraints and narrowing the parameter space for achieving* Q^{*}*. Notably, hypergraphs with* $m = 4$ *hyperedges exhibit additional* (m, χ) *combinations than those limited to* $m = 3$*, and* $\Lambda_{4,3} < \Lambda_{3,2}$*, suggesting that decomposition is more challenging in hypergraphs with larger hyperedges.*

We further extend this analysis to simplicial complexes, where $\beta_{\Delta} = 0$ *determines whether decomposition is attainable (Fig. 4e). These results highlight a fundamental finding, i.e., the existence of* Q^{*} *is not guaranteed universally but is restricted to specific parameter regimes. Consequently, the applicability of our framework depends on whether the underlying dynamics fall within these regimes. This observation underscores the importance of* Q^{*} *not only as a technical requirement, but also as a critical criterion delineating when higher-order contagion processes can, or cannot, be faithfully reduced to lower-order representations.*

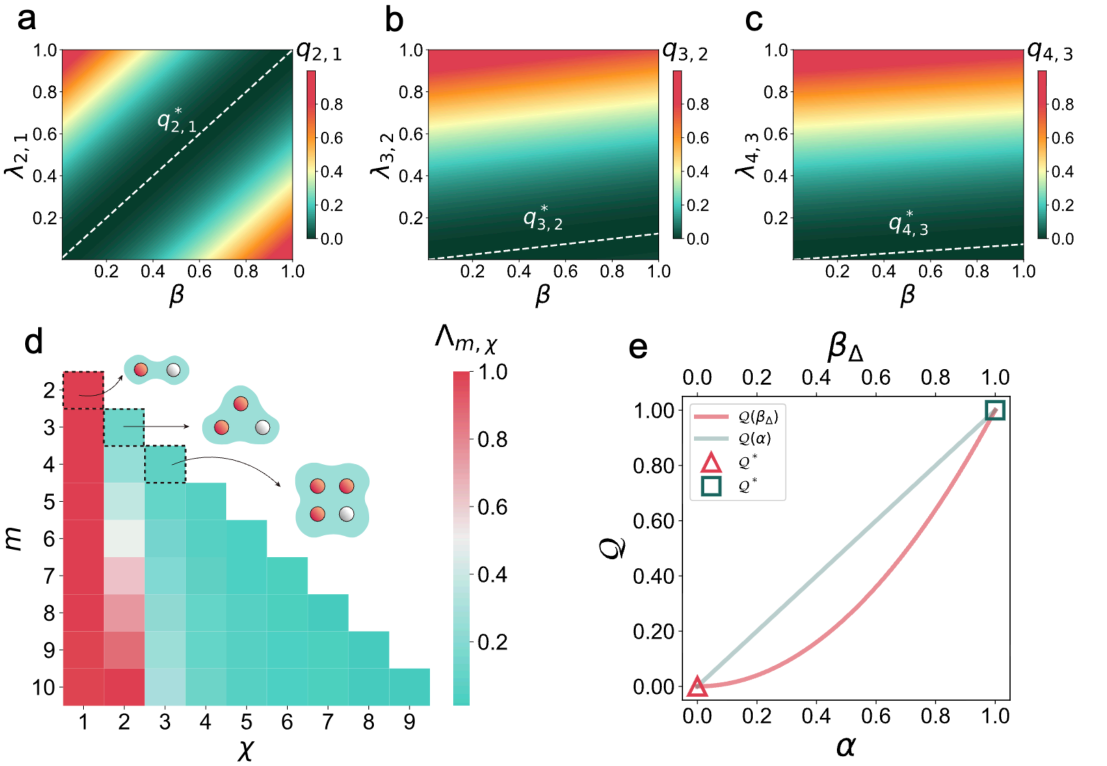

Fig. R1. (Fig. 4 in the revised manuscript) *Q^* in dynamics on hypergraphs and simplicial complexes.* ***a-c*** *Variation of $q_{m,\chi}$ with respect to $\lambda_{m,\chi}$ and β in contagion dynamics on hypergraphs ($\mathbb{I}_{\Upsilon=\mathcal{H}}$) with $(m,\chi)=(2,1),(3,2)$ and $(4,3)$. The dashed line indicates the condition $q^*_{m,\chi}$ required to achieve Q^*. Here, we focus on $\kappa=2$.* ***d*** *Permissible range of $\lambda_{m,\chi}$ required to achieve Q^* for contagion dynamics on hypergraphs, denoted as $\Lambda_{m,\chi}$, shown for different hyperedge sizes m and corresponding numbers of infected nodes χ. The same κ settings are used.* ***e*** *Variation of Q with respect to β_Δ in contagion dynamics on simplicial complexes (red line), where the red triangle denotes $Q=Q^*$. The green line shows Q for two opinion dynamics on hypergraphs, with the green square indicating Q^*. We note that α represents a factor controlling the nonlinear scaling of influence from neighboring hyperedges in the opinion updating mechanism in opinion dynamics, as detailed in the following Section 2.3 and the Methods section.*

2.1 Fig. 4 and Eq. (4) show that Q is different for different m and X. If in the hypergraphs there are different hyperedges of different sizes and with different number of infected, how this is impacting Q^*?

Reply: We sincerely thank the reviewer for this insightful and constructive comment. As noted above, the previous results did not sufficiently illustrate how variations in m and χ affect Q^*. To address this concern, we first defined a component $q_{m,\chi}^{\kappa}$ to explicitly characterize the value of Q under different hyperedge sizes m and numbers of infected nodes χ within the hyperedges when the mapping ratio κ is fixed. Under this definition, the condition Q^* for dynamics on hypergraphs is satisfied if $q_{m,\chi}^{\kappa} = 0$ for all $(m, \chi) \in \mathcal{Z}$, denoted as $\left(q_{m,\chi}^{\kappa}\right)^*$. Here, $\mathcal{Z}$ represents the set of distinct (m, χ) pairs observed during the process.

Furthermore, we systematically investigated how variations m and χ influence Q^*. Since achieving Q^* requires that $\left(q_{m,\chi}^{\kappa}\right)^*$ is satisfied for all $(m, \chi) \in \mathcal{Z}$, we evaluated $\left(q_{m,\chi}^{\kappa}\right)^*$ across a broad range of m and χ (see Fig. R1a–c). To quantitatively capture the restrictiveness of the decomposition, we defined $\Lambda_{m,\chi}$ as the permissible range of $\lambda_{m,\chi}$ for which $q_{m,\chi}^*$ holds. Fig. R1d illustrates the resulting trends, showing that larger group interactions or denser local infection levels can reduce the feasible parameter space, thereby decreasing the feasibility of decomposition.

Page 7, Section 2.2:

For the dynamical factor, in order to explicitly characterize the nonlinearity inherent in node infections, we introduce the measure Q*, defined as:*

$$Q = \mathcal{A} \cdot \mathbb{I}_{\Upsilon=\mathcal{H}} + \mathcal{B} \cdot \mathbb{I}_{\Upsilon=\mathcal{C}}, \tag{4}$$

where $\mathcal{A} = \sum_{(m,\chi)\in Z} q_{m,\chi}^{\kappa}$ *and* $\mathcal{B} = \beta_{\delta}^{2}(\delta > 1)$. *Here,* $\mathbb{I}$ *is an indicator function, where* $\mathbb{I}_{\Upsilon=\mathcal{H}}$ *equals 1 if the system* Υ *is a hypergraph and 0 if it is a simplicial complex. The component* $q_{m,\chi}^{\kappa}$ *is defined as* $q_{m,\chi}^{\kappa} = [\lambda_{m,\chi}^{\kappa} - \beta(\mathbb{I}_{\kappa<m}\, \chi^{-\nu} \sum_{a=\tau}^{\tau^*} a\binom{\chi}{a}\binom{m-\chi-1}{\kappa-a}) + \mathbb{I}_{\kappa\geq m}\, \chi^{1-\nu})]^2$.

The measure of Q *thus indicates the degree of restrictiveness associated with the proposed transformable conditions. Specifically, when C2 (or C3) is satisfied for dynamics on a hypergraph (or a simplicial complex), the measure reduces to* $Q = 0$. *In such cases, we denote* Q *as* Q^* *for clarity.*

Notably, when the indicator $\mathbb{I}_{\Upsilon=\mathcal{H}} = 1$ *and* κ *is fixed, the condition* Q^* *is fulfilled if* $q_{m,\chi}^{\kappa} = 0$ *for all* $(m, \chi) \in \mathcal{Z}$, *which we denote as* $\left(q_{m,\chi}^{\kappa}\right)^*$.

Pages 8-9, Section 2.2:

Q^* as a criterion for dynamic transformation. *The feasibility of decomposition into structural and dynamical components critically depends on the value of* Q^*. *For contagion dynamics on hypergraphs, achieving* Q^* *requires that* $q_{m,\chi}^{\kappa} = 0$ *for all observed* $(m, \chi) \in \mathcal{Z}$. *Here, we fix* $\kappa = 2$ *as a representative scenario and perform the subsequent analysis. Since* κ *is fixed throughout, we henceforth denote* $\lambda_{m,\chi}^{\kappa}$ *and* $q_{m,\chi}^{\kappa}$ *by* $\lambda_{m,\chi}$ *and* $q_{m,\chi}$, *respectively (and* $\left(q_{m,\chi}^{\kappa}\right)^*$ *by* $q_{m,\chi}^*$*) for brevity. To evaluate when condition of* Q^* *can be satisfied, we systematically investigate* $q_{m,\chi}^*$ *across across a broad range of hyperedge sizes* m *and numbers of infected nodes* χ *within the hyperedges. As shown in Fig. 4a–c, when the interaction size is small (*$m = 2$*) and the* *number of infected nodes is low ($\chi = 1$), the admissible interval of $\lambda_{m,\chi}$ that allowing a mapping between contagion on a hypergraph and that on its projected multi-edge representation remains relatively broad, which in turn promotes decomposition. However, for $(m,\chi) = (3,2)$ or $(4,3)$, the feasible domain of $\lambda_{m,\chi}$ rapidly contracts. This narrowing indicates that, larger group interactions or denser local infection levels may impose stricter constraints on the existence of a valid mapping between hypergraph contagion and that on multi-edge dyadic graphs, thus reducing the feasibility of decomposition. For instance, Fig. 4b shows that when $\lambda_{3,2} > 0.2$, no valid mapping exists, and decomposition becomes infeasible.*

To quantitatively capture the difficulty of decomposition, we define $\Lambda_{m,\chi}$ as the permissible range of $\lambda_{m,\chi}$ for which $q^*_{m,\chi}$ holds. The analysis in Fig. 4d demonstrates that the diversity of $\Lambda_{m,\chi}$ increases with larger hyperedges, while the values of $\Lambda_{m,\chi}$ systematically shrink as χ increases, imposing stricter constraints and narrowing the parameter space for achieving Q^*. Notably, hypergraphs with $m = 4$ hyperedges exhibit additional (m,χ) combinations than those limited to $m = 3$, and $\Lambda_{4,3} < \Lambda_{3,2}$, suggesting that decomposition is more challenging in hypergraphs with larger hyperedges.

We further extend this analysis to simplicial complexes, where $\beta_\Delta = 0$ determines whether decomposition is attainable (Fig. 4e). These results highlight a fundamental finding, i.e., the existence of Q^* is not guaranteed universally but is restricted to specific parameter regimes. Consequently, the applicability of our framework depends on whether the underlying dynamics fall within these regimes. This observation underscores the importance of Q^* not only as a technical requirement, but also as a critical criterion delineating when higher-order contagion processes can, or cannot, be faithfully reduced to lower-order representations.

2.2 The entropy is calculated for Q^* fixing the parameters differently for each m and X? For example, in caption of Fig. 3 the authors say "... where \lambda satisfies Eq. 3", so this means a different \lambda for different m and X?

Reply: We sincerely thank the reviewer for these comments. As clarified above, Q^* is defined as a point at which the consistency condition holds simultaneously for all (m,χ) pairs that may arise during the contagion process on hypergraphs. Accordingly, the entropy at Q^* is always evaluated on the self-consistent solution. The corresponding $\lambda^{\kappa}_{m,\chi}$ values are determined from the self-consistency equations, and therefore can indeed differ across different (m,χ) pairs. For instance, in Fig. 3 the self-consistent solution used to compute Q^* is given by $\lambda^2_{2,1} = \lambda^2_{3,1} = \beta$ and $\lambda^2_{3,2} = (2\beta + \beta_\Delta)/2^\nu$. To avoid ambiguity, we have updated the caption of Fig. 3 in the revised manuscript to explicitly specify these values, as follows:

Page 6, Section 2.2:

In ***a****,* $\Delta\Phi_1(t)$ *is calculated as* $\Delta\Phi_1(t) = \Phi^{\mathcal{Q}}(t) - \Phi^{\mathcal{Q}^*}(t)$, *with* $\mathcal{Q}(\lambda = 0.005, \nu = 4)$ *and* $\mathcal{Q}^*(\nu = 1)$, *where* $\lambda_{2,1}^2 = \lambda_{3,1}^2 = \beta$ *and* $\lambda_{3,2}^2 = (2\beta + \beta_\Delta)/2^\nu$ *for* $\mathcal{Q}^*$.

3 I still find quite unclear how the authors treat the \lambda parameter: if it "represents a constant infection rate" how it can "assume different values under different settings of m and X"? In particular, the conditions for mapping the process to the simplicial contagion case are different for different m and X, but a general hypergraph is made by different hyperedges of different sizes (m) and with a different number of infected nodes over time within them (X): so the conditions for a specific m and X are usually not valid for others and cannot be fulfilled all simultaneously, since \lambda is constant? This is partially linked to the previous point.

Reply: We sincerely thank the reviewer for this question. We agree that our previous phrasing could lead to confusion. In the revised manuscript, we now make explicit that the "constant infection rate" refers to constancy within a given (m, χ) class, while λ is allowed to take different constant values across different (m, χ) classes. This is a modeling choice that enables us to systematically characterize the precise circumstances under which the two dynamical processes coincide. In this formulation, m and χ serve as the quantities that reconcile the discrepancies between hypergraph contagion and simplicial contagion.

Thus, for a general heterogeneous hypergraph, where hyperedges of different sizes coexist and where χ varies over time, the mapping conditions to simplicial contagion must hold simultaneously for all (m, χ) pairs that are actually observed during the process, and not for a single fixed (m, χ) pair. The revised text now clearly states this.

In this revision, we have removed the previous confusing sentences and rewrote the formal description of λ in the main text. Furthermore, we have clarified that the mapping conditions (now Eq. 2 and Eq. 3 in the manuscript) are required to hold for all (m, χ) pairs observed during the process, rather than for any single fixed pair.

Page 5, Section 2.1:

We denote by $\chi = \chi_h(t)$ *the number of I-state nodes in each hyperedge* $h\,(h \in \mathcal{E}_i)$ *adjacent to the S-state node* i *at time* t*, where* $\mathcal{E}_i$ *is the set of hyperedges incident to* i*. In most formulations of contagion dynamics on hypergraphs,* λ *is assumed to be a uniform basic infection rate across all hyperedges and time steps. To explore the relationship between dynamics on hypergraphs and simplicial complexes in* *depth, in this study, we relax this assumption and consider that λ need not be uniform across all hyperedges, but may take distinct values for hyperedges with different size m and number of infected nodes χ at different time steps. This parametrization provides a flexible yet controlled framework for systematically comparing different contagion dynamics and for elucidating their potential equivalence.*

Page 5, Section 2.1:

We find that, for all combinations of (m, χ) observed during the contagion process on hypergraph (here, we denote $\mathcal{Z}$ as the set of distinct (m, χ) pairs observed during the process), the consistency between two dynamical processes is ensured when $\lambda^{\kappa}_{m,\chi}$ and β_δ satisfy a specific relationship. Specifically, this consistency holds under the following condition (Condition 1, C1):

$$\lambda^{\kappa}_{m,\chi} = \frac{1}{\chi^{\nu}} \begin{cases} \sum_{a=\tau}^{\tau^*} \binom{\chi}{a} \binom{m-\chi-1}{\kappa-a} \sum_{b=1}^{a} \binom{a}{b} \beta_b, & \kappa < m, \\ \sum_{a=1}^{\chi} \binom{\chi}{a} \beta_a, & \kappa \geq m. \end{cases} \quad \forall (m, \chi) \in \mathcal{Z}, \qquad (2)$$

where $\tau = max\big(1, \kappa + 1 - (m - \chi)\big)$ and $\tau^* = min(\kappa, \chi)$. We note that this equation does not prescribe λ as a functional form of m and χ. Instead, it identifies the circumstance under which the two dynamical processes coincide, with the parameters m and χ serving as the key quantities that reconcile their difference. We note that the proposed formulation is flexible, the case $\nu = 1$ corresponds merely to the linear limit, serving as a special instance within this general framework. Further details regarding the dynamic transformation can be found in the Supplementary Information. Combining Eq. 2 with the condition defined as $\beta_\delta = 0$ for $\delta > 1$ (Condition 2, C2), the contagion dynamics on $\mathcal{H}$ become equivalent to those on its projected dyadic graph with multiple edges when the following condition (Condition 3, C3) is satisfied:

$$\lambda^{\kappa}_{m,\chi} = \beta \begin{cases} \chi^{-\nu} \sum_{a=\tau}^{\tau^*} a \binom{\chi}{a} \binom{m-\chi-1}{\kappa-a}, & \kappa < m, \\ \chi^{1-\nu}, & \kappa \geq m. \end{cases} \quad \forall (m, \chi) \in \mathcal{Z}. \qquad (3)$$

4 The discussion on the limitations of the work are improved, however I think that the discussion on the existence of Q^* should also be more stressed in the main text (not only in the Discussion): especially regarding the GDW opinion dynamics, which shows that intrinsically higher-order processes do not fall (easily) in the group of transformable processes (and this is very relevant). Moreover, I was expecting them to be transformable at least from the structural point of view, if the underlying hypergraph has only pairwise interactions.

Reply: We sincerely thank the reviewer for this suggestion. We fully agree that highlighting the existence (or non-existence) of the transformation operator Q^* in intrinsically higher-order opinion dynamics is important, particularly in the context of the group-based DW (GDW) model. In response, we have added a dedicated subsection in the main text entitled "Existence of Q^* in intrinsically higher-order opinion dynamics", where we explicitly discuss this point.

In this new subsection, we consider the typical GDW model on hypergraphs proposed in [R1] (provided at the end of this response), which is intrinsically higher-order. We formally present the update rule and illustrate that, due to the group-level tolerance condition and the nonlinear scaling with hyperedge size, the GDW dynamics cannot be straightforwardly mapped to a pairwise multigraph process, preventing the straightforward existence of Q^* for generic hypergraphs.

Nevertheless, we clarify a notable case: for 2-uniform hypergraphs, in which all hyperedges are pairwise, the nonlinear term in the GDW update rule reduces to 1, and the dynamics effectively coincide with those on a simple graph. In this special case, the structural contribution from hyperedges becomes trivial, and the transformation operator Q^* exists. This demonstrates that, while GDW dynamics are generally intrinsically higher-order and not easily transformable, the existence of Q^* can be restored under specific structural constraints. All relevant equations and explanations have been incorporated into the main text to make this point explicit, the details are provided below.

Page 12, Section 2.3:

Existence of Q^* in intrinsically higher-order opinion dynamics. *Beyond the opinion dynamics discussed above, we further consider the group-based DW (GDW) model on hypergraphs [40], which is inherently higher-order. In a typical GDW model [46], a hyperedge is randomly selected at each iteration, and if the group-level opinion variance among its nodes falls below a tolerance threshold, all nodes within that hyperedge adopt the group's average opinion. Formally, the GDW update rule is given by* $\frac{1}{(|h_r|-1)^{\alpha'}}\sum_{i\in h_r}\left(o_i(t)-\overline{o}_{h_r}(t)\right)^2<\epsilon$, *where* h_r *denotes a randomly selected hyperedge at time* t, α' *is an adjustable model parameter, and* $\overline{o}_{h_r}(t)$ *is the average opinion of its nodes. If this rule is satisfied, each node updates as* $o_i(t+1)=\overline{o}_{h_r}(t)$ *for all* $i\in h_r$*; otherwise, opinions remain unchanged,* $o_i(t+1)=o_i(t)$.

As previously noted, the existence of a transformation operator Q^* *is essential for connecting such higher-order dynamics with their projected multi-edge counterparts. However, for GDW dynamics this mapping is inherently difficult. The discrepancies arise because (i) the expected opinion increments induced by a hyperedge do not match* *those in the multigraph DW model, and (ii) the tolerance condition is evaluated collectively over an entire group rather than on individual pairs. These features make GDW intrinsically higher-order and prevent it from being easily transformed into an equivalent pairwise process.*

Nevertheless, we consider a notable case of a specific structure, namely 2-uniform hypergraphs, in which all hyperedges involve only pairwise interactions. In this setting, each randomly selected hyperedge h_r *contains two nodes, which we denote as* i_1 *and* i_2*. Since* $(|h_r| - 1) \equiv 1$*, the nonlinear factor in the update rule,* $\frac{1}{(|h_r|-1)^{\alpha'}}$*, reduces to 1. Consequently, the GDW update condition simplifies to* $\left(x_{i_1} - x_{i_2}\right)^2 < 2\epsilon$*, indicating that the opinion dynamics on a 2-uniform hypergraph therefore reduce to those on graphs. In this case, all dynamical contributions associated with the nonlinear term* $\frac{1}{(|h_r|-1)^{\alpha'}}$ *are absorbed, and the random selection of a single edge per update ensures that dynamics on the multi-edge graphs and simple graphs coincide on average, i.e., the structural contribution effectively vanishes. This confirms that, although GDW dynamics on hypergraphs are challenging to fall in the group of transformable processes, the special case of 2-uniform hypergraphs with only pairwise interactions restores the existence of* Q^**.*

Minor issues.

1.1 There are still many notation problems and inaccuracies (some even if I already highlighted them in the previous review round): for example, the definition of X is introduced in page 13, but should appear before, in page 5 already (since it's used there).

Reply: We sincerely thank the reviewer for this suggestion. We carefully re-checked the entire manuscript for notation consistency and resolved the remaining issues. Specifically, the definition of χ has now been moved forward to the first place where it appears (page 5 in the revised version). This ensures that the symbols are formally introduced before being used. In addition, we re-verified the related condition and reformulated it explicitly into a piecewise form in the main text to avoid ambiguity (now Eq. 2 and Eq. 3). Consistently, all corresponding formulations in the Methods (now Eq. 16 and Eq. 17) and in the Supplementary Information (now Eq. 22 and Eq. 23) have been updated to the same piecewise notation. Furthermore, we carefully re-examined the entire manuscript for notation accuracy and clarity, and we have revised all issues identified during this process. All corresponding changes have been marked in red for the reviewer's convenience.

Page 5, Section 2.1:

We denote by $\chi = \chi_h(t)$ the number of I-state nodes in each hyperedge $h\,(h \in \mathcal{E}_i)$ adjacent to the S-state node i at time t, where $\mathcal{E}_i$ is the set of hyperedges incident to i.

Page 5, Section 2.1:

$$\lambda_{m,\chi}^{\kappa} = \frac{1}{\chi^{\nu}} \begin{cases} \sum_{a=\tau}^{\tau^*} \binom{\chi}{a} \binom{m-\chi-1}{\kappa-a} \sum_{b=1}^{a} \binom{a}{b} \beta_b, & \kappa < m, \\ \sum_{a=1}^{\chi} \binom{\chi}{a} \beta_a, & \kappa \geq m. \end{cases} \quad \forall (m,\chi) \in \mathcal{Z}, \tag{2}$$

$$\lambda_{m,\chi}^{\kappa} = \beta \begin{cases} \chi^{-\nu} \sum_{a=\tau}^{\tau^*} a \binom{\chi}{a} \binom{m-\chi-1}{\kappa-a}, & \kappa < m, \\ \chi^{1-\nu}, & \kappa \geq m. \end{cases} \quad \forall (m,\chi) \in \mathcal{Z}. \tag{3}$$

Page 16, Section 4.2:

$$\lambda_{m,\chi}^{\kappa} = \frac{1}{\chi^{\nu}} \begin{cases} \sum_{a=\tau}^{\tau^*} \binom{\chi}{a} \binom{m-\chi-1}{\kappa-a} \sum_{b=1}^{a} \binom{a}{b} \beta_b, & \kappa < m, \\ \sum_{a=1}^{\chi} \binom{\chi}{a} \beta_a, & \kappa \geq m. \end{cases} \quad \forall (m,\chi) \in \mathcal{Z}. \tag{16}$$

$$\lambda_{m,\chi}^{\kappa} = \beta \begin{cases} \chi^{-\nu} \sum_{a=\tau}^{\tau^*} a \binom{\chi}{a} \binom{m-\chi-1}{\kappa-a}, & \kappa < m, \\ \chi^{1-\nu}, & \kappa \geq m. \end{cases} \quad \forall (m,\chi) \in \mathcal{Z}. \tag{17}$$

Page 7, Supplementary Note 4:

$$\lambda_{m,\chi}^{\kappa} = \frac{1}{\chi^{\nu}} \begin{cases} \sum_{a=\tau}^{\tau^*} \binom{\chi}{a} \binom{m-\chi-1}{\kappa-a} \sum_{b=1}^{a} \binom{a}{b} \beta_b, & \kappa < m, \\ \sum_{a=1}^{\chi} \binom{\chi}{a} \beta_a, & \kappa \geq m. \end{cases} \quad \forall (m,\chi) \in \mathcal{Z}. \tag{22}$$

$$\lambda_{m,\chi}^{\kappa} = \beta \begin{cases} \chi^{-\nu} \sum_{a=\tau}^{\tau^*} a \binom{\chi}{a} \binom{m-\chi-1}{\kappa-a}, & \kappa < m, \\ \chi^{1-\nu}, & \kappa \geq m. \end{cases} \quad \forall (m,\chi) \in \mathcal{Z}. \tag{23}$$

1.2 In Eq.s (12,13) on the right-hand side there should be a subscript as at the first member.

Reply: Thanks for this suggestion. We have verified the notation and updated the right-hand side of Eq. 12 and Eq. 13 to include the appropriate subscript, consistent with the first term. The updated equations are now reflected in the revised manuscript as follows.

Page 15, Section 4.2:

$$\frac{dI_{\mathcal{G}}(t)}{dt} = \left(1 - I_{\mathcal{G}}(t)\right) \cdot \langle k^* \rangle \cdot \beta \cdot I_{\mathcal{G}}(t). \tag{12}$$

$$\frac{dI_{\mathcal{C}}(t)}{dt} = \sum_{\delta=1}^{max|u|,u\in U} (1 - I_{\mathcal{C}}(t)) \cdot \langle k_{\delta}^* \rangle \cdot \beta_{\delta} \cdot (I_{\mathcal{C}}(t))^{\delta}. \tag{13}$$

1.3 What is the "bound c" in Fig. 5 caption? Maybe it should be \epsilon?

Reply: We thank the reviewer for this comment. We have checked this notation issue and revised the term “bound c” in the caption of Fig. 5. In the main text, the bound in the opinion dynamics is now consistently denoted by ϵ. Specifically, the revised description in the caption reads:

Page 10, Caption of Fig. 5:

The value of ϵ is set to 0.1 for the synthetic network and 0.003 for the Email-Enron, while the hypergraph DW model parameter α is 0.5 and 0.8, respectively.

1.4 A statement in Supp. Note 4 is still incorrect: the minimum number of infected in the simplex could be 0 potentially.

Reply: We thank the reviewer for pointing this out. We agree with the reviewer that in principle the number of infected nodes in the simplex could be zero. To avoid ambiguity, we have revised the description to clarify this case.

Page 6, Supplementary Note 4:

If $\chi = 0$, no contagion event can be supported on this hyperedge, and therefore in the mapped κ-simplex we have $\beta_\delta = 0$ for all admissible orders δ in this simplex. In the following, we therefore focus on hyperedges with at least one infected node ($\chi \geq 1$). Under this condition, the number of infected nodes in the mapped κ-simplex ranges from $max\left(1, \kappa + 1 - (m - \chi)\right)$ to $min(\kappa, \chi)$.

Page 15, Section 4.2:

For configurations where $\chi = 0$, contagion cannot occur through this hyperedge, hence in the mapped κ-simplex we have $\beta_\delta = 0$ for all admissible orders δ. We therefore focus on hyperedges with $\chi \geq 1$.

1.5 There is still usage of “network dynamics” in the text.

Reply: We thank the reviewer for this comment. We have carefully checked the manuscript and updated all occurrences of "network dynamics" to the more precise term "dynamics on networks." The specific revisions are listed below.

Page 7, Section 2.2:

While the preceding section established the fundamental framework for capturing local infection probabilities, a deeper understanding requires moving beyond node-level descriptions to examine the system-wide behavior of dynamics on networks.

Page 7, Section 2.2:

By leveraging entropy, we can identify and quantify the key factors governing dynamic transformations, thereby constructing a comprehensive scheme to unravel the distinctions between dynamics on higher-order networks and pairwise networks.

1.6 Fig. 4 of SI: still panels a and b are inverted with respect to the caption and a colorbar should be added to indicate the meaning of the colours under the curves.

Reply: We thank the reviewer for this comment. We have corrected panels a and b in Fig. 4 of the Supplementary Information so that they are consistent with the caption. Regarding the colors under the curves, we initially used them to indicate the gap between the two dynamical processes. However, we realized that the color shading might introduce unnecessary visual complexity and could potentially confuse the reader. Importantly, the gap is clearly visible from the curves themselves without the color shading. Therefore, we have removed the color shading and updated Fig. 4 in the Supplementary Information accordingly (see Fig. R2 in this response), which makes the gap between the two curves more directly apparent.

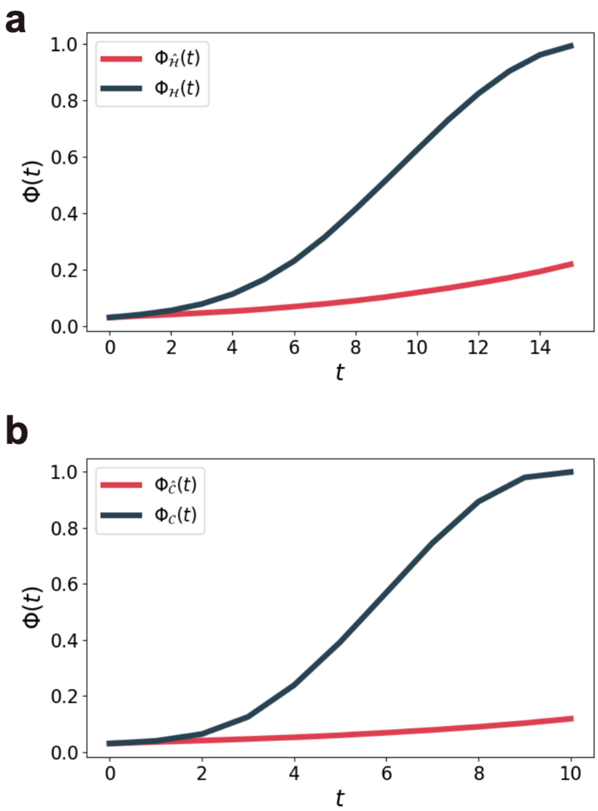

Fig.R2. (Fig. 4 in the Supplementary Information) *Encoding empirical systems with higher-order interactions as dyadic graphs leads to information loss in dynamics. The variance of information entropy Φ during contagion dynamics is analyzed in* ***a*** *a hypergraph $\mathcal{H}$,* ***b*** *a simplicial complex $\mathcal{C}$, and their projected simple graphs. Notably, the hypergraph and simplicial complex are derived from real datasets of High-school and Primary-school. As time steps increase, a growing disparity in Φ emerges between dynamics on hypergraphs (black) or simplicial complexes (black) and their projected graphs (red). The gap between the black and red curves indicate the variation in entropy change during the dynamics, highlighting the differences between dynamics on higher-order networks and those on their corresponding simple projections. Each time step t represents the average over 500 simulations of the SI contagion process.*

1.7 In SI, at the end of page 11: \Delta I_1 and I_2 are not defined for hypergraphs.

Reply: We thank the reviewer for this comment. We have added definitions of both ΔI_1 and ΔI_2 in the Supplementary Information. The details of the revision are provided below.

Page 11, Supplementary Note 7:

Here, in hypergraphs, we denote $\frac{dI_{\mathcal{H}}^{\mathcal{Q}}(t)}{dt} - \frac{dI_{\mathcal{H}}^{\mathcal{Q}^*}(t)}{dt}$ *and* $\frac{dI_{\widetilde{\mathcal{H}}}(t)}{dt} - \frac{dI_{\widehat{\mathcal{H}}}(t)}{dt}$ *as* ΔI_1 *and* ΔI_2*, respectively.*

Page 11, Supplementary Note 7:

Consequently, within the hypergraph contagion framework, it follows that the quantity $\Delta I^* = \frac{dI^{Q}_{\mathcal{H}}(t)}{dt} - \frac{dI_{\widehat{\mathcal{H}}}(t)}{dt}$ *is equivalent to the sum of* ΔI_1 *and* ΔI_2*.*

1.8 The last paragraph of the Introduction "To the best of our… dynamical systems" is repeated twice.

Reply: We sincerely thank the reviewer for this comment. We have removed the repeated text and updated the last paragraph of the Introduction. We believe this revision improves clarity and minimizes redundancy in the manuscript. The revised sentences now read:

Page 3, Section 1:

To the best of our knowledge, this study is the first to offer a comprehensive analysis for the transformability of dynamics on higher-order networks via the lens of system disorder. In addition, we provide a foundational understanding of the roles played by both structural and dynamical factors in dynamic transformations, thereby shedding light on the unique characteristics of higher-order dynamical systems.

1.9 In Fig. 2 caption, \beta is said to vary from 0.005 to 0.1, but it varies from 0.01 (see legend). Sometimes panels are indicated in bold and sometimes with "( )".

Reply: We thank the reviewer for pointing this out. We have carefully checked and corrected the description of β in the caption of Fig. 2 in the main text. The revised description now accurately reflects the range of β used, as indicated in the legend.

In addition, we have reviewed the figure captions throughout both the main text and the Supplementary Information, and updated them to ensure that all panels are consistently indicated in bold.

Page 4, Caption of Fig. 2:

a *Average infection density* $\overline{I}(t)$ *for contagion dynamics on a hypergraph and its projected simplicial complex, based on an empirical high-school social network. For the hypergraph (dots),* $\lambda^2_{2,1} = \lambda^2_{3,1} = \beta$, $\lambda^2_{3,2} = (2\beta + \beta_\Delta)/2^\nu$*; for the simplicial complex (lines),* $\beta_\Delta = 0.5$. β *varies from 0.01 to 0.1, with* $\kappa = 2$.

1.10 What is U in Eq. (9)?

Reply: We thank the reviewer for this comment. In Eq. 9, U denotes the set of all simplices in the simplicial complex $\mathcal{C}$. We have now added this definition in the main text to ensure clarity. The added description is as follows.

Page 15, Section 4.2:

where U denotes the set of all simplices in the simplicial complex $\mathcal{C}$.

1.11 At the end of Sec. 4.3, there is a typo (repeated twice) with a dot after "\mathcal(D)" that should not be there.

Reply: We thank the reviewer for pointing this out. We have corrected the typographical errors at the end of Section 4.3 in the main text, where the extra dot after $\mathcal{D}$ appeared twice. The updated descriptions now read as follows.

Page 18, Section 4.3:

Similar to the entropy indicator used in contagion dynamics, a high value of $\mathcal{D}$ in opinion dynamics means that individuals in the network hold very different opinions.

Page 18, Section 4.3:

In contrast, a low value of $\mathcal{D}$ suggests that most individuals share the same opinion, reflecting a consensus state.

1.12 Caption of Fig. 3 is unclear: what are the "dotted line", "dark-colored" and "light-colored" bars cited in the caption referring to panels a and b?

Reply: We sincerely thank the reviewer for this comment. In the previous revision, some redundant phrases related to the "dotted line," "dark-colored," and "light-colored" bars remained in the caption. We have now removed these redundancies and clarified the markings corresponding to panels a and b. The updated description is as follows.

Page 6, Section 2.2:

Note that, for clarity, the total entropy difference $\Delta\Phi^*$ (scatter points marked with "$\times$"), closely matches the sum of $\Delta\Phi_1$ and $\Delta\Phi_2$ (shown as bars).

2 In caption of Fig. 4 should be stated what is \alpha (since here it appears before than the Sec. in which it is introduced)

Reply: We sincerely thank the reviewer for this comment. To improve clarity, we have added a statement defining α in the caption of Fig. 4, as it appears before the section in which it is introduced. The updated description is detailed below.

Page 8, Caption of Fig. 4:

We note that α represents a factor controlling the nonlinear scaling of influence from neighboring hyperedges in the opinion updating mechanism in opinion dynamics, *as detailed in the following Section 2.3 and the Methods section.*

3 The information on numerical simulations is not enough: how are the different realizations created? Different initial conditions or different networks? When are the simulations stopped, and which initial conditions are used? This should be added in the text, for example with a dedicated small paragraph in the methods or in the captions. Moreover, the authors should check all the captions to see if everywhere is indicated: (i) how simulations are run; (ii) on which structure.

Reply: We sincerely thank the reviewer for this comment. We acknowledge that the information on numerical simulations was previously insufficient. We have now added detailed descriptions in the captions of the relevant figures, including the initial conditions used in each simulation, the stopping criteria, and the network structures on which the simulations are run. Additional clarifications have also been included in the Suppementary Information. The updated captions are provided below.

Page 4, Caption of Fig. 2:

The relationships of dynamics across network representations. a *Average infection density $\bar{I}(t)$ for contagion dynamics on a hypergraph and its projected simplicial complex, based on an empirical high-school social network. For the hypergraph (dots), $\lambda_{2,1}^{2} = \lambda_{3,1}^{2} = \beta$, $\lambda_{3,2}^{2} = (2\beta + \beta_{\Delta})/2^{\nu}$; for the simplicial complex (lines), $\beta_{\Delta} = 0.5$. β varies from 0.01 to 0.1, with $\kappa = 2$. Note that the $\lambda_{m,\chi}^{\kappa}$ represents the basic infection rate isolated by hyperedge size m, the number of infection nodes in the hyperedge χ and with the mapping ratio κ, see Methods for details.* ***b*** *Comparison of $\bar{I}(t)$ for dynamics on simplicial complex (dots) and those on projected dyadic graph (lines). Results for each type of contagion under the different parameter settings shown in **a** and **b** are averaged over 500 independent simulations with $\mathcal{T} = 30$. In each simulation, a single node is randomly initialized in the infected state, while all other nodes are set to the susceptible state.* ***c-d*** *F1-score variation as the system approaches critical states C1 and C2, respectively. Lower F1-scores in **c** indicate reduced accuracy in distinguishing hypergraph-based contagion, while higher F1-scores in **d** reflect improved classification of simplicial complex dynamics. The SVM classifier uses node degree and infection order features from simulations with $\lambda = 0.04, \nu = 1$ (hypergraphs) and $\beta = 0.04, \beta_{\Delta} = 0.8$ (simplicial complexes), see Methods for details of the experimental settings. Results are averaged over 10^3 runs with $\mathcal{T} = 50$.*

Page 6, Caption of Fig. 3:

Identification and quantification of contributing factors in contagion dynamics. a-b *Temporal evaluation of $\Delta\Phi_1(t) + \Delta\Phi_2(t)$ in SI contagion processes simulated on* *real-world datasets of primary school and high school interactions. In **a**, $\Delta\Phi_1(t)$ is calculated as $\Delta\Phi_1(t) = \Phi^{\mathcal{Q}}(t) - \Phi^{\mathcal{Q}^*}(t)$, with $\mathcal{Q}(\lambda = 0.005, \nu = 4)$ and $\mathcal{Q}^*(\nu = 1)$, where $\lambda_{2,1}^2 = \lambda_{3,1}^2 = \beta$ and $\lambda_{3,2}^2 = (2\beta + \beta_\Delta)/2^\nu$ for $\mathcal{Q}^*$. $\Delta\Phi_2(t)$ is derived as $\Phi_{\widetilde{\mathcal{H}}}(t) - \Phi_{\widehat{\mathcal{H}}}(t)$. In **b**, for the simplicial complex $\mathcal{C}$, $\Delta\Phi_1(t)$ is evaluated by setting $\mathcal{Q}(\beta_\Delta = 0.9)$ and $\mathcal{Q}^*(\beta_\Delta = 0)$, while $\Delta\Phi_2(t)$ is calculated similarly to **a**. Note that, for clarity, the total entropy difference $\Delta\Phi^*$ (scatter points marked with "×"), closely matches the sum of $\Delta\Phi_1$ and $\Delta\Phi_2$ (shown as bars). Results are averaged over 500 independent simulations with $\mathcal{T} = 20$. **c-d** Comparison of theoretical predictions ($\Delta\Phi^T$, solid lines) from the SI model with simulation results ($\Delta\Phi^S$, bars) for $\Delta\Phi_1(t)$ and $\Delta\Phi_2(t)$, with the propagation duration of $\mathcal{T} = 15$. Strong agreement is observed between theory and simulation. **e** Comparison of quantitative evaluation of the mean infection density $\bar{I}(t)$ between the original and the refined models. Theoretical predictions $\bar{I}^T(t)$ (solid lines) align closely with simulation results $\bar{I}^S(t)$ (dots), as shown for simplicial complexes $\bar{I}_{\mathcal{H}_3}(t)$, projected multi-edge graphs $\bar{I}_{\widetilde{\mathcal{H}}_3}(t)$, and simple graphs $\bar{I}_{\widehat{\mathcal{H}}_3}(t)$. The inset presents the non-logarithmic results of $\bar{I}(t)$ with error bars. Note that the simplicial complexes utilized here are shown in SSC networks in Supplementary in detail. Simulation of contagion dynamics are over 500 independent Monte Carlo realizations, with $\mathcal{T} = 100$. For the simulation of contagion dynamics across the network representations shown in **a-e**, a single node was randomly initialized in the infected state, while all other nodes were set to the susceptible state. The mean-field solutions for $\bar{I}_{\mathcal{H}_3}(t)$ are obtained by numerically integrating the corresponding differential equations using the LSODA algorithm implemented in SciPy (Python).*

Page 10, Caption of Fig. 5:

Validations in DW and Voter opinion dynamics. a *Opinion variations of nodes in $\mathcal{H}$ in a simulation of DW model. The initial opinion values are set to follow a uniform distribution. As time progresses, continuous opinions among nodes evolve and eventually converge to a steady state. **b-c** The relationships among the dynamical uncertainty $\Delta\Phi_1$, the structural uncertainty $\Delta\Phi_2$, and the total differences of system disorder ($\Delta\Phi^*$) underlie the transformability between higher-order and pairwise networks in both synthetic and empirical systems. The value of ϵ is set to 0.1 for the synthetic network and 0.003 for the Email-Enron, while the hypergraph DW model parameter α is 0.5 and 0.8, respectively. The simulations in **a-c** were averaged over 1000 independent simulations of the DW opinion dynamics on each network representation, with each simulation run for 1000 time steps. In each simulation, the initial opinion states of nodes were initialized according to a uniform distribution over [0,1). **d** Opinion variations of nodes in $\mathcal{H}$ in a simulation of Voter model. The initial opinion values are distributed uniformly. Over time, discontinuous opinions among nodes evolve and eventually converge to a steady state. **e-f** The relationships among the* *dynamical uncertainty $\Delta\Phi_1$, the structural uncertainty $\Delta\Phi_2$, and the total differences of system disorder ($\Delta\Phi^*$) underlie the transformability between higher-order and pairwise networks in both synthetic and empirical systems. We set model parameter α to 0.5 in both **e** and **f**. The opinion dynamics are simulated for 2000 time steps. Note that the synthetic network in panels **b** and **e**, with $|V| = |E| = 100$, is generated using HyperCL. The values of $\Phi(t)$ were averaged over 1000 independent simulations of the Voter opinion dynamics on each network representation, with each simulation run for 2000 time steps. In each simulation, the initial opinion states of nodes were initialized according to a uniform distribution over $\{1,2,\dots,10\}$.*

Page 11, Caption of Fig. 6:

***Generalizability of the unified framework. a** Comparison of $\Delta\ddot{\Phi}^*$ and $\Delta\ddot{\Phi}_1 + \Delta\ddot{\Phi}_2$ in DW dynamics within system Υ across both synthetic and empirical systems. Synthetic hypergraphs with varying topologies are generated using HyperCL, where the degree distribution exponents are set to 2, 3, and 5 for scale-free hypergraphs (SFH), Barabási–Albert hypergraphs (BAH), and Erdős–Rényi hypergraphs (ERH), respectively, transitioning from scale-free to uniform degree distributions. Empirical systems, including Email-Enron, High-School, NDC-classes-full, and Primary-School networks, are analyzed, with detailed descriptions provided in the Supplementary Information. **b** Comparison of $\Delta\ddot{\Phi}^*$ and $\Delta\ddot{\Phi}_1 + \Delta\ddot{\Phi}_2$ in Voter dynamics within Υ for both synthetic and empirical systems. Each value is averaged over independent 500 simulation runs. The simulation settings for the DW and Voter models were identical to those used in Fig. 5.*

Page 12, Supplementary Note 8:

We note that the results for each type of contagion under different parameter settings, as shown in the figures, are averaged over 500 independent simulations. In each simulation, one node is randomly selected and initialized in the infected state, while all other nodes are set to be susceptible.

Page 18, Supplementary Note 9:

We note that, for the DW dynamics, results are averaged over ten simulations. Each simulation is run for a fixed total number of time steps (10^4, 10^3, and 5×10^3 in Supplementary Fig.10, Fig.11 and Fig. 13, respectively). This procedure yields consistent and stable outcomes in the DW model, with initial opinions uniformly distributed in [0,1). For the Voter model, results were averaged over 1000 simulations of 2000 time steps each, with initial opinions uniformly distributed in $\{1,2,\cdots,10\}$.

4 Why when increasing the density of the hypergraphs, the dynamical factor is more relevant? A short justification should be added in the main text.

Reply: Thanks for this comment. To clarify why the dynamical factor becomes more relevant with increasing hypergraph density, we have added a brief mechanistic justification in the main text. In short, higher density increases the number of interactions per node and the redundancy of propagation pathways, which amplifies the accumulation and propagation of nonlinear effects across the network. Consequently, the dynamical factor plays a stronger role in the observed differences, while the structural factor remains relevant. Section 2.3 in the main text has been updated with the following descriptions.

Pages 11-12, Section 2.3:

This can be attributed to the fact that higher density of hypergraphs increases both the number of interactions per node and the redundancy of propagation pathways. This allows the nonlinear effects in the opinion updating mechanism to accumulate more significantly at the local node level and to propagate more efficiently across the network, thereby amplifying their overall impact. As a result, the dynamical factor tends to contribute more substantially to the observed differences, even though structural factor remains relevant.

Response to the comments of Reviewer #2

Reviewer #2 (Remarks to the Author):

The revised article, "Transformability of Higher-order Network Dynamics" greatly improves upon its original draft. Some lingering issues/comments:

Reply: We sincerely thank the reviewer for the valuable comments and have carefully revised the manuscript in accordance with each suggestion.

1 I realized that Ref. 25 is not about contagion so shouldn't be cited when talking about contagion. I think that Ref. 28 or https://doi.org/10.1063/5.0020034 might be more appropriate in the second paragraph of the introduction.

Reply: We sincerely thank the reviewer for this suggestion. We have replaced previous Ref. 25 with the reference provided by the reviewer ([R2], provided at the end of the response), now cited as [25] in the revised manuscript, which is more appropriate for the context of contagion dynamics. The corresponding text in the second paragraph of the Introduction has been updated accordingly.

Page 1, Section 1:

The prevalence of group interactions in real-world systems has led to the emergence of higher-order networks [15-17], such as hypergraphs [18-20] and simplicial complexes [21-23], as foundational tools for studying contagion dynamics [25, 25], which overcome the limitations of traditional models.

2 Not to be pedantic, but the manuscript states, "Secondly, the contagion dynamics are governed by the evolution of individual node states (e.g., infection probabilities), which gives rise to disorder at the system level, hereafter referred to as system disorder." I don't think that "governed" is the appropriate word here. I would say that temporal node states describe the system and infection probabilities govern these transitions.

Reply: We sincerely thank the reviewer for this comment. We agree that the term "governed" was not the most appropriate choice. We have updated the sentence in the last paragraph of the Introduction to improve clarity and precision.

Page 3, Section 1:

Secondly, in contagion dynamics, temporal node states describe the system and infection probabilities govern these transitions, leading to disorder at the system level, hereafter referred to as system disorder.

3 The last paragraph of the introduction is much improved.

Reply: We sincerely thank the reviewer for the kind comment and are glad that the revision improves clarity.

4 I recommend that it be published after these minor corrections are made.

Reply: We sincerely thank the reviewer for the recommendation. We greatly appreciate the careful reading and helpful suggestions, which have allowed us to improve the manuscript.

References

[R1] Hickok, A., Kureh, Y., Brooks, H. Z., Feng, M. & Porter, M. A. A bounded confidence model of opinion dynamics on hypergraphs. SIAM Journal on Applied Dynamical Systems 21, 1–32 (2022).

[R2] Landry, N. W. & Restrepo, J. G. The effect of heterogeneity on hypergraph contagion models. Chaos: An Interdisciplinary Journal of Nonlinear Science 30 (2020).

Response to the comments of Reviewer #1

Reviewer #1 (Remarks to the Author):

During this second revision phase, the authors addressed my concerns and amended the text accordingly. Some of the modifications and responses are in the right direction, however some parts seem not convincing to me. I detail the reasons for these considerations below: these points should be addressed by the authors before accepting the paper for publication in Communication Physics.

Reply: We sincerely thank the reviewer for their comments on our work. Below, we respond in detail to each of the concerns raised.

1 Many of the figures' captions still lack crucial information or present contrasting information, despite having requested to clarify this part in both my first and second report. For example, the caption of Fig. 3 says that the simulations are run on the primary and high-school dataset, but only one curve is shown, and then also an SSC random networks is cited; Fig. 4 does not indicate the value of \nu; Fig. 5a,d do not indicate the underlying network;...

Reply: We sincerely thank the reviewer for carefully pointing out the remaining issues in several figure captions and for their patience. We agree that figure captions should be as self-contained and unambiguous as possible. In the revised manuscript, we have made a concerted effort to review the captions across the manuscript and have revised them for clarity and consistency, with particular attention to specifying (i) the underlying network or dataset used, (ii) whether the network is empirical or synthetic and how it is generated, (iii) the relevant model parameters (including ν, β, β_Δ, etc.), and (iv) the correspondence between panels and datasets or network representations. Below we summarize the key clarifications that we have made in response to the reviewer's examples.

First, regarding Fig. 3, we have clarified that panels (a-b) report SI contagion simulations on two empirical higher-order datasets (primary-school and high-school contact data). We have also clarified that panels (c-d) and (e) have been produced on synthetic simplicial complex networks (SSC3 and SSC4, respectively) generated using the configuration-model construction, and we now cite the appropriate references for the generative model used in our study. Additionally, we have specified the relevant parameters and have pointed to the Supplementary Information for the reported topological properties of SSC3/SSC4. The revised caption distinguishes between the empirical and synthetic settings, briefly explains why different network classes are used across panels, and avoids the potentially confusing juxtaposition of empirical datasets and SSC networks in the previous wording.

Second, in Fig. 4, we have added the value of the nonlinearity parameter ν in both the caption and the main text, indicating that Fig. 4 corresponds to $\nu = 4$.

Additionally, we have noted in the caption that the sensitivity to ν is examined separately in the Supplementary Information.

Third, for Fig. 5, we have revised the caption to state the underlying network used in panels (a) and (d), namely synthetic hypergraphs generated via the HyperCL model (including network size and generation settings). Moreover, we have made the opinion-dynamics parameters, initialization rules, and simulation settings more explicit to improve self-consistency.

Finally, beyond these figure-specific edits, we have also checked the remaining captions in the same spirit and have made additional adjustments needed to improve clarity and consistency. We hope these revisions address the reviewer's concern and improve the readability and self-contained nature of the figures.

Page 6, Caption of Fig. 3:

Identification and quantification of contributing factors in contagion dynamics. ***a-b*** *Temporal evaluation of the additive approximation* $\Delta\Phi_1(t)+\Delta\Phi_2(t)$ *for SI contagion on* ***a*** *primary-school and* ***b*** *high-school. Here, we represent the primary-school data as a hypergraph in* ***a*** *and the high-school data as a simplicial complex in* ***b****. In* ***a****,* $\Delta\Phi_1(t)$ *is calculated as* $\Delta\Phi_1(t)=\Phi^{\mathcal{Q}}(t)-\Phi^{\mathcal{Q}^*}(t)$*, with* $\mathcal{Q}(\lambda=0.005,\nu=4)$ *and* $\mathcal{Q}^*(\nu=1)$*, where* $\lambda_{2,1}^2=\lambda_{3,1}^2=\beta$ *and* $\lambda_{3,2}^2=(2\beta+\beta_\Delta)/2^\nu$*.* $\Delta\Phi_2(t)$ *is derived as* $\Phi_{\widehat{\mathcal{H}}}(t)-\Phi_{\widetilde{\mathcal{H}}}(t)$*. In* ***b****, we evaluate* $\Delta\Phi_1(t)$ *by setting* $\mathcal{Q}(\beta_\Delta=0.9)$ *and* $\mathcal{Q}^*(\beta_\Delta=0)$*, while* $\Delta\Phi_2(t)$ *is computed analogously to* ***a****. Note that, for clarity, the total entropy difference* $\Delta\Phi^*$ *(scatter points marked with "×"), closely matches the sum of* $\Delta\Phi_1$ *and* $\Delta\Phi_2$ *(shown as bars). Results of* ***a-b*** *are averaged over 500 independent simulations with* $\mathcal{T}=20$*.* ***c-d*** *Comparison of theoretical predictions (*$\Delta\Phi^T$*, solid lines) from the SI model with simulation results (*$\Delta\Phi^S$*, bars) for* $\Delta\Phi_1(t)$ *and* $\Delta\Phi_2(t)$ *on a synthetic network (i.e., SSC3, see Supplementary for details) generated by the configuration-model construction (see Supplementary Note, following [28]). Results of* ***c-d*** *are averaged over 500 independent simulations with* $\beta=0.005$*,* $\beta_\Delta=0.5$ *and* $\mathcal{T}=15$*. Strong agreement is observed between theory and simulation.* ***e*** *Comparison of quantitative evaluation of the mean infection density* $\bar{I}(t)$ *between the original and the refined models on a larger synthetic network (i.e., SSC4, see Supplementary for details), with* $\beta=0.01$ *and* $\beta_\Delta=0.1$*. Theoretical predictions* $\bar{I}^T(t)$ *(solid lines) align closely with simulation results* $\bar{I}^S(t)$ *(dots), as shown for simplicial complexes* $\bar{I}_{\mathcal{H}_3}(t)$*, projected multi-edge graphs* $\bar{I}_{\widehat{\mathcal{H}}_3}(t)$*, and simple graphs* $\bar{I}_{\widetilde{\mathcal{H}}_3}(t)$*. The inset presents the non-logarithmic results of* $\bar{I}(t)$*. Dashed lines correspond to the classical mean-field approximation, whereas solid lines are obtained from our extended heterogeneous mean-field equation (see Supplementary Information). The topological properties of SSC3 and SSC4 are reported in Table 2 in Supplementary Information. Simulation of contagion dynamics are over 500 independent Monte Carlo* *realizations, with* $\mathcal{T} = 100$*. For the simulation of contagion dynamics across the network representations shown in* ***a-e****, a single node is randomly initialized in the infected state, while all other nodes are set to the susceptible state. The mean-field solutions for* $\bar{I}_{\mathcal{H}_3}(t)$ *are obtained by numerically integrating the corresponding differential equations using the LSODA algorithm implemented in SciPy (Python).*

Page 8, Caption of Fig. 4:

Q^* in dynamics on hypergraphs and simplicial complexes. ***a-c*** *Variation of* $q_{m,\chi}$ *with respect to* $\lambda_{m,\chi}$ *and* β *in contagion dynamics on hypergraphs* ($I_{\Upsilon=\mathcal{H}}$) *with* $(m,\chi) = (2,1), (3,2)$ *and* $(4,3)$*, respectively. The dashed line indicates the condition* $q^*_{m,\chi}$ *required to achieve* Q^**. Here, we focus on* $\kappa = 2$ *and* $\nu = 4$*.* ***d*** *Permissible range of* $\lambda_{m,\chi}$ *required to achieve* Q^* *for contagion dynamics on hypergraphs, denoted as* $\Lambda_{m,\chi}$*, shown for different hyperedge sizes* m *and corresponding numbers of infected nodes* χ *(with the same* $\kappa = 2$ *and* $\nu = 4$ *as in panels* ***a-c****). A logarithmic colorbar is used to resolve small values of* $\Lambda_{m,\chi}$*, and the displayed values remain strictly positive over the explored domain.* ***e*** *Variation of* Q *with respect to* β_Δ *in contagion dynamics on simplicial complexes (red line), where the red triangle denotes* $Q = Q^*$*. The green line shows* Q *for two opinion dynamics on hypergraphs, with the green square indicating* Q^**. We note that* α *represents a factor controlling the nonlinear scaling of influence from neighboring hyperedges in the opinion updating mechanism in opinion dynamics, as detailed in the following Section 2.3 and the Methods section.*

Page 10, Caption of Fig. 5:

Validations in DW and Voter opinion dynamics. ***a*** *Opinion variations of nodes in one simulation of the DW model on a synthetic hypergraph generated by HyperCL [20]. We set* $\epsilon = 0.1$ *and* $\alpha = 0.5$*, and run the simulation for 1000 time steps. As time progresses, continuous opinions among nodes evolve and eventually converge to a steady state.* ***b-c*** *The relationships among the dynamical uncertainty* $\Delta\Phi_1$*, the structural uncertainty* $\Delta\Phi_2$*, and the total differences of system disorder* ($\Delta\Phi^*$) *underlie the transformability between higher-order and pairwise networks in both synthetic and empirical systems. The value of* ϵ *is set to 0.1 for the synthetic network and 0.003 for the Email-Enron, while the hypergraph DW model parameter* α *is 0.5 and 0.8, respectively. The simulations in* ***a-c*** *were averaged over 1000 independent simulations of the DW opinion dynamics on each network representation, with each simulation run for 1000 time steps. In each simulation of* ***a-c****, the initial opinion states of nodes were initialized according to a uniform distribution over* $[0,1)$*.* ***d*** *Opinion variations of nodes in one simulation of Voter model on the synthetic HyperCL hypergraph. We set* $\epsilon = 0.1$ *and* $\alpha = 0.5$*, and run the simulation for* 10^4 *time steps. Over time, discontinuous opinions among nodes evolve and eventually converge to a steady state.*

e-f *The relationships among the dynamical uncertainty* $\Delta\Phi_1$*, the structural uncertainty* $\Delta\Phi_2$*, and the total differences of system disorder (*$\Delta\Phi^*$*) underlie the transformability between higher-order and pairwise networks in both synthetic and empirical systems. The value of* ϵ *is set to 0.1 for the synthetic network and 0.001 for the Email-Enron, while* α *is fixed at 0.5. The values of* $\Phi(t)$ *in* ***e-f*** *are averaged over 1000 independent simulations of the Voter opinion dynamics on each network representation, with each simulation run for 2000 time steps. In each simulation of* ***e-f****, the initial opinion states of nodes were initialized according to a uniform distribution over* $\{1,2,\cdots,10\}$*. Note that the synthetic networks shown in panels* ***a****,* ***b****,* ***d*** *and* ***e****, with* $|V| = |E| = 100$*, are generated using HyperCL with the hyperdegree exponent* $\gamma = 2$.

2. The framework is now much clearer: to transform the higher-order process into the pairwise one, the higher-order contagion probabilities must have specific values for each size of the group (m) and for each number of infected individuals in it (X). This has clarified the framework, showing that the constraints for transformability are very strong (and potentially unrealistic).

However the authors' considerations on the existence of Q^* are unclear: I am mainly referring to the paragraphs "As shown in Fig. 4a-c, ... hypergraphs with larger hyperedges." at the end of pag. 8 and beginning of pag. 9. The authors claim that when the group size is small (m=2) and there are few infected individuals (X=1) the range of parameters for which the higher-order/pairwise mapping can occur is broader than the case with large sizes and many infected individuals (m=4, X=3). However, Fig. 4 shows that for each value of \beta there exists a single \lambda_m,X that allows transformability for each m,X considered in the same way. It seems that the authors are changing point of view, assuming that \lambda_m,X is fixed and \beta is searched for the mapping: therefore if (m,X) are large and \lambda_m,X is large then the corresponding allowed \beta does not exist. This approach is a bit confusing, since for the full transformability to exist \beta must exist and be the same for every m,X and the point of view is different from the rest of the paper. The authors should clarify this point better and make it less confusing.

Reply: We sincerely thank the reviewer for these comments and appreciate the opportunity to clarify this point more explicitly. In the revised manuscript, we have carefully restructured the descriptions around Fig. 4 to avoid the ambiguity noted by the reviewer and to make our viewpoint consistent throughout the paper. Specifically, we have (i) stated that β is a global parameter of the pairwise contagion process; (ii) clarified that our analysis focuses on the remaining admissible freedom in $\lambda_{m,\chi}$ needed to achieve Q^*, rather than "searching for β"; and (iii) introduced $\Lambda_{m,\chi}$ as a statistic that quantifies how restrictive the decomposition is in terms of the remaining admissible span of $\lambda_{m,\chi}$ over the explored β domain.

First, we have clarified a key requirement for transformability, namely that β is a global parameter of the pairwise contagion process and therefore must take the same value for all $(m,\chi) \in \mathcal{Z}$.

Second, since β is treated as a global parameter, our analysis focuses on the remaining admissible flexibility in $\lambda_{m,\chi}$ under the mapping constraint $q_{m,\chi} = q^*_{m,\chi}$ over the same explored β domain. In Fig. 4a-c, we have visualized the solution locus defined by the mapping constraint $q_{m,\chi} = q^*_{m,\chi}$, and our interest has been the $\lambda_{m,\chi}$-span covered by this locus over the explored β range. As the reviewer notes, for each fixed β, the mapping constraint yields a compatible $\lambda_{m,\chi}$, accordingly, the reported $\lambda_{m,\chi}$-span refers to the range of $\lambda_{m,\chi}$ values obtained over the same explored β range, rather than to fixing $\lambda_{m,\chi}$ and then "searching for β". We find that this admissible $\lambda_{m,\chi}$-span is comparatively wider for small interaction size and low infection level (e.g., $(m,\chi) = (2,1)$), but contracts for larger channels (e.g., $(3,2)$ and $(4,3)$), indicating increasingly restrictive mapping constraints under the same explored β domain.

Third, to quantify the restrictiveness of the decomposition and to avoid ambiguity, we have introduced $\Lambda_{m,\chi}$, defined as the permissible range of $\lambda_{m,\chi}$ values for which the mapping condition can be satisfied within the explored β range. By construction, $\Lambda_{m,\chi}$ measures the remaining flexibility of $\lambda_{m,\chi}$ within its feasible interval. As shown in Fig. 4d for the representative case $\nu = 4$, $\Lambda_{m,\chi}$ tends to decrease as χ increases, indicating that denser local infection levels impose increasingly stringent constraints on achieving Q^*. Also, allowing larger hyperedges introduces additional (m,χ) channels that must be satisfied simultaneously under the same global β, thereby suggesting that decomposition is more challenging in hypergraphs with larger hyperedges.

We hope that the revised presentation resolves the confusion and makes the logic underlying the existence of Q^* more transparent. The specific revisions implemented in the manuscript are provided below.

Pages 8-9, Section 2.2:

Q^* as a criterion for dynamic transformation. *The feasibility of decomposition into structural and dynamical components critically depends on the value of Q^*. For contagion dynamics on hypergraphs, achieving Q^* requires that $q^{\kappa}_{m,\chi} = 0$ for all observed $(m,\chi) \in \mathcal{Z}$. Here, we fix $\kappa = 2$ as a representative scenario and perform the subsequent analysis. Since κ is fixed throughout, we henceforth denote $\lambda^{\kappa}_{m,\chi}$ and $q^{\kappa}_{m,\chi}$ by $\lambda_{m,\chi}$ and $q_{m,\chi}$, respectively (and $\left(q^{\kappa}_{m,\chi}\right)^*$ by $q^*_{m,\chi}$) for brevity. A key point is that the rate β is a global parameter of the pairwise contagion process and must take the same value for all $(m,\chi) \in \mathcal{Z}$ in order for full transformability to hold. Accordingly, we focus on the remaining freedom in $\lambda_{m,\chi}$ when imposing the mapping condition $q_{m,\chi} = q^*_{m,\chi}$ within the explored domain of β. To assess when Q^* can be achieved, we* *systematically examine the mapping condition $q_{m,\chi} = q^*_{m,\chi}$ across a broad range of hyperedge sizes m and numbers of infected nodes χ within the hyperedges. In Fig. 4, we set $\nu = 4$. As shown in Fig.4a–c, when the interaction size is small ($m = 2$) and the number of infected nodes is low ($\chi = 1$), the admissible interval of $\lambda_{m,\chi}$ that allows a mapping between contagion on a hypergraph and that on its projected multi-edge representation remains relatively broad, which in turn promotes decomposition. However, for $(m,\chi) = (3,2)$ or $(4,3)$, the feasible domain of $\lambda_{m,\chi}$ rapidly contracts. This narrowing indicates that, under the same explored β range, larger group interactions or denser local infection levels tend to impose more restrictive mapping constraints, thereby reducing the feasibility of achieving Q^* and the associated decomposition.*

To capture the difficulty of decomposition, we define $\Lambda_{m,\chi}$ as the permissible range of $\lambda_{m,\chi}$ values, i.e., the $\lambda_{m,\chi}$-span of the solution set $q_{m,\chi} = q^*_{m,\chi}$ within the explored β domain. By construction, $\Lambda_{m,\chi}$ characterizes the remaining flexibility of $\lambda_{m,\chi}$ within its feasible interval. In the representative setting of Fig. 4d ($\nu = 4$), we observe that $\Lambda_{m,\chi}$ tends to decrease as χ increases, indicating that denser local infection levels impose increasingly stringent constraints on achieving Q^*. Notably, allowing larger hyperedges introduces additional (m,χ) channels that must be satisfied simultaneously under the same global β, suggesting that decomposition is more challenging in hypergraphs with larger hyperedges. The sensitivity of $\Lambda_{m,\chi}$ to ν is examined in Supplementary Information.

3. *\Lambda_m,X is still a good measure: if it becomes 0, it means that regardless of \beta, the only way to transform one process into the other is if there is zero probability of infection for those m,X. In Fig. 4d, it is not clear whether some (m,X) give \Lambda_m,X=0 or simply very small. Perhaps it is better to use a logarithmic scale of the colorbar and indicate if the values are zero? If they are zeros, the authors should also comment on this in the text.*

Reply: We sincerely thank the reviewer for the suggestion. In the revised manuscript, we have (i) revised Fig. 4d (shown as Fig. R1d in this response) to use a logarithmic colorbar to better resolve small values of $\Lambda_{m,\chi}$, and (ii) explicitly clarified in the caption and the main text whether any $\Lambda_{m,\chi}$ values are exactly zero over the explored parameter domain.

First, following the reviewer's suggestion, we have adopted a logarithmic scale for the colorbar in Fig. 4d. This improves visual discrimination among small but nonzero $\Lambda_{m,\chi}$ values that were difficult to distinguish on a linear scale.

Second, we confirm that, over the explored parameter domain shown in Fig. 4d, $\Lambda_{m,\chi}$ remains strictly positive for all displayed (m,χ) (i.e., we do not observe any entries with $\Lambda_{\text{m},\chi} = 0$ in Fig. 4d). Therefore, the green regions in Fig. 4d correspond to highly restrictive, but non-vanishing, admissible $\lambda_{m,\chi}$-ranges, rather than to cases where transformability would require suppressing the corresponding higher-order infection channel entirely.

In addition, we have added a brief clarification in the caption to emphasize the above point.

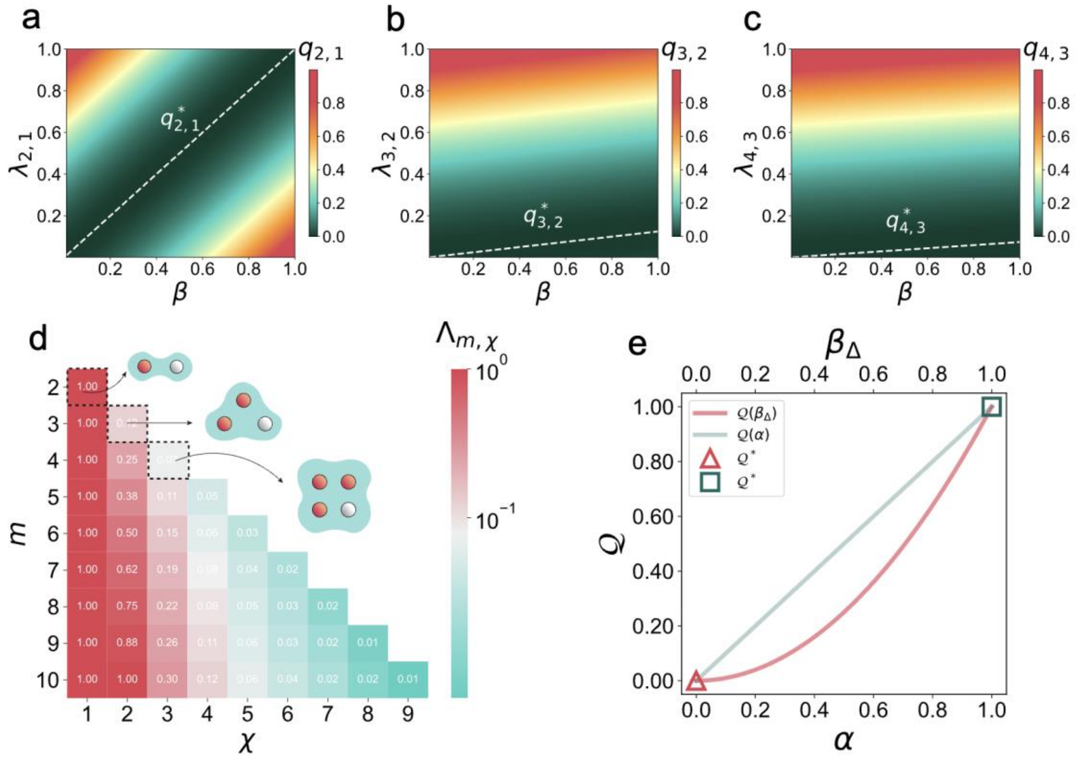

Fig. R1. (Fig. 4 in the manuscript) $\boldsymbol{Q^*}$ ***in dynamics on hypergraphs and simplicial complexes. a-c*** *Variation of* $q_{m,\chi}$ *with respect to* $\lambda_{m,\chi}$ *and* β *in contagion dynamics on hypergraphs (*$I_{\Upsilon=\mathcal{H}}$*) with* $(m,\chi) = (2,1), (3,2)$ *and* $(4,3)$*, respectively. The dashed line indicates the condition* $q^*_{m,\chi}$ *required to achieve* Q^**. Here, we focus on* $\kappa = 2$ *and* $\nu = 4$*.* ***d*** *Permissible range of* $\lambda_{m,\chi}$ *required to achieve* Q^* *for contagion dynamics on hypergraphs, denoted as* $\Lambda_{m,\chi}$*, shown for different hyperedge sizes* m *and corresponding numbers of infected nodes* χ *(with the same* $\kappa = 2$ *and* $\nu = 4$ *as in panels* ***a-c****. A logarithmic colorbar is used to resolve small values of* $\Lambda_{m,\chi}$*, and the displayed values remain strictly positive over the explored domain.* ***e*** *Variation of* Q *with respect to* β_Δ *in contagion dynamics on simplicial complexes (red line), where the red triangle denotes* $Q = Q^*$*. The green line shows* Q *for two opinion dynamics on hypergraphs, with the green square indicating* Q^**. We note that* α *represents a factor controlling the nonlinear scaling of influence from neighboring hyperedges in the opinion updating mechanism in opinion dynamics, as detailed in the following Section 2.3 and the Methods section.*

4. For which value of \nu are the results in Fig. 4 obtained? \nu determines the non-linearity of the higher-order process, so I imagine it plays a key role in the existence of Q^*.

Reply: We thank the reviewer for emphasizing the role of ν, which controls the nonlinearity of the higher-order contagion process. In the revised manuscript, (i) we have now explicitly reported the value used in Fig. 4 (i.e., $\nu = 4$) in both the main text and the figure caption, and (ii) we have included a sensitivity analysis in the Supplementary Note to clarify how the results depend on ν.

First, we have added a statement that Fig. 4a-d were obtained with $\nu = 4$.

Second, to assess sensitivity to ν, we have repeated the same analysis for $\nu = 2, 3,$ and 5 while keeping $\kappa = 2$ fixed (shown as Fig. R2 in this response and as Fig. 10 in Supplementary Note 9). We find that for $\nu = 3, 4,$ and 5, the qualitative trends reported in Fig. 4d are preserved. For $\nu = 2$, we observe a localized exception for channels with $\chi = m - 1$, where the relative ordering of $\Lambda_{m,\chi}$ can be reversed (e.g., $\Lambda_{4,3} > \Lambda_{3,2}$). Importantly, this exception does not alter our main conclusion: full transformability still requires satisfying all $(m, \chi) \in \mathcal{Z}$ constraints simultaneously under a single global β, and the feasibility of achieving Q^* remains governed by this global-consistency requirement.

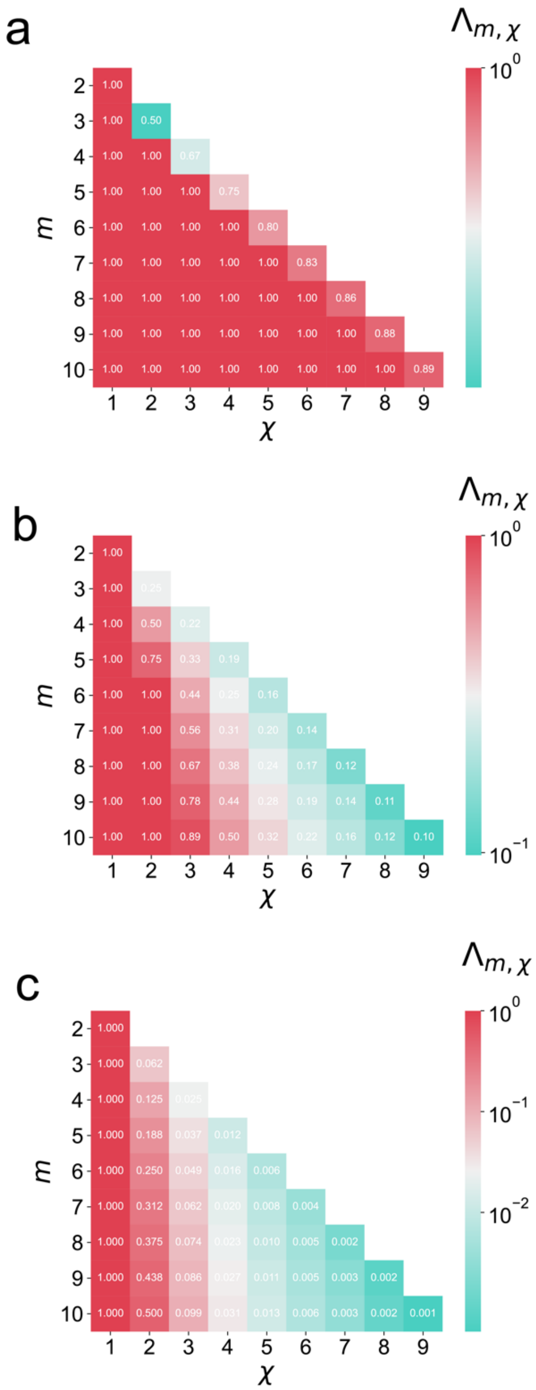

Fig. R2. (Fig. 10 in Supplementary Note 9) *Sensitivity of* $\Lambda_{m,\chi}$ *to the nonlinearity parameter* ν*. The permissible* $\lambda_{m,\chi}$*-range* $\Lambda_{m,\chi}$ *is shown for* $\nu = 2$ *(panel* ***a****),* $\nu = 3$ *(panel* ***b****), and* $\nu = 5$ *(panel* ***c****), with* $\kappa = 2$ *fixed. The colorbar is logarithmic to resolve small values of* $\Lambda_{m,\chi}$*.*

Page 18, Supplementary Note 9:

To examine the sensitivity of the results reported in Fig. 4 ($\nu = 4$*) in the main text to the nonlinearity parameter* ν*, we performed the same analysis for* $\nu = 2, 3$ *and* 5*, while keeping* $\kappa = 2$ *fixed. The corresponding results are shown in Fig. 10. The* *qualitative trends for* $\nu = 3$ *and* $\nu = 5$ *are consistent with Fig. 4, whereas for* $\nu = 2$ *we observe a localized exception for channels with* $\chi = m - 1$. *Importantly, this exception does not affect our main conclusion: full transformability still requires satisfying all* $(m, \chi) \in \mathcal{Z}$ *constraints simultaneously under a single global* β, *and the feasibility of achieving* Q^* *remains governed by this global-consistency requirement.*

Article title: Transformability of Dynamics on Higher-order Networks
Manuscript Number: COMMSPHYS-25-1130C

Response to the comments of Reviewer #1

Reviewer #1 (Remarks to the Author):

In this final round of review, the authors carefully addressed all my concerns and revised the manuscript accordingly.

I am satisfied with the changes implemented and with their response.

I consider the actual version of the paper ready, hence I suggest publication of the paper in Communications Physics.

Finally, I would like to express my appreciation to the authors for their work of revision, which was very attentive and effective, improving the paper significantly.

Reply: We sincerely thank the reviewer for the recommendation and for the time spent on reviewing our manuscript. We greatly appreciate the careful reading and helpful suggestions, which have helped us improve the manuscript.

Review

The article, “Transformability of Higher-order Network Dynamics” explores when hypergraph dynamics can be mapped (“transformed” in the parlance of the article) to pairwise networks, when hypergraph dynamics can be mapped to dynamics on a simplicial complex, and when when dynamics on a simplicial complex can be mapped to pairwise network dynamics. The manuscript treats this as a classification problem and determines parameter regimes for which both processes are indistinguishable, and thus, the dynamics are equivalent. The manuscript derives mathematical conditions for when these dynamics are interchangeable and validates these predictions with numerical simulations. Overall, I find this manuscript interesting and potentially valuable to the higher-order and pairwise network science community.

Most of my comments on the manuscript are related to its lack of clarity. Some of the mathematical details are not sufficiently described and jargon and inadequately described terminology detracts from the paper’s narrative. That being said, I think with an extensive revision, that the paper would be improved greatly, and I would be able to more accurately determine the merit of this piece.

Some more detailed comments and questions:

- The in-text references don’t seem (?) to correspond to the articles in the bibliography. Is the numbering off somehow? As one example: In the introduction, the manuscript states “Nowadays, higher-order networks have become foundational tools for studying contagion dynamics [22–24]” and navigating to the bibliography, Refs. 22-24 are:
    - [22] “How do hyperedges overlap in real-world hypergraphs?” (for which the formatting seems off…)
    - [23] “Networks beyond pairwise interactions: Structure and dynamics.”
    - [24] “Higher-order interactions shape collective dynamics differently in hypergraphs and simplicial complexes.”

  Of these, only the last reference seems directly relevant, although the second one is relevant in a very general sense. I didn’t exhaustively check the references, but I would suggest a double-check on all the references.
- Typographical errors:
    - In the abstract: “interplays” should be “interplay”
    - In the introduction: I don’t believe that “examplied” is a word.
    - There are numerous punctuation errors including missing commas, spaces prior to commas, etc.
    - Reword “between individual neighbors.” to “with a single neighbor.”
- In the introduction and the abstract, the terms “transformable” and “inter-transformed” are used without explicitly explaining what these terms mean. I would add a sentence or two of introduction. Later, in Section 2.3, the manuscript mentions “generalizability”. Is this the same thing?

- This sentence is filled with jargon and imprecision: “Secondly, as the dynamical process inherently reflects the variations of node states within a system, which can be characterized through the evolution of system instability, we naturally leverage information entropy to globally quantify the evolution of instability generated throughout these contagion processes.” What do “reflect” and “variations” mean in this context? I would say that the dynamical process determines node state transitions; is that what this clause means? What does “evolution of system instability” mean? Is this saying that the fixed points and their stabilities are changing in time?
- The introduction starts with a broad overview of higher-order dynamics and offers a nice overview of current modeling limitations, but the introduction should be more grounded in the framework that this manuscript introduces. Specifically, the last paragraph of the introduction is filled with technical jargon (and, as I note above, imprecision) and a lack of overview into what it is that this manuscript accomplishes.
- In Fig. 2, the caption uses notation and terminology that is not introduced until later in the paper ($kappa$, for example). In addition, I think that more description in both the figure and the caption would help.
- When defining the infection rate as χ^ν, I think a reference to Ref. 3 in my list of relevant references would be appropriate (or Ref. [29] in the manuscript). Also: what does the “mapping ratio” mean?
- In Fig. 2, the mention of a “projected simplicial complex” reminded me of an “induced simplicial complex” introduced in Ref. 4 in the list below.
- In Fig. 1(c), the x-label is chopped off. Consider using tight_layout() in pyplot.
- Why not distinguish hypergraphs from graphs in Fig. 2 and why not derive an additional condition, similar to C1 and C2? Especially since this is illustrated in Fig. 1. In my opinion, this is just as important, if not more, than the other comparisons.
- Equations (2) and (3) seem fundamental to the message of the paper. Yet there is no build-up to the presentation of these conditions, all derivation is relegated to Supplementary Note 4, and there is hardly any discussion of the intuitive interpretation of these results.
- The manuscript states that “we classify dynamics using a model of Support Vector Machine”, but more information is needed to reproduce the results of this paper. I assume that the population-level time series (not nodal timeseries) are fed into the SVM? How was the number of time steps determined?
- Overall, I thought that the way sections 2.2 and 2.3 were written felt like an abrupt shift from the prior section. I think that they should be re-written to better motivate why these sections are important to the paper.
- The section title “A unified framework from the perspective of system instability” is a confusing title. First, how is it unified? That could be spelled out more clearly. Second, there are many mentions of “system instability” in the manuscript. As a dynamical systems person, I would use

this to refer to equilibria and their stability, but the manuscript seems (?) to be using this to refer to “avalanche-like” behavior, where the system accelerates toward complete infection. In Eq. (4), I am unclear how this would scale with maximum edge size. Also I found the notation of condition C2 confusing, following Eqs. (2) and (4) ($\beta_\delta=0(\delta>1)$ and $\beta_\delta^2(\delta>1)$).

- More details need to be shared about the entropy. Is this computed on the population average or on a node-by-node basis? How do you deal with continuous nodal states (binning, etc.)?
- Where does Q show up in the results? I understand that Q just indicates the system state, but I don’t understand why it’s introduced and then in Fig. 3, for example, it’s never used.
- In plots 3(c) and (d), $\phi1$ and $\phi2$ should be ϕ_1 and ϕ_2 respectively.
- In Section 2.3, the manuscript stated, “The scattered points, aligned along the diagonal, highlight the generalizability and robustness of our unified framework and delineate the transitions in dynamical behavior.” I must have missed this, because this is not clear to me.
- I found the notation very hard to follow, relying on tildes, umlauts, hats, with non-intuitive (and sometimes inconsistent letters. The scripts on the letters made it more challenging to read.
- Releasing a public GitHub and/or Zenodo repository would make the results in the manuscript more reproducible and I strongly recommend that one be released with the revision.

Some relevant references:

1. Rachith Aiyappa et al., Emergence of simple and complex contagion dynamics from weighted belief networks.Sci. Adv.10,eadh4439(2024).DOI:10.1126/sciadv.adh4439: The authors show that including belief networks on a pairwise network can lead to both simple and complex contagions.
2. Leonie Neuhäuser, Andrew Mellor, and Renaud Lambiotte, Multibody interactions and nonlinear consensus dynamics on networked systems, Phys. Rev. E 101, 032310 DOI: https://doi.org/10.1103/PhysRevE.101.032310: The authors show that “higher-order” linear dynamics are always reducible to pairwise dynamics.
3. Guillaume St-Onge, Vincent Thibeault, Antoine Allard, Louis J. Dubé, and Laurent Hébert-Dufresne, Social Confinement and Mesoscopic Localization of Epidemics on Networks. Phys. Rev. Lett. 126, 098301 DOI: https://doi.org/10.1103/PhysRevLett.126.098301
4. Landry, N.W., Young, JG. & Eikmeier, N. The simpliciality of higher-order networks. EPJ Data Sci. 13, 17 (2024). https://doi.org/10.1140/epjds/s13688-024-00458-1